Interactions Of Class A And Class L Amphipathic Helical Peptides With Model Membranes

Ivan V. Polozov, M. Sc.

A Thesis Submitted to the School of Graduate Studies in Partial Fulfillment of the

Requirements for the Degree

Doctor of Philosophy

McMaster University

1997

DOCTOR OF PHILOSOPHY (1997) McMASTER UNIVERSITY

(Biochemistry) Hamilton, Ontario

TITLE: Interactions of Class A and Class L amphipathic helical peptides with model membranes

AUTHOR: Ivan V. Polozov, M.Sc. (Moscow Inst. of Physics and Technology)

SUPERVISOR: Dr. Richard M. Epand, Professor

NUMBER OF PAGES: xvii, 169

Abstract

Amphipathic α-helix, that is an α-helix with opposing hydrophilic and hydrophobic faces oriented along the long axis of the helix, is an often encountered secondary structural motif in biologically active peptides and proteins. In this thesis, there were systematically studied membrane interactions of two amphipathic α-helical peptides: the 18L peptide, which belongs to the class L (lytic peptides), and the Ac-18A-NH_2 peptide of the class A (apolipoprotein) according to classification of Segrest et al. (1990). It was found previously [Tytler et al., 1993] that class A and class L peptides have opposing effects on some properties of biological and model membranes. In order to elucidate the molecular mechanism responsible for this so-called reciprocal effect in biological membranes, we studied a number of aspects of membrane interactions of 18L and Ac-18A-NH_2 peptides including equilibrium and kinetics membrane binding, permeabilization, fusion and conductance. These functionally different peptides also displayed a number of similarities in membrane interactions and thus parallel studies of these two peptides provide an insight into the general features of amphipathic peptide membrane interactions.

It was found that membrane binding equilibrium and kinetics for both peptides can be described as monomer partitioning with saturation at high peptide/lipid ratios. The rate of peptide-membrane association is relatively close to the diffusion limit. Increase in membrane affinity correlates with a decrease in dissociation rate, i.e. with slower peptide exchange. Both for cationic 18L and zwitterionic Ac-18A-NH_2, the presence of acidic lipids increased membrane binding constants by two orders of magnitude. We have shown that the dynamic

character of the peptide membrane equilibrium can be used for selective peptide targeting and disruption of membranes with specific lipid composition. Titration calorimetry experiments show that the free energy of binding results from an entropic contribution. The free energy of peptide-membrane association is in the range of 8.5-12.8 kcal/mol.

In regards to effects on membrane domain organization, 18L and Ac-18A-NH_2 peptides displayed more similarities than differences. While binding with high affinity to fluid membranes, peptides were unable to penetrate into the lipid membrane in the gel state. If trapped kinetically by cooling from the fluid phase, peptides dissociated from the gel membrane on the time scale of several hours. Charge-charge interactions were capable of inducing lateral domain formation in fluid membranes. Both peptides had affinity for anionic lipids which resulted in about 30 percent enrichment of acidic lipids within several nanometers of the peptide's tryptophan, but there was no long-range order in peptide-induced lipid demixing. Peptide insertion in fluid acidic membranes was accompanied by only a small increase in bilayer surface and a decrease in polarity in the membrane core. Peptide-lipid charge-charge interactions were also capable of modulating existing domain composition in the course of the main phase transition in mixtures of anionic phosphatidylglycerol with zwitterionic phosphatidylcholine. We were unable to observe any peptide-induced lateral phase separation in fluid zwitterionic membranes with nonbilayer phase propensity. Peptides actually improved lipid mixing within the temperature range of the main phase transition of the DMPC:DMPE binary system.

Peptide-membrane permeabilizing activity was significantly affected by the presence of acidic lipids and, in zwitterionic membranes, the presence of nonbilayer forming lipids. In anionic membranes (DOPC:DOPG, DOPG) both peptides caused leakage in the range of bound peptide/lipid ratios of 1:100 to 1:10 and on the time scale of seconds. In zwitterionic

vesicles in the range of bound peptide/lipid ratios 1:50 to 1:10, 18L caused both leakage and fusion on the time scale of hundreds of seconds. At the same peptide/lipid ratios, higher lipid concentrations favoured more fusion and less leakage. Ac-18A-NH_2 caused vesicle leakage, but not fusion. The lytic activity of 18L increased and that of Ac-18A-NH_2 decreased with an increase in the content of an inverted phase forming lipid. A reciprocal effect of 18L and Ac-18A-NH_2 was observed in both the vesicle leakage and vesicle fusion assays with zwitterionic lipids. Reciprocal effects of 18L and Ac-18A-NH_2, were restricted only to membranes with a high propensity for nonbilayer phase formation (DOPE, Me-DOPE, DOPC:DOPE, DOPC:Me-DOPE). The decrease in the content of nonbilayer phase forming lipid or addition of acidic lipids reduces or eliminates the reciprocal effects. This suggests that nonbilayer phase propensity is the physical property responsible for observation of reciprocal effects of A- and L-class peptides in biological membranes.

Analysis of the mechanism of 18L induced permeabilization of zwitterionic membranes have shown that 18L peptide destabilises membranes, leading to a transient formation of large defects (diameter > 3 nm) which generally results in contents leakage, but in the presence of bilayer-bilayer contact can lead to vesicle fusion. This defect formation is accompanied by phospholipid flip-flop and or peptide translocation. Peptide insertion into the membrane also significantly reduces membrane stability to mechanical tension making it susceptible to osmotic lysis. This mechanism may be general for the action of class L peptides.

The results presented in this thesis appear, in part, in following publications:

Papers

Polozov, I. V. , Polozova, A. I. , Mishra, V.K., Anantharamaiah, G. M., Segrest, J. P., and Epand, R. M. (1997) *Biochim. Biophys. Acta (in press)*. Studies of kinetics and equilibrium membrane binding of class A and class L model amphipathic peptides.

Polozov, I.V., Polozova, A.I., Molotkovsky, J.G., Anantharamaiah, G.M., Segrest, J.P., and Epand, R.M. (1997) *Biochim. Biophys. Acta (in press)*. Amphipathic peptide affects the lateral domain organization of lipid bilayers.

Polozov, I.V., Polozova, A.I., Woolley, G.A., Tytler, E.M., Anantharamaiah, G.M., Segrest, J.P., Epand, R.M. (1997) *Biochemistry* 36, 9237-9245. Role of lipids in the permeabilization of membranes by class L amphipathic helical peptides.

Epand, R.M., and Polozov, I.V. (1996) In "Nonmedical applications of liposomes", Y. Barenholz and D.D. Lasic, eds., CRC Press, Boca Raton, 105-111. Liposomes and Membrane Stability.

Polozov, I.V., Polozova, A.I., Anantharamaiah, G.M., Segrest, J.P., and R.M. Epand. (1994) *Biochem. Mol. Biol. Intern. 33*, 1073-1079. Mixing rates can markedly affect the kinetics of peptide-induced leakage from liposomes.

Polozov, I.V., Anantharamaiah, G.M., Segrest, J.P., and R.M. Epand (1997) Manuscript in preparation. Osmotically induced membrane tension modulates permeabilization of membranes by class L amphipathic helical peptides.

Polozov, I.V., Anantharamaiah, G.M., Segrest, J.P., and R.M. Epand (1997) Manuscript in preparation. Amphipathic peptides affect phospholipid flip-flop and membrane asymmetry.

Abstracts

Polozov, I. V. , Polozova, A. I. , Mishra, V.K., Anantharamaiah, G. M., Segrest, J. P., and Epand, R. M. (1996) Biophys J., 70, A95, Mechanism of membrane permeabilization by L class amphipathic lytic peptides (Abstract).

Polozov, I. V. , Polozova, A. I. , Mishra, V.K., Anantharamaiah, G. M., Segrest, J. P., and Epand, R. M. (1996) Biophys J., 70, A94, Evidence that nonbilayer phase propensity is important for biological membranes. Use of amphipathic peptide analogs with opposite effects. (Abstract).

Polozov, I.V., Polozova, A.I., Molotkovsky, J.G., Anantharamaiah, G.M., Segrest, J.P. and Epand, R.M. (1995) Biophysical J., 68, A433, Amphipathic peptides effects on the lateral domain organization of lipid bilayers (Abstract).

Polozov, I.V., Polozova, A.I., Anantharamaiah, G.M., Segrest, J.P. and Epand, R.M. (1994) FASEB Summer Conference on Membrane Biophysics. Interaction of helical amphipathic peptides with model membranes.

Acknowledgments

First of all I would like to thank Dr. Richard M. Epand for the expert supervision of this thesis. His liberal approach provided freedom for pursuing new ideas, while being extremely available for discussions and fast in editing. Also I would like to thank my suprevisory committee members: Dr. A.M. Edwards, Dr. G. E Gerber, Dr. D.S-C. Yang for their comments and criticism.

Special thanks to my wife Alla, who not only supported me through this years, but contributed to this work in her short stay as a postdoc in this laboratory and in multiple discussions afterwards.

My parents significantly contributed to this project by bringing me up with respect to science and then by guiding me to the overseas direction.

I am grateful to all members of the Dr. Epand's lab, past and present, for discussions and their patience during multiple group meetings and presentations, and for the company throughout all this years: Dr. Raquel Epand, Dr. Marian Mosior, Dr. John Katsaras, (Dr.) Jim Cheetham, (Dr.) Tina McCallum, Dr. G. Andrew Woolley, Alan Stafford, Dr. Ling Miao, Dr. Adriana Colotto, Dr. Zhi Huang, Yoshikatsu Ogawa, Thorsten Wieprecht, Robert Bruins, Jenifer Giorgione, Joses Jones, Dr. Zhe Zhou, and summer and project students too.

I would like to thank my collaborators: Dr. G.M. Anantharamaiah and Dr. J.P. Segrest, for peptides synthesis and purification; Dr. Julian G. Molotkovsky for providing the fluorescent lipid probes; Dr. Yury Tarahovsky for the EM photographs; Dr. G. Andrew Woolley for BLM conductance measurements and Dr. Shlomo Nir for fruitful discussions.

Finally I would like to acknowledge financial support of Department of Biochemistry, McMaster University.

TABLE OF CONTENTS

ABBREVIATIONS

18L, GIKKFLGSIWKFIKAFVG;

Ac-18A-NH_2, N-Acetyl-DWLKAFYDKVAEKLKEAF-amide;

ANTS, aminonaphthalene-3,6,8-trisulfonic acid;

ABD-PE, 1-hexadecanoyl-2-[12-[(7-aminobenz-2-oxa-1,3-diazol-4-yl]aminododecanoyl]- *sn*-glycero-3-phosphoethanolamine;

AA, 12-(9-anthryl)-11-*trans*-dodecenoic acid;

APC, 1-acyl-2-[*trans*-12-(9-anthryl)-11-dodecenoyl]-*sn*-glycero-3-phosphocholine;

APE, 1-acyl-2-[*trans*-12-(9-anthryl)-11-dodecenoyl]-*sn*-glycero-3-phosphoethanolamine;

APG, 1-acyl-2-[*trans*-12-(9-anthryl)-11-dodecenoyl]-*sn*-glycero-3-phosphoglycerol;

APL, anthrylvinyl-labelled phospholipid (any of APC, APE or APG);

ΔG_b, the free energy of peptide-membrane binding;

diPhyPC, diphytanoylphosphatidylcholine;

diSC_2(5), 3-3'-diethylthiacarbocyanine iodide;

DMPC, 1,2-dimyristoyl-*sn*-glycero-3-phosphocholine;

DMPE, 1,2-dimyristoyl-*sn*-glycero-3-phosphoethanolamine;

DMPG, 1,2-dimyristoyl-*sn*-glycero-3-phosphoglycerol;

DOPC, 1,2-dioleoyl-*sn*-glycero-3-phosphocholine;

DOPE, 1,2-dioleoyl-*sn*-glycero-3-phosphoethanolamine;

DOPG, 1,2-dioleoyl-*sn*-glycero-3-phosphoglycerol;

DPA, dipicolinic acid;

DPPC, 1,2-dipalmitoyl-*sn*-glycero-3-phosphocholine;

DPPG, 1,2-dipalmitoyl-*sn*-glycero-3-phosphoglycerol;

DPX, *p*-xylenebis-(pyridinium bromide);

DT, sodium dithionite ($Na_2S_2O_4$);

E, fluorescence resonance energy transfer efficiency.

FITC-dextran, fluorescein isothiocyanate-labelled dextran (M.W. 20,000 and 10,000);

FRET, fluorescence resonance energy transfer;

IMC, intrinsic monolayer curvature.

K, the equilibrium peptide-membrane binding constants;

k_a, the rate constant of peptide-membrane association;

k_d, the rate constant of peptide-membrane dissociation;

L, lipid concentrations;

LUV, large unilamellar vesicles;

Me-DOPE, N-methyl-dioleoylphosphatidylethanolamine;

MLV, multilamellar lipid vesicles;

NBD-PE, 1-hexadecanoyl-2-(12-[7-nitrobenz-2-oxa-1,3-diazol-4-yl]amino)dodecanoyl- *sn*-glycero-3-phosphoethanolamine;

NBD-PC, 1-hexadecanoyl-2-(12-[7-nitrobenz-2-oxa-1,3-diazol-4-yl]amino)dodecanoyl-*sn*-glycero-3-phosphocholine;

P_0, peptide concentration;

P_b, the peptide concentrations in membrane;

P_{be}, equilibrium amount of peptide bound to the membrane;

P_f, the peptide concentration in water;

PPC, 1-acyl-2-[9-(3-perylenoyl)nonanoyl]-*sn*-3-glycerophosphocholine;

PA, 9-(3-perylenoyl)nonanoic acid;

R, a rate constant of single exponential time course of peptide-membrane binding;

r, bound peptide/lipid ratio;

Tb, terbium III chloride;

T_H, bilayer to hexagonal phase transition temperature;

T_m, temperature of the main (L_β to L_α) phase transition.

FIGURES

TABLES

1. Introduction

Lipid-peptide interactions are known to play a key role in many biological phenomena. Interactions of peptides with membranes also provide a model system for a number of aspects of lipid-protein interactions.

Detailing of membrane interactions of class A and class L amphipathic α-helical peptides, the subject of this thesis, requires at least a small overview on the current idea of the structure of biomembranes and on the definition and classification of the amphipathic motif in proteins and peptides.

1.1 Current concept of the structure of biomembranes

The hypothesis that a lipid bilayer constitutes the core of biological membranes has been first put forward by Gorter and Grendel back in 1925. Formation of lamellar phases by hydrated lipids has been established by the diffraction studies of Palmer and Schmitt [Bear et al., 1941; Palmer and Schmitt, 1941]. The view of biomembranes as two-dimensional solutions of proteins in a lipid bilayer emerged from a series of works throughout the sixties and is now known as the fluid mosaic model of Singer and Nicholson (1972) (Fig. 1.1.1A). This model of high heuristic value, made it possible to put forward a series of hypotheses about membrane structures and functions which largely defined the course of membrane studies. Twenty five years later the model still holds although this years of scrutinising necessarily resulted in ajustments of the original model.

There appeared an increased appreciation of membrane structure complexity. A current cartoon of a eucariotic plasma membrane (Fig. 1.1.1B) illustrates typical

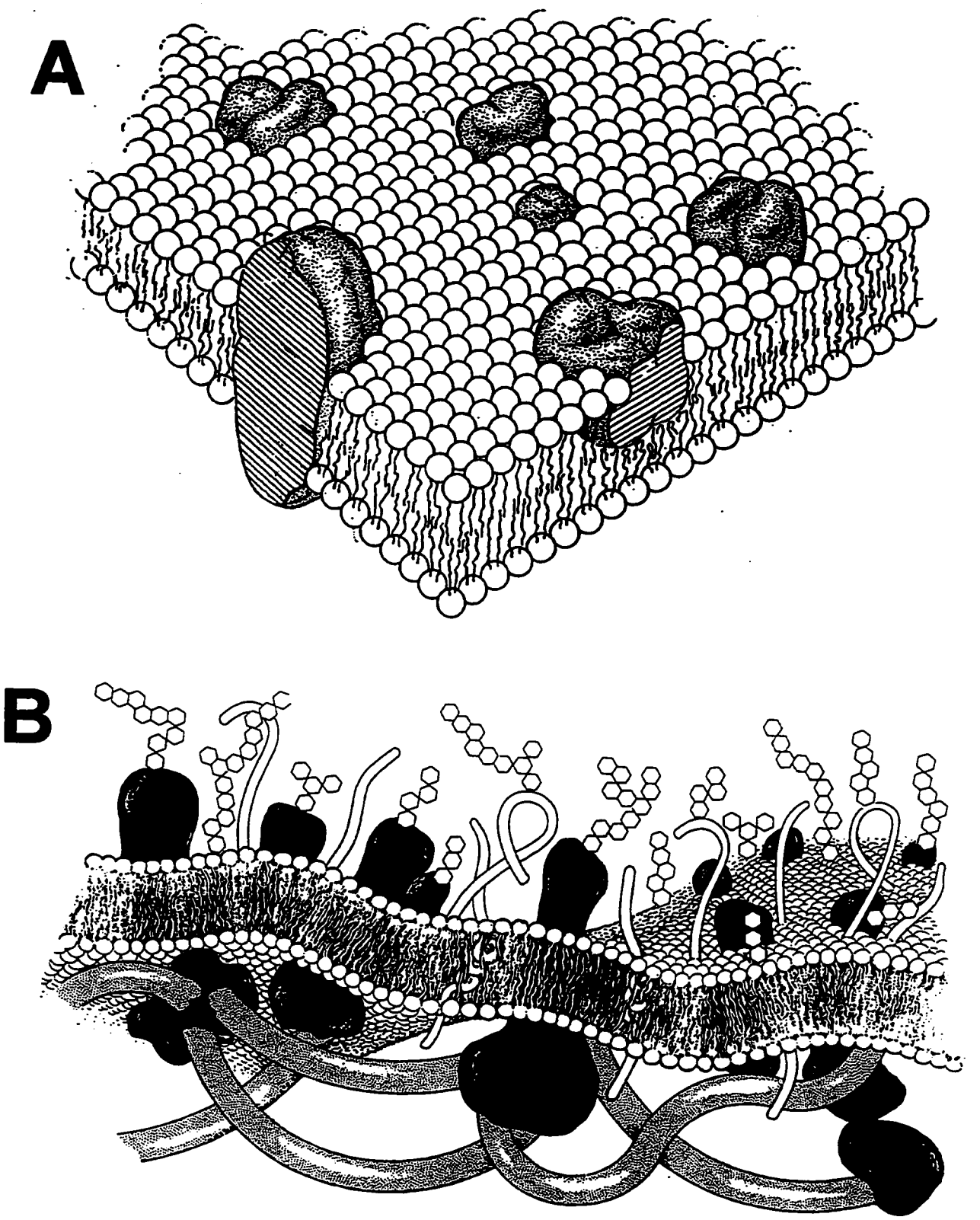

Figure 1.1.1 A. Schematic representation of biomembrane as a lipid bilayer with randomly distributed membrane imbedded proteins (the fluid mosaic model). From Singer and Nicholson, 1972.
B. Schematic illustration of plasma membrane of eucariotic cell. Typical components are pictured only approximately to scale. From Bloom et al., 1991.

components of biomembranes pictured only approximately to scale [Bloom et al., 1991]. The lipid bilayer core, made up of diacyl-lipids and sterols, serves as the permeability barrier. Low permeability of the lipid bilayer to ions and other polar solutes makes it possible to precisely regulate the aqueous composition of a membrane enclosure by means of a relatively small amount of protein pumps and channels, amphiphilic-glycosylated proteins inserted into the membrane. To support the bilayer, a subsurface network of proteins has been developed and attached to the bilayer in ways that are not precisely understood at present. The added rigidity allows cells greater deformability and movement. Finally large extrafacial peptidoglycan moieties emanate from the bilayer; the macromolecular "roughness" of this glycocalyx serves the function of cell-surface recognition and can cause both adhesion or repulsion, as required. Some lipids (glycolipids) also have complex carbohydrate headgroups. Generally, the lipid bilayer is also asymmetric in composition [review Devaux, 1993]. Complex glycolipids, like gangliosides, usually have absolute specificity for the outer leaflet of the membrane, while phospholipids usually display preferential distribution, with PC mostly on the outer monolayer and PE and PS on the inner one.

Organisation of biomembranes, other than plasma membranes of eucariotic cells, varies markedly depending on the function of the membrane, but are similar in having lipid, protein and carbohydrate components. While the majority of membrane functions are mediated by proteins, the view of the lipid bilayer as an inert passive support for membrane proteins is completely irrelevant. There is some progress in understanding the ways properties of the lipid bilayer are related to membrane functions. Below in this section I shall briefly review several aspects of bilayer structure in relation to membrane activities.

1.1.1 Enigma of lipid diversity

The abundance of different lipid species in biological membranes is a direct indication that the lipid bilayer is more than an inert support for membrane proteins. A single lipid species with the propensity to form a liquid crystalline bilayer would be sufficient to fulfil the role of a membrane as a permeability barrier. Nevertheless, all biomembranes are composed of many different lipid classes, and within a given class, an enormous diversity of molecular species with a specific acyl chain composition is found. Perhaps, in the future this diversity will be explained by a diversity of reasons. Naturally many of the lipid species have particular biological functions, depending on their chemical and biochemical properties. Many minor membrane lipids appear to be essential in cellular signalling pathways or otherwise have a high bioactivity. Similar function were also proposed for (parts of) more abundant lipid classes. However, it seems possible that in many cases the overall lipid composition of biological membranes is regulated in order to maintain some physical properties of membranes. Several different properties have been deemed to be the most important ones, such as membrane fluidity [Shinitzky, 1984], critical LUV formation temperature [Gershfeld, 1989; Gershfeld and Murayama, 1988], membrane nonbilayer phase propensity or intrinsic monolayer curvature strain [Gruner, 1985; Epand and Epand, 1994; Österberg et al., 1995; Morein et al., 1996].

Naturally, excess variability of lipid composition serves the function of accommodating to environmental conditions. This was used as an approach to study the importance of the physical properties of a lipid bilayer. Lipid extracts from cold blooded animals or bacteria grown at different temperatures or at different harsh environmental

conditions have been compared in search of invariable features. Advanced studies [reviewed in de Kruijff et al., 1997] were possible for such bacteria as *E. coli* because of the availability of mutants in the biosynthesis of the major phospholipids. These studies also suggest the importance of nonbilayer phase propensity (negative intrinsic monolayer curvature) for membrane functions.

1.1.2 Lipid polymorphism and roles of non-bilayer forming lipids

While it is established that a lipid bilayer forms the core (permeability barrier) of most biological membranes, it is known since pioneering works of Luzzati [Luzzati and Hanson, 1962; Luzzati, 1968] that individual lipid components and even total lipid extracts from biological sources do not necessarily form stable bilayers. Rather the lamellar arrangement was found to be only one of a number of phases adopted by lipids. Roughly, non-bilayer forming lipids can be classified as those forming or promoting inverted phases (inverted hexagonal H_{II} and/or cubic Q_{II} , Fig.. 1.1.2.1) and those forming or promoting micellar-like phases.

There exist several theoretical approaches to the molecular basis of the nonlamellar phase behaviour of membrane lipids. The most widely used is the approach based on the "shape" of the lipid molecule [Israelachvilli et al., 1977, 1980; Israelachvilli, 1991] and the considerations of "spontaneous monolayer curvature" [Gruner, 1985; Gruner et al., 1989]. The "shape" concept is the simpler of the two. Its main assumption is that for any lipid (amphiphile) molecule the type of possible aggregates is determined by the geometric properties of the molecule. The main parameter of the concept is the critical parameter S -

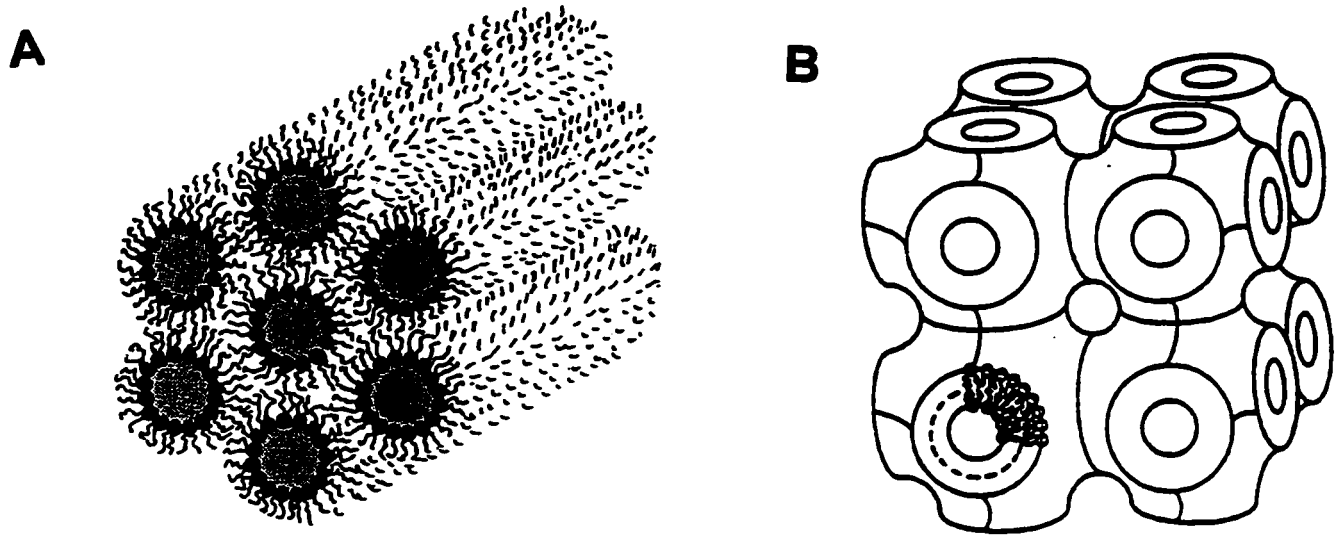

Figure 1.1.2.1. Examples of lipid nonlamellar phases. A Inverted hexagonal phase H_{II}. B. Inverse bicontinuous cubic phase Im3m (Q^{229}). From Seddon, 1990.

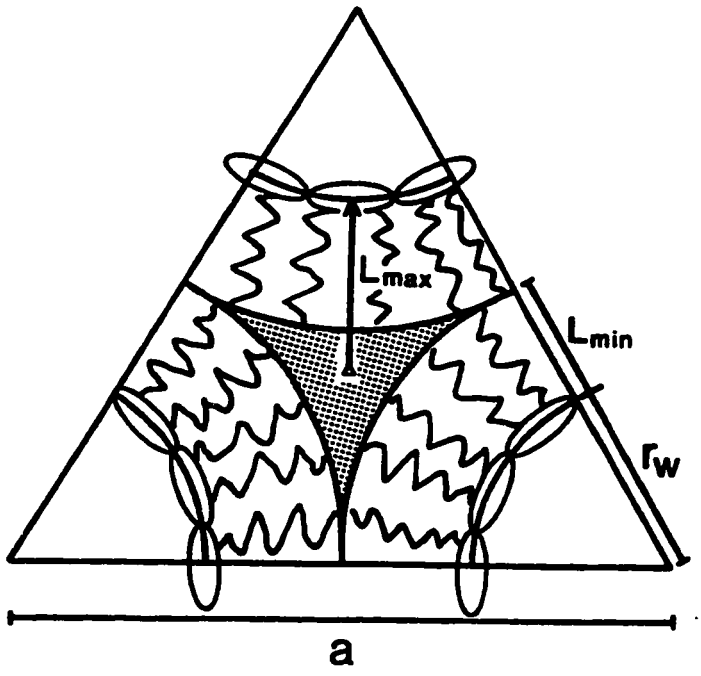

Figure 1.1.2.2 Packing frustration in the H_{II} phase. From Seddon, 1990.

shape factor, defined as $S = v/a_o l_c$. Where v is the hydrocarbon chain volume, a_o is the optimal headgroup cross-sectional area, and l_c - critical chain length. Major structures possible for different values of the critical parameter are shown in the Fig. 1.1.2.3. Cone-shaped molecules, those with $S < 0.5$, are likely to form micelles; cylindrical ones ($S = 0.5$-1) should form lamellar arrangements and those with packing parameter values above 1 should form inverted phases. Despite the simplicity of this concept, it has proven to be useful for the rationalisation of many aspects of the phase behaviour of many membrane lipids. Parameters of the system can be understood as rigid geometric characteristics, and thus may be used for rough estimates of the phase state of the lipid. But, actually, all of the system parameters (v, a_o, l_c) are the effective values depending on a number of system parameters such as temperature, hydration, ionic strength, hydrogen bonding, etc. Thus this model is of limited use for the prediction of subtle changes in phase behaviour.

Gruner and co-workers have proposed an alternative approach, centred around the concept of spontaneous intrinsic monolayer curvature (C_o). This concept arises naturally from the fact that within a lipid monolayer, forces arising from interactions between headgroups, in the interface, and between hydrocarbon chains do not pass through the "centre of mass" of the monolayer. Thus the monolayer would have a tendency to curl, which in the lamellar phase is opposed by the other monolayer. For monolayers with negative curvature, the curvature stress can be released by formation of an inverted arrangement, e.g. the inverted rods of the hexagonal phase (H_{II}). In this arrangement exposure of the hydrophobic residues to the aqueous media is relieved by parallel packing of hydrophobic rods. However, as it is clear from the Fig 1.1.2.2, there still remains a

Lipid	Critical packing parameter $v/A_0\ l_c$	Critical packing shape	Structures formed
Single-chained lipids (detergents) with large head-group areas:	$< \frac{1}{3}$	Cone 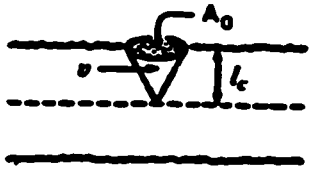	Spherical micelles 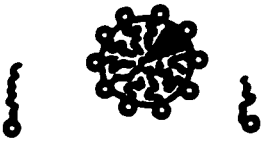
Single-chained lipids with small head-group areas:	$\frac{1}{3} - \frac{1}{2}$	Truncated cone or wedge 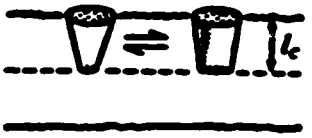	Globular or cylindrical micelles 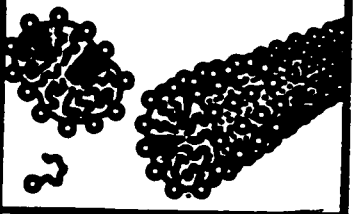
Double-chained lipids with large head-group areas, fluid chains:	$\frac{1}{2} - 1$	Truncated cone 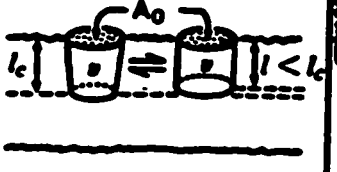	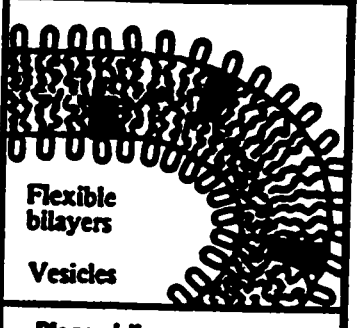
Double-chained lipids with small head-group areas, anionic lipids in high salt, saturated frozen chains:	~ 1	Cylinder 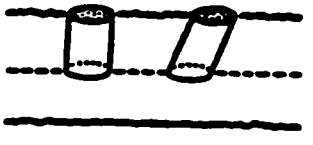	Planar bilayers 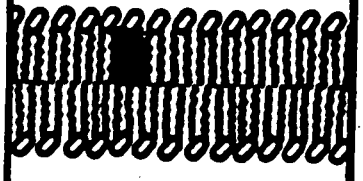
Double-chained lipids with small head-group areas,	> 1	Inverted truncated cone 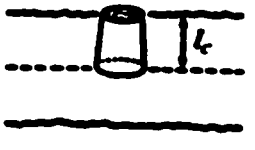	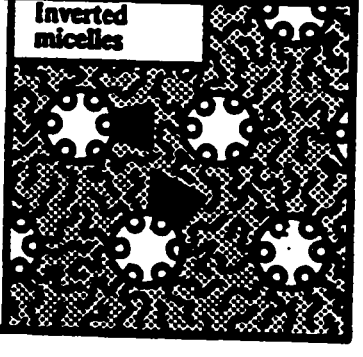

Figure 1.1.2.3 Packing properties of lipids and the aggregate structures that may be formed, for various values of the "critical shape parameter" ($S = v/a_o l_c$). From Israelachvilli et al., 1980.

frustration in the chain packing. All of the hydrophobic regions must be filled to a uniform liquid alkane density, but in order to fill the triangular regions in the centre (shaded), some of the chains must stretch away from their optimal conformational state. Thus the balance of curvature stress and hydrophobic packing constraints defines the phase state of the lipid. The main parameter of this concept is the $R_o=1/C_o$ - the radius of spontaneous monolayer curvature. In the lamellar arrangement the free energy associated with the curvature stress can be defined as $E = k\cdot(1/R-1/R_o)^2$ where k is the bending modulus of the monolayer and R is its radius of curvature.

It has been proposed by Kirk and Gruner (1985) that R_o values of inverted phase forming lipids can be measured via the first-order repeat of H_{II} phases formed in the presence of small quantities of alkanes. The rationale behind their suggestion was that small percent of alkanes should relieve the hydrocarbon chain packing stress by filling the interstitial volume between H_{II} rods and thus the lipid monolayers should relax to their spontaneous curvatures. Unfortunately, the assumption that alkanes will not affect the R_o by directly intercalating in the monolayer was proved to be unfounded [Siegel et al., 1989; Sjolund et al., 1987]. Thus values of the intrinsic radius of curvature measured according Kirk and Gruner (1985) should be taken with caution. The absence of a reliable method to measure the R_o of the monolayer hampers application of this formalism. Support for the existence of intrinsic monolayer curvature stress in Me-DOPE bilayer was recently provided by Epand and Epand (1994).

Besides formation of inverted phases, there exists another possibility to alleviate the intrinsic monolayer curvature stress in bilayers - by global rearrangement of lipids towards

the formation of a bicontinuous cubic phase (Fig. 1.1.2.1). It is now generally believed that the bicontinuous cubic phases are based upon "minimal surfaces" which have at each point zero net curvature. In the minimal surface, bicontinuous in three dimensions, each monolayer creates a net mean negative curvature at the water membrane interface (towards the water), yet without creating potential voids (and hence chain packing problems) within the hydrocarbon region.. Thus the concept of intrinsic monolayer curvature is useful for the explanation of the formation of bicontinuous cubic phases.

Existence of non-lamellar phase forming lipids in biological membranes led investigators to suggest that these non-lamellar phases may play a role in biological functions [Cullis and deKruijff, 1979]. Much of the focus in this area was addressed to the question of the possible existence of nonlamellar structures in biological membranes. There is some electron microscopy evidence which suggests that some biological specimens contain extensive domains of cubic structures [Landh, 1995]. Some inverted phase formation probably takes place in the tight junctions between cells [Wegener and Galla, 1996; Borovyagin and Sabelnikov, 1989].

Besides a direct role of non-lamellar structures in biological systems, there is an increasing number of example to illustrate that certain membrane properties are modulated by the presence of non-lamellar lipids [reviewed in Epand, 1996; Epand, 1997]. This includes modulation of the functions of membrane proteins and membrane associated enzymes as well as membrane fusion.

1.1.3 Membrane domain organisation

According to the fluid mosaic concept [Singer and Nicholson, 1972], the lipid bilayer was viewed as a two dimensional solvent, fluid and homogeneous, with a possible exception of specific protein-lipid interactions. Fluidity of biomembranes was often emphasized afterwards [Shinitzky, 1984; Gennis, 1989], but currently this term is used less often because of its too broad definition and different set of properties implied by different authors. The idea of homogeneity of the bilayer of a biomembrane, arose from the fact that biomembrane lipids are above their main phase transition temperatures. This proved to be not necessarily true. For example, brain sphingomyelin undergoes a main phase transition in the range of 30°-50°C, that is at physiological conditions [Dobereiner et al., 1994]. Resistance of some membrane fractions (glycolipid-enriched membrane fraction [Rogers and Rose, 1996; Schroeder et al., 1994]) to detergent solubilization was also explained by the solid state of this biomembrane domain. Besides, lipid-lipid immiscibility is not restricted to the gel state. A number of cases of fluid-fluid phase immiscibility have been shown in model membranes [Hong-wei and McConnell, 1975; Berclaz and McConnell, 1981]. High content of cholesterol in biomembranes is often cited as another reason to consider the biomembrane lipid matrix as homogeneous, arguing that cholesterol plasticizes membranes and eliminates the main phase transition. However, recent studies [Bloom et al., 1991; Vist and Davis, 1990; McMullen and McElhaney, 1995] show that cholesterol effects on the lipid lateral organization are diverse and concentration

dependent and serve better as evidence of the existence of complex lateral organization than of its absence.

The concept of a homogeneous lipid bilayer for many years directed experimental efforts just at detection of some deviation from equilibrium. By now things have progressed to such a point that nobody argues about the possibility of existence of some complex lateral organization in membranes and generally the focus moved to characterization of this organization and identification of its biological importance [for reviews: Bergelson et al., 1995; Welti and Glaser, 1994; Raudino, 1995; Jacobsen and Vaz, 1992].

In very general terms, the thermodynamic causes for phase separations are well established and may be attributed to a balance of mutually antagonistic forces: intermolecular attractive or repulsive forces tend to aggregate or separate certain molecular species, whereas entropy tends do drive the system toward homogeneity. Relatively small differences in pair-interaction energies can lead to phase separations in biological membranes. Since biological membranes are dynamic non-equilibrium structures, complex lateral membrane organization also may be the result of kinetic rather than thermodynamic factors. The domains can arise over a large range of time- and length-scales, from dynamic organization on the nanometer scale [Mouritsen and Jorgensen, 1994; Bloom et al., 1991; Jacobsen and Vaz, 1992] to the domains of micron scale, presenting fractions of the entire cell surface [Luan et al., 1995].

Existence of membrane lateral phase separation may have some important biologically relevant consequences. For example, when two phases are present in a bilayer,

a new fundamental variable parameter appears, which is the lateral connectivity of each phase. When a phase is self-connected throughout the plane of the bilayer it is said to be percolating. Conversely, not percolating phase is constituted of disconnected domains. The percolation threshold of a given phase is the area fraction of that phase above which the percolating cluster exists. Below the percolation threshold long range diffusion in that phase can not occur over distances larger than the dimensions of phase domains. Relatively small change in the phase state of the membrane can result in the change of the percolation state of domains. This can have profound impact on the rates of reaction between components having preference for the same phase [Almeida et al., 1993; Almeida and Vaz, 1995]. Diffusion rates and effective local component concentrations are also expected to be strongly modulated in the more general case of diffusion in heterogeneous membrane.

Two dimensional lateral phase separation can also have consequences on the three dimensional structure of the membrane. For example, brain sphingomyelin (bSM) undergoes main phase transition between 30°C and 50°C, which is accompanied with solid-fluid phase separation. Heating through this regime bSM giant unilamellar vesicles leads to the continuous budding and fission of small vesicles, the lipid composition of which differs from that of the mother vesicle [Dobereiner et al., 1994].

Existence of membrane domains is closely linked with the existence of lipid diversity [Chapter 1.1.1]. Knowledge of the phase organization of lipid systems progressed significantly since the early seventies. Within the lamellar organization a number of lipid phases have been identified. While their biological relevance is not known yet, there is no *a priori* reason to exclude it. Complex phase diagrams have been

found even for simple binary lipid mixtures. More complex organization is expected with an increase in the complexity of mixtures. However, progress in the analysis of complex mixtures is limited by the available experimental techniques. Approaches used to study membrane lateral organization can be divided into macroscopic bulk techniques and microscopic probe based techniques [Bloom et al., 1991], while lateral organization of membranes occurs in the so called mesoscopic range (1-100 nm). Both types of techniques provide indirect information about heterogeneity in the system rather than direct information on spatial and temporal domain organization. Simultaneous application of both types of techniques is advantageous. A wide range of methods have been applied to studies of phase separations in the lateral organization of model systems, including calorimetry [McMullen and McElhaney, 1995], or X-ray diffraction [Caffrey, 1989], many spectroscopic techniques such as fluorescence [Paltauf and Schmid, 1989; Bergelson et al, 1985; Welti and Glaser, 1994.], FTIR [Mantsch and McElhaney, 1991], ESR [Hong-wei and McConnell, 1975; Berclaz and McConnell, 1981; Marsh, 1995] and NMR [Bloom et al., 1991] spectroscopy, then freeze fracture electron microscopy [Borovyagin and Sabelnikov, 1989; Luna and McConnell, 1978], small angle neutron scattering (SANS) [Knoll et al., 1981; 1983] and fluorescence recovery after photobleaching (FRAP) [Axelrod et al., 1976; Jovin and Vaz, 1989]. The choice of techniques applicable to studies of biological membranes is significantly narrower. The most commonly used are fluorescent methods (including FRAP and fluorescence microscopy) [Welti and Glazer, 1994; Luan et al., 1995; Chen et al., 1997], the latest and

the most promising are the single particle tracking (SPT) [Sheetz et al., 1989; Sheetz et al., 1995] and near-field optical microscopy [Hwang et al., 1995].

Probe based techniques always have to address the question of how good the probe parallels the properties of native components. Below will be described the reasons for the synthesis and application of anthrylvinyl- and perylenoyl-labelled lipid probes, which were used in this project in a number of applications, including studies of membrane lateral organization.

1.1.3.1 Lipid-specific probes

The first generation of fluorescent probes used in membrane studies were non-polar or amphiphilic substances, such as pyrene, 1,6-diphenyl-1,3,5,-hexatriene (DPH), 8-anilino-1-napthalensulfonate (ANS), and cyanine dyes. The location of such probes inside the membrane is uncertain. Application of such fluorescent probes to studies of membrane domain organization is further hampered by unknown or difficult to define partitioning of the probe between various membrane domains. These uncertainties led to an idea to use as membrane probes, fluorescently modified lipids. Two types of modifications are possible: fluorescent groups can be introduced either in headgroup or in the hydrocarbon tails of the molecule. There exist applications for both types of probes, but since fluorophors usually are relatively bulky and hydrophobic, lipid modification in the headgroup is definitely more perturbing than modification in the acyl chains. Lipid probes having a fluorophor attached to one of the hydrocarbon chains retain the natural polar headgroup and thus were termed lipid-specific [Bergelson et al., 1985]. Several series of lipid-specific probes have been

synthesized [review, Bergelson et al., 1985; Paltauf and Schmid, 1989]. Many of them are now commercially available [Haugland, 1996] which contributes to their increase in popularity for the studies of membrane structure and dynamics [reviews: Welti and Glazer, 1994; Bergelson et al., 1985; 1992; 1995; Paltauf and Schmid, 1989].

Even subtle changes in the structure of lipid molecule have drastic consequences on its phase behavior. For example, introduction to a saturated chain of just one double bond lowers the temperature of the main phase transition by 30°-50°C. Thus it is impossible to make a non-perturbing fluorescent probe. Perhaps the least perturbing fluorophor is parinaric acid, a naturally occurring fatty acid, with 4-conjugated double bonds. However, its high susceptibility to oxidation complicates its application and interpretation of results [Welti and Silbert, 1982]. This disadvantage can be overcome by the use of small aromatic molecules. Several derivatives of anthracene have been used by various laboratories: 2-anthryl [De Boney and Tocanne, 1984], 2-anthroyl [Kaplun et al., 1978] 9-anthryl [Stoffel and Michaelis, 1976], 9-anthroyl [Waggoner and Stryer, 1970; Lanelle and Toccanne, 1982]. Use of 9-anthrylvinyl (AV) as a fluorophor was proposed by Molotkovsky et al. (1979) (Fig. 1.1.3.1.1). This fluorophor has a *trans*-double bond conjugated with anthracene aromatic rings.This increased its extinction coefficient and quantum yield compared to other anthracene derivatives. The red-shifted AV fluorescence excitation maximum to 370 nm (near UV) makes possible to use it as an acceptor for resonance energy transfer from tryptophan. Its fluorescence lifetime of ~9 ns makes this probe's fluorescence anisotropy sensitive to the phase state of the lipid [Bergelson et al., 1985]. Indeed, AV-labelled fluorescent PC, was sensitive not only to the main phase transition of DMPC but also to its

A

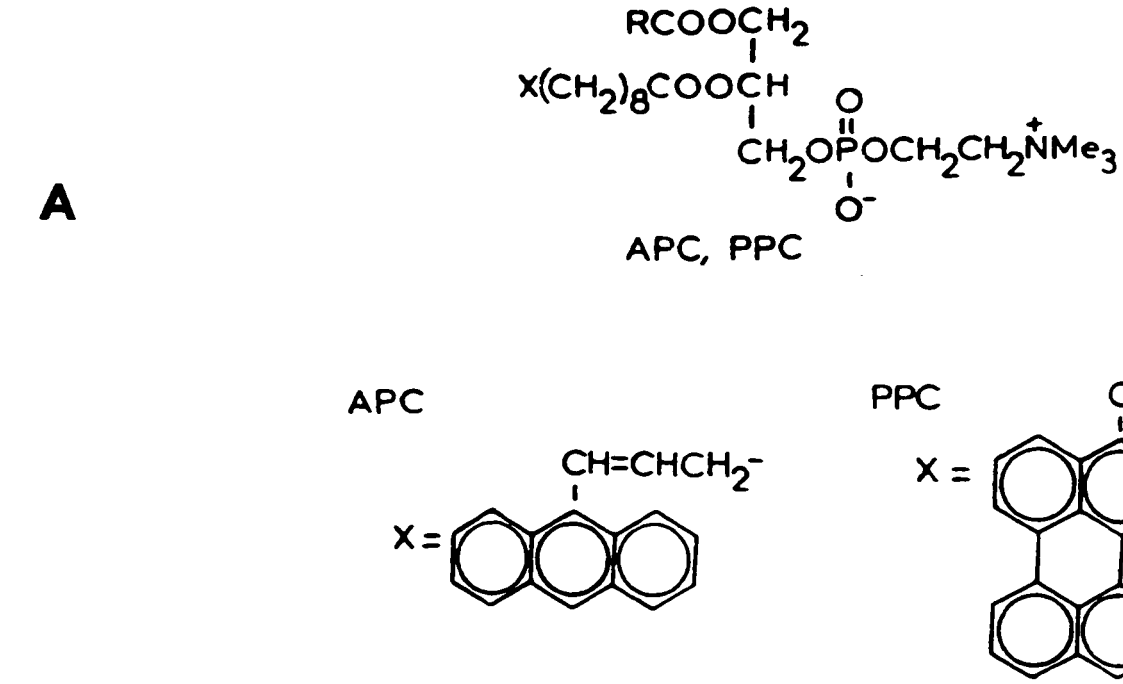

B

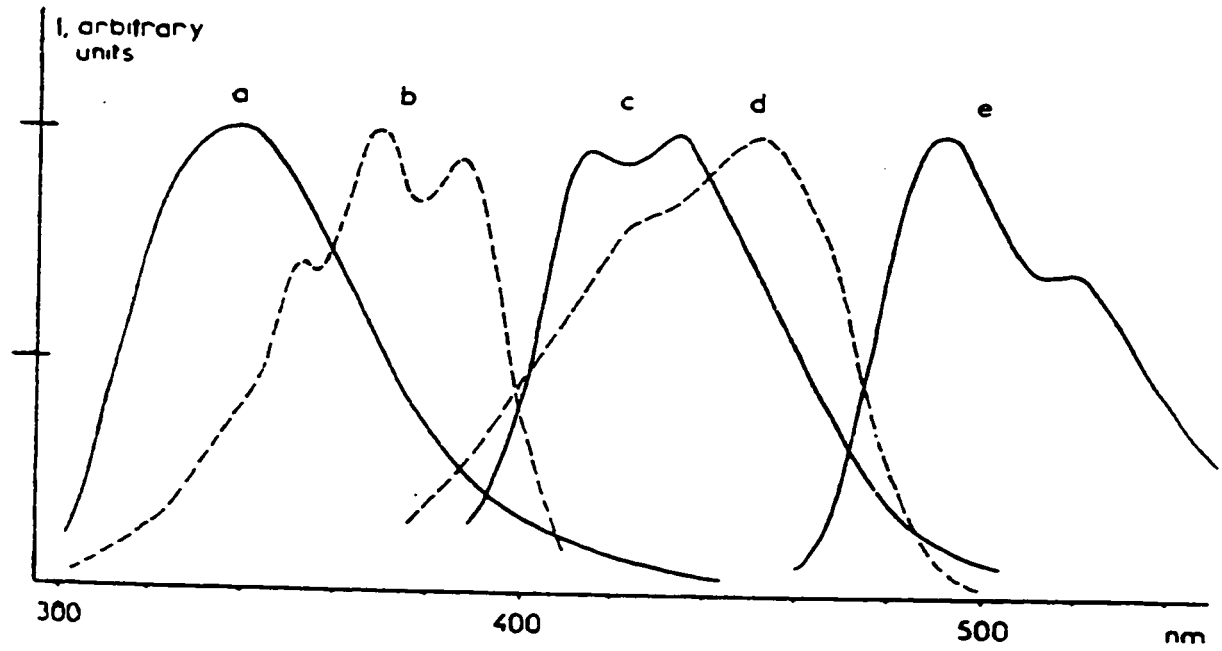

Figure 1.1.3.1.1 **A.** Chemical formulas of 9-anthrylvinyl- and 3-perylenoyl-labelled phosphatidylcholines (APC and PPC). **B.** Normalized spectra of (a) fluorescence emission of tryptophan (protein in HDL_2, λ_{ex} 294 nm); (b) excitiation of AA in dioxane (λ_{em} 430 nm); (c) emission of AA in dioxane (λ_{ex} 370 nm); (d) excitiation of PA in dioxane (λ_{em} 520 nm); (e) emission of PA in dioxane (λ_{ex} 450 nm). From Molotkovsky et al., 1984.

pretransition ($P_{\beta'}$--L_{α}) which is not resolved by other fluorescent probes [Polozov et al., 1994a]. This serves as an indirect evidence of the low perturbing properties of AV fluorophor. Also there is direct support provided by proton magnetic resonance spectroscopy of sonicated PC vesicles containing anthrylvinyl-labelled phosphatidylcholine (APC) which demonstrated that APC induced a noticeable upfield shift only at the level of the acyl terminal CH_3 groups and a part of the methylenes, while the resonances of the choline protons remained completely unaltered [Molotkovsky et al., 1982]. There have been synthesized a large assortment of AV-labelled lipids including triglyceride, all major classes of phospholipids [review: Bergelson et al., 1985; Bergelson, 1992], and a number of glycolipids [Molotkovsky et al., 1991]. Probes with C_{12}- and C_6-acyl chain spacers have been synthesized which in principle makes it possible to estimate the depth of insertion of membrane protein or membrane-active peptide tryptophans.

The so called "two probe approach" was put forward for the application of these probes to the studies of lipid membrane domain organization [Bergelson et al., 1985]. One can expect that probe-induced perturbances will be similar for probes with different headgroups but the same fluorophors in the hydrophobic area. Thus, to analyze multicomponent lipid system, one can conduct parallel experiments with probes with various headgroups. It is likely that difference in probes fluorescence parameters (anisotropy, energy transfer) is determined by the headgroup of the probe molecule and thus is indicative of the difference in state of the "host lipids". As a control for this hypothesis, it was shown that in a homogeneous (one-component) membrane, when all probes disregarding their headgroups have a similar environment (as defined by

neighboring molecules), all probes have similar parameters, however, they are different in a heterogeneous mixture [Polozov et al., 1994a; Gromova, 1990]. The phase transition of APC is below 0°C, so it is understandable that in the high melting mixtures APL's have some preference for the fluid phase, regardless of their headgroups.

Perylenoyl-labelled lipids (Fig. 1.1.3.1.1) have been synthesized as an acceptor for the anthrylvinyl excitation energy [Molotkovsky et al., 1984] and this property was used in studies of lipid-lipid [Polozov et al., 1994a] and peptide-lipid interactions [Gromova et al., 1990; Gawrisch et al., 1993]. Unlike perylene, the excitation and emission main maxima of which are very close to each other, the 3-perylenoyl group displays a considerable Stokes shift, and the position of the emission maxima depends on the solvent polarity. This sensitivity was used for estimates of the lipid bilayer water permeability [Molotkovsky et al., 1987]. The position of excitation and emission maxima of 3-perylenoyl fluorophor are in the visible range which makes these lipid-specific probes convenient for fluorescence microscopy. Taken together anthrylvinyl and perylenoyl labelled lipid-specific probes complement each other for a variety of membrane applications.

1.1.4 Membrane asymmetry and coupled bilayer hypothesis

While details of the mechanism of maintenance of membrane asymmetry and its relationship to biological functions are yet not understood [Allan and Kallen, 1994], there is accumulating knowledge about this important structural feature of biomembranes. It is well established that in model membranes, lipids exchange between two leaflets of the bilayer (flip-flop) very slowly, on the scale of hours or days [Kornberg and McConnell, 1971]. This low rate suggests that bilayer asymmetry is

defined kinetically rather than thermodynamically. This view evolved from that of twenty years ago [Bergelson and Barsukov, 1977] when asymmetry of biomembranes was hypothesized to have a similar origin as the spontaneous asymmetry of sonicated small unilamellar vesicles, which was explained in terms of adaptation to the curvature stress of the bilayer.

As briefly mentioned above [Chapter 1.1] the major motif in biomembrane lipid asymmetry is the location of aminophospholipids and acidic phospholipids on the cytoplasmic side of biomembranes. This is true both for plasma and organelle membranes, although since analysis of membrane asymmetry in organelles is more complicated, there is less certainty about their arrangement [Bergelson and Barsukov, 1977; Devaux, 1992]. All phospholipids in the plasma membrane of eukaryotic cells are subject to a slow passive transbilayer movement. In addition, aminophospholipids are rapidly moved from the exoplasmic to the cytoplasmic leaflet of the plasma membrane at the expense of ATP hydrolysis, which is an indication of protein involvement in the maintenance of aminophospholipid asymmetry. Search for the candidate flippase proteins culminated in reconstitution of flippase activity in proteoliposomes by a 110 kDa Mg^{2+}-dependent ATP-ase [Auland et al., 1994].

Though the principal pathways of transbilayer movement of phospholipids probably apply to all eukaryotic plasma membranes, studies of the actual kinetics of phospholipid redistribution have been largely confined to non-nucleated cells (erythrocytes), which have relatively inert plasma membrane. Regulation of membrane asymmetry and composition is likely to be more complicated in other metabolically

more active cells. There are data that in human skin fibroblasts the rate of aminophospholipid translocation is at least an order of magnitude higher than that in human erythrocytes [Pomorski et al., 1996]. Experiments on nucleated cells are complicated by endocytosis and metabolism of the lipid probes inserted into the plasma membrane. There are data that external addition of SM analogs to human skin fibroblasts results in its fast uptake via endocytosis mediated by lateral membrane segregation [Chen et al., 1997]. Thus the endocytic pathway can also influence plasma membrane composition and asymmetry.

Experiments with hepatocytes of transgenic mice [Smith et al., 1994; Smitt et al., 1993] suggest that P-glycoprotein (P-gp), responsible for the multi-drug resistance (MDR) of cancer cells, is a PC-translocator (flippase) promoting the transfer of PC from the inner to the outer leaflet of the plasma membrane, and ultimately is responsible for secretion of PC into bile.

Random non-directed transbilayer diffusion rates in biomembranes are also higher than in model membranes, thus the existence of non-specific flippases was postulated. However, it might be that higher rates are just the consequence of the high content of proteins in biomembranes. It has been found that some lytic peptides [Fattal et al., 1994; Matsuzaki et al., 1996] at the permeabilising peptide lipid ratios, induce high rates of lipid flip-flop. This disruption of lipid asymmetry may just be a side effect or may be related to peptide lytic activities. It is not known how general protein or peptide induced lipid flip-flop can be. A report by Epand et al. (1994) suggests that apolipoprotein A-I decrease the rates of lipid flip-flop and thus protects erythrocytes

against the generation of procoagulant activity. This observation of diverse peptide effects on membrane asymmetry prompted us to compare effects of amphipathic lytic peptides and apolipoprotein analogs on phospholipid flip-flop in model membranes [Chapter 3.5].

It is worth mentioning that postulating the existence of specialized proteins involved in all processes changing lipid asymmetry may be excessive. For example, recent studies on Ca^{2+}-induced lipid scrambling in model membranes containing phosphatidylinositol 4,5-bisphosphate (PIP_2) [Sulpice et al., 1996] suggested that this lipid scrambling is a direct result of Ca^{2+} -PIP_2 interactions.

One of the consequences of the asymmetry of the membrane is that two leaflets of the bilayer membrane can respond differently to a particular perturbation. Such a perturbation, for example, can result in the expansion of one layer relative to the other, thereby producing a curvature of that membrane. Back in seventies this concept was introduced in the studies of shape changes in erythrocytes and lymphocytes [Sheetz et al., 1976] induced by membrane insertion of amphiphilic compounds. Introduction of small differences between the surface of two monolayers can lead to great changes in the shape and morphology of vesicles including vesicle fission or fusion [Sackmann, 1994]. In cells, where large shape changes are moderated by the cytoskeleton, monolayer surface mismatch will create membrane curvature stress which is likely to affect functions of the membrane.

Other biological consequences of membrane asymmetry are directly related to possible changes in monolayer composition. It is possible to make a parallel between

membrane polarization and membrane asymmetry. Change in membrane polarization can cause cascades of physiological reactions. Similarly, exposure of PS has been involved in formation of procoagulation activity and also as a signal for the initiation of apoptosis. Acidic lipids flip-flop was correlated with protein translocation. It is likely that the list will be significantly enlarged as functional roles of membrane asymmetry become fully appreciated.

1.1.5 Osmotic effects and membrane tension

The lipid bilayer of a cell membrane constitutes a continuous selective barrier to solutes in living cells. In contrast, it has a high permeability to water which diffuses along the hydrocarbon chains [Reeves and Dowben, 1970; Deamer et al., 1996; Marrink et al., 1996]. These differences in permeation rates promote the well known phenomena of swelling and shrinkage as a response to the osmotic disbalance between the outer and the inner cell media. Red blood cells are subjected to the osmotic stresses on their passage through kidney. Generally, cells have multiple mechanisms of dealing with osmotic stress by carefully adjusting solute concentrations in order to avoid osmotic lysis.

Effects of osmotic pressure on vesicles were studied for many years. There is a consensus that vesicles respond elastically to changes in osmotic pressure, but when the elastic limit is reached a pore formation occurs. As pores grow in size they release excess pressure with partial release of vesicle content and then reseal immediately afterwards [Hallet, 1993; Ertel, 1993]. However, there is still some controversy about the critical values of stress that bilayers can withstand. There are two reasons for this

uncertainty. First, preparation of homogeneous monodisperse osmotically sensitive vesicles was a problem before the appearance of extrusion techniques. Second, even with extruded vesicles there is a question of the extent of initial vesicle inflation. There are data that extruded vesicles are not spherical when prepared in a buffer [Mui et al., 1993; Clerc and Thompson, 1994]. Thus initial vesicle response to osmotic downshift might be the result of vesicle shape change, rather than elastic expansion. Osmotic stress can be spontaneously present in other common used vesicle preparations. Even when some precautions are taken there is still some uncertainty about the osmotic compensation of vesicles. Multilamellar vesicles were found to be under osmotic stress as sealing of the vesicles occurs prior to completion of lipid hydration [Gruner et al., 1985]. Contrary to that, the freeze-thaw procedure used for preparation of LUV was shown to produce osmotically swollen vesicles [Chapman et al., 1991].

Another aspect of osmotic effects on vesicle structure was brought to attention lately. It was shown that relatively small changes in osmotic strength can strongly affect the structure of the membrane-water interface, changing the state of lipid polar headgroup hydration [Disalvo et al., 1996; White et al., 1996].

Osmotic swelling of liposomes can also serve as a model for the more general area of tension effects on biological or model membranes. The rheological properties of membranes are believed to influence both blood flow and cell fusion. The postulated molecular bases for such phenomena as cellular osmoregulation, blood pressure homeostasis, and fluid translocation through higher plants invoke membrane stretch receptors or sensors. Mechanosensitive ion channels have been revealed through the

application of patch clamping techniques to animal, plant and bacterial cells [Morris, 1990] and biochemical measurements have indicated that turgor sensitive regulatory proteins and enzymes may be present in bacterial cytoplasmic membranes [Csonka and Hanson,1991]. The mechanism of this putative mechanosensors is largely unknown. More to that, it is generally unknown how tension will affect functions of any membrane protein. However, recent studies suggest that membrane tension can modulate activities of membrane active peptides and proteins. For example, it has been shown [Opsahl and Webb, 1994] that change of the tension of BLM modulates the conductance of the alamethicin ion-channel. Recently, effects of melittin were shown to be modulated by an osmotic gradient [Benachir and Lafleur, 1996]. These examples show that a study of tension effects on vesicles is necessary in order to discriminate it from other effects, this is especially necessary in the case of studies of vesicle aqueous content leakage.

To conclude, after many years of liposome research, still relatively little is known about the mechanical properties of vesicles, especially, regarding their dependence on lipid composition.

1.2 Aspects of peptide-lipid interactions

1.2.1 Amphipathic α-helix in lipid-peptide interactions. Class A and class L amphipathic α-helix.

The amphipathic α-helix, that is an α-helix with opposing hydrophilic and hydrophobic faces oriented along the long axis of the helix, is an often encountered secondary structural motif in biologically active peptides and proteins. Amphipathic helices

were first described as a unique structure/function motif involved in lipid interaction by Segrest et al. (1974). Prior to this Perutz et al. (1965) had noted that α-helices in globular proteins often have narrow nonpolar edges along the long axis of the helix facing the nonpolar interior of the protein. Since that time amphipathic helical domains have been described for a number of globular, lipid-associating and complex transmembrane proteins [reviews, Epand, 1993; Segrest et al., 1990].

Naturally occurring amphipathic helices have been classified into seven major types (A, H, L, G, K, C, and M) on the basis of their hydrophobicity and the size and charge distribution of their hydrophilic domain [Segrest et al., 1990]. (Table 1.2.1.1 and Figure 1.2.1.1). There were identified three classes of lipid-associating amphipathic α–helices: class A - apolipoproteins, H - hormones and L - lytic peptides. Another membrane related class consists of transmembrane sequences of complex membrane proteins (class M). Others are classes of helices involved in protein-protein interactions. This includes, class G, typical of globular α–helical proteins; class K, found in calmodulin-binding domains of calmodulin regulated Kinases; and class C, found in coiled-coil proteins.

Since the concept of amphipathic helix classes was derived from the fact that amphipathic helices differ in both structure and function, it is quite possible that as more protein sequences will be known the classification of amphipathic α–helices will be extended. There might be identified completely new classes. Also subclasses may be introduced into major classes upon detailed analysis, including into consideration additional new parameters [Segrest et al., 1994].

Average Properties of Seven Different Classes of Amphipathic Helixes

Property	Classes A (Apolipoproteins)	H (Polypeptide hormones)	L ("Lytic" polypeptides)	G (Globular proteins)	K (Calmodulin-regulated protein kinases)	C (Coiled-coil proteins)	M (Transmembrane proteins)
Mean hydrophobic moment per residue	0.42	0.54	0.37	0.32	0.38	0.22	0.12
Mean hydrophobicity per residue of nonpolar face	0.73	0.57	0.74	0.64	0.55	0.80	0.74
Mean charged residue density per 11mer of helix							
Positive	1.9	2.4	1.6	1.3	3.0	2.1	0.09
Lys/Arg ratio	2.0	0.8	30	5.7	0.8	1.3	0.6
Negative	2.0	0.5	0.4	1.3	0.2	2.5	0.25
Total	3.9	2.9	2.0	2.6	3.2	4.6	0.3
Mean ± charge ratio	0.9	4.8	4.0	1.1	15	0.8	0.4
Mean localization of charged residues by quadrant							
Nonpolar face / Positive / Polar face							
Nonpolar face / Negative / Polar face							
Mean angle subtended by polar face	≥180	≤100	≤100	≥180	≥180	≥320	≤60

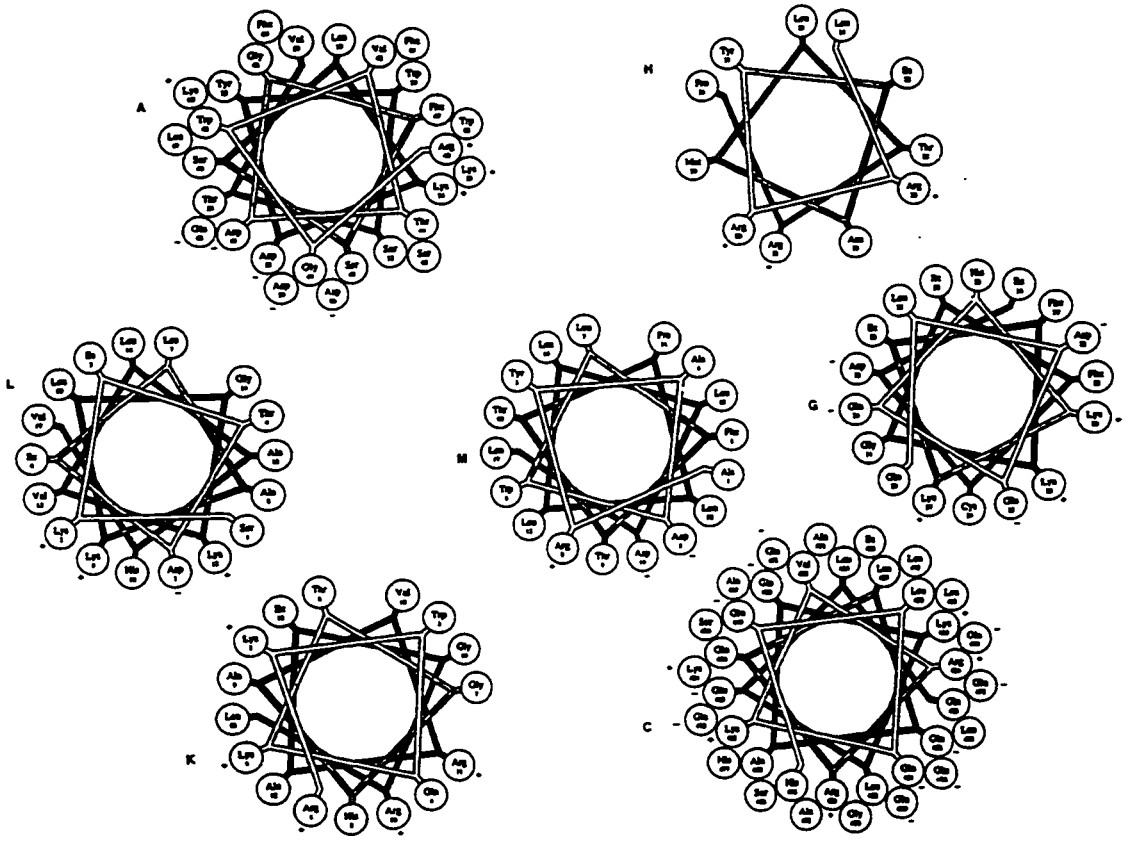

Table 1.2.1.1 Average properties of seven different classes of amphipathic α-helices. From Segrest et al. 1990.

Figure 1.2.1.1 "Schiffer-Edmundson" wheel diagrams of examples representing the different classes of amphipathic helixes. Class A, apolipoprotein C-III (residues 40-67); Class H, pancreatic polypeptide (24-34); Class L, bombolitin I; Class M, bacteriorhodopsin, helix C; Class G, myohemerythrin helix (18-38); Class K, rabbit smooth musclemyosin light chain kinase (2-17); and Class C, myosin c-β (448-483). From Segrest et al. 1990.

This classification provided a significant insight into the specificity of the amphipathic helical motif for particular biological functions. Comparison of new putative amphipathic α–helices with already known and classified sequences, may lead to the identification of similarities and suggestion of putative functions.

Below will be described in more details properties of class A and class L amphipathic α–helices as they are directly related to the subject of this thesis.

1.2.1.1 Class A: Apolipoproteins

Apolipoproteins are the protein components of plasma lipoproteins and through their lipid-associating characteristics these proteins allow the transport of the otherwise water-insoluble lipids in plasma. Certain apolipoproteins have an additional metabolic function through their interaction with cell surface receptors or activation of lipolytic enzymes. There are two subclasses of apolipoproteins, those capable of moving between lipoprotein particles and those that stay with one particle from biosynthesis to catabolism. Numerous experiments have shown the amphipathic helices to be responsible for the lipid associating properties of the exchangeable apolipoproteins.

All the major human apolipoprotein genes have been cloned and sequenced. The most striking feature of these exchangeable apolipoproteins is the presence of internal 22-residue-long repeats. Most importantly, this repeat unit has the periodicity of an amphipathic α–helix. This class A amphipathic helix found in natural apolipoproteins has a high mean hydrophobic moment and has a distinctive structure of the polar face: unique clustering of negatively charged residues at the centre and positively charged residues at the

polar-nonpolar interface. A mean radial angle subtended by the polar face is more than 180°. In addition, the polar face of the class A amphipathic helix has the second highest density of charged residues; in an average 22-mer amphipathic helix of class A there are 4 Lys/Arg and 4 Glu/Asp residues.

This characteristic distribution of polar residues was found important for the high lipid affinity of class A peptide analogs. "Reversed" peptides - with altered distribution of cationic and anionic residues - were synthesized. Their membrane affinity was found to be significantly lower. The so called "snorkel hypothesis" was put forward suggesting that long hydrophobic stems of lysyl residues are inserted deeply into the bilayer (Figure 1.2.1.1.1) and thus contribute to the hydrophobicity of the peptide [Anantharamaiah et al., 1993].

1.2.1.2 Class L: Lytic peptides

The venom of several hymenopterae species, such as bees and wasps, contain large amounts of small cationic amphipathic α–helical peptides responsible for some of the toxic effects of these insect bites [Argiolas and Pisano, 1985; Hirai et al., 1979]. Key physiological properties include mast cell degranulation and phospholipase A_2 activation. A family of structurally similar peptides, the magainins have been described in the skin of frogs from several species [Zasloff, 1987]. The magainins are thought to act as antibiotics by permeabilization of membranes of prokaryotes [Zasloff et al., 1988].

All of the peptides of the class L consist entirely of an amphipathic helix. The class L helices have high hydrophobic moments and are highly positively charged. There are two clusters of positively charged aminoacid residues in the polar face which is narrower (<100°) than in most of other classes. The charged residues are mostly lysines.

It is worth mentioning that melittin, an extensively studied amphipathic lytic peptide from bee venom, does not belong to the class L, since its sequence most closely resembles that of transmembrane proteins (class M) [Segrest et al., 1990].

1.2.2 Model peptides as an approach for studies of peptide-membrane interactions

With advances in peptide synthesis, model peptide approaches become popular for a wide range of applications, including studies of amphipathic peptide-membrane interactions. The concept of an amphipathic α–helix provides a framework for understanding the structure-function relationships among natural peptides and proteins. Comparison of natural and synthetic model peptides provides a test of the relevance of putative amphipathic structures for peptide activities. Also the concept of amphipathic α–helix renders an approach for *de novo* design of peptides with desired properties.

Several different approaches to the design of model amphipathic peptides were used in a number of applications. A minimalistic approach has been used to design lytic peptides with only Lys and Leu residues [Cornut et al., 1994; 1996]. A more conservative approach than complete *de novo* design is to introduce substitutions of one or several

residues in natural sequences. For example, series of magainin analogs were designed to have variation only in hydrophobicity, only in charge or only in hydrophobic moment [Dathe et al., 1996, 1997]. To test the importance of helix formation, helix breaking D aminoacid residues were introduced at various positions of potential amphipathic helix [Wieprecht et al., 1996; Shai and Oren, 1996; Oren et al., 1997]. All D peptides are usually synthesized to prove that some particular peptide activity is not mediated by a protein receptor. (However, it was reported that somehow calmodulin interacts with amphiphilic peptides (class K) composed of all D-amino acids [Fisher et al., 1994]). An interesting approach to study peptide membrane binding and self association is to introduce fluorescent probes [Rapaport and Shai, 1994], or to use tryptophan as an intrinsic fluorescent probe and move it around the peptide sequence [Matsuzaki et al., 1994]. An example of more sophisticated use of model peptides is the successful modelling of several ion channels physiological characteristics by a cross-linked bundle of synthetic peptides corresponding to amphipathic sequences from transmembrane sections of these proteins [Oblat-Montal et al., 1993; Grove et al., 1993].

Classification by Segrest et al. (1990) can serve as a natural start for model studies. Jones et al. (1992) suggested an algorithm for averaging a series of superimposed aminoacid sequences. Based on this analysis, an archetypical peptide analog of class L amphipathic helices, 18L (GIKKFLGSIWKFIKAFVG, Fig. 1.2.2.1), has been designed *de novo* [Tytler et al., 1993]. A series of class L peptide analogs was designed and synthesized in which (i) the bulk of interfacial amino acids changed; (ii) the bulk of positive residues was increased by dimethylation of Lys residues or by replacing the Lys residues with Arg;

or (iii) the angle subtended by the polar face was changed. Several modifications of 18L peptide were used to assess the importance of the glutamic acid residue in the centre of hydrophobic sequence [Tytler et al., 1995]. The motif of the class L sequence was also modified by designing an amphipathic helical peptide, K18L, in which the cluster of glycine residues was removed from the polar face of the amphipathic helix [Epand et al., 1993].

An archetypical peptide analog of class A amphipathic helices, 18A (DWLKAFY-DKVAEKLKEAF, Fig. 1.2.2.1), has been designed *de novo* [Anantharamaiah et al., 1985]. 18R peptide, a modification of 18A differing in radial charge distribution, but still overall zwitterionic, was used to asses the importance of charge distribution [Epand et al. 1989, 1987; Anantharamaiah et al., 1985]. Since 18A is essentially a fragment from an apolipoprotein sequence, a tandem repeat of 18A sequences was synthesized and used in a number of studies of membrane interactions [Mishra et al., 1995; Anantharamaiah et al., 1985; Srinivas et al., 1990; Chung et al., 1985]. Peptides with Lys substituted for Arg were used to obtain evidence for the snorkel hypothesis [Mishra et al., 1994]. The acetylamide derivative (Ac-18A-NH_2) of the 18A peptide have been shown to mimic better the properties of apolipoproteins [Venkatachalapathi et al., 1993], since this blocked peptide has a more stable α–helical structure because of the removal of the unfavourable charge-helix dipole interactions.

This brief overview of approaches to the design of model peptides for studies of peptide membrane interactions was not intended to be comprehensive, but rather to introduce background on 18L and 18A (Ac-18A-NH_2) peptides, whose membrane interac-

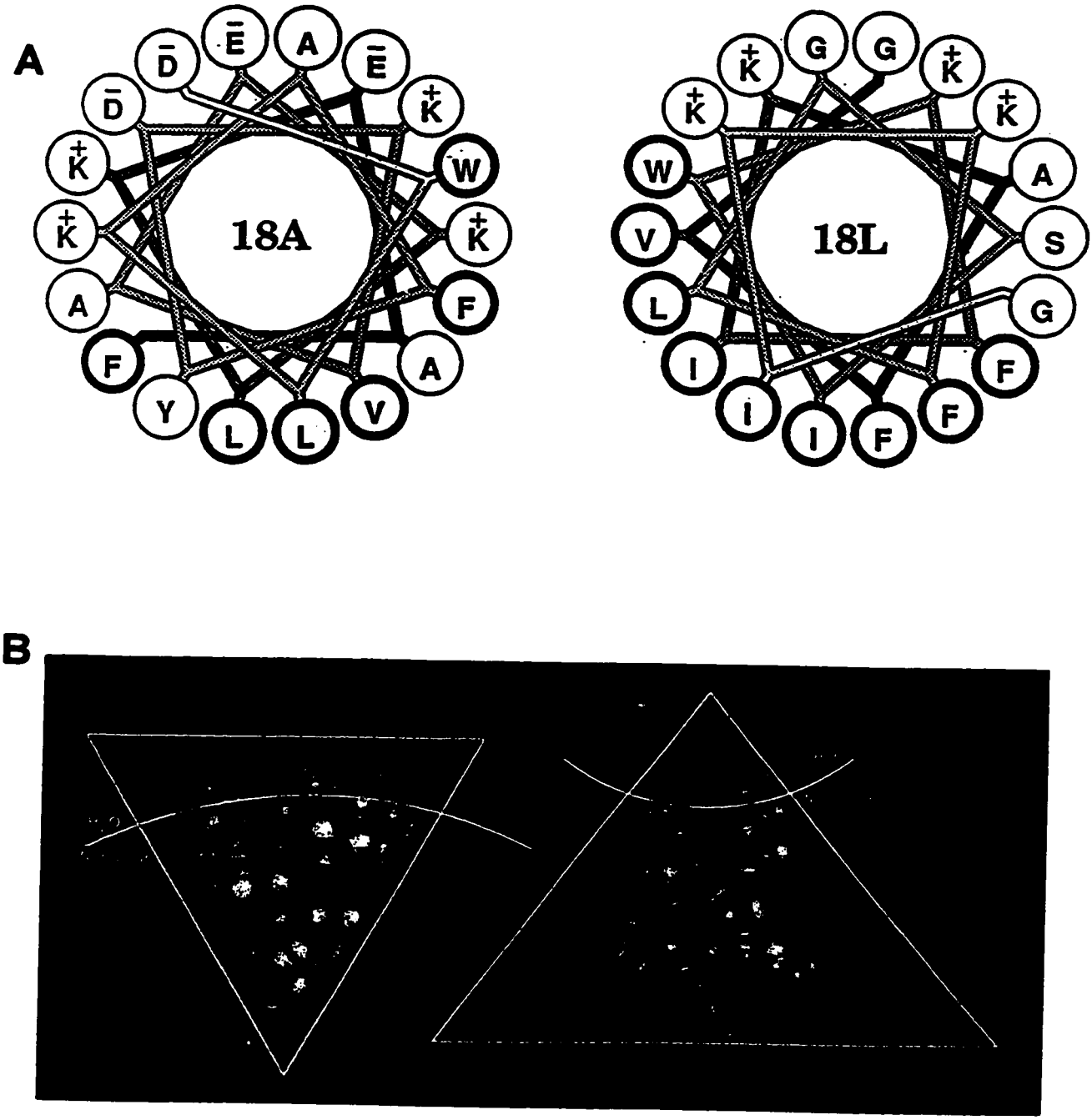

Figure 1.2.2.1. **A.** "Schiffer-Edmundson" helical wheel diagrams of 18A (DWLKAFYDKVA-EKLKEAF) and 18L (GIKKFLGSIWKFIKAFVG), the archetypical peptides of class A and class L respectively.

B. Molecular models of 18A and 18L illustrating positive monolayer curvature caused by class A and negative monolayer curvature promoted by class L peptides. Projection along the axis of the α–helix. From Tytler et al., 1993.

tions were extensively studied in this work. The amino acid sequence and helical wheel representation of 18L and 18A (Ac-18A-NH_2) peptides are shown in Figure. 1.2.2.1.

1.2.3 Reciprocal effect of class A and class L peptides

It has been found previously that class A and class L peptide analogs have an opposing activity on a number of biological phenomena such as erythrocyte lysis or neutrophil activation (Tytler et al., 1993). This opposing activity was not mediated by a protein receptor and was related to the different effects of class A and class L peptides on the biomembranes. Experiments with model peptides were conducted in order to understand molecular mechanism responsible for this opposing effect.

It was previously suggested to use the shift in the temperature of L_α-H_{II} phase transition (T_H) measured by DSC as a general approach to determination of effects of any membrane active substance on intrinsic monolayer curvature or non-bilayer phase propensity of the membrane and correlate this with its functional activities. This approach have been used successfully for a number of low molecular weight membrane modulators [Cheetham, 1993] and was extended to the studies of peptide-membrane interactions [Tytler et al., 1993].

Experiments on the T_H shift of dipalmitoleoylphosphatidylethanolamine (DPoPE) from bilayer to hexagonal phase were performed with series of class A (including apolipoprotein A-I) and class L peptides. This lipid was chosen, because it's T_H = 43.5 °C is relatively low and thus effects are not complicated by temperature denaturation of peptides. class A helices were shown to increase and class L to decrease the T_H, thus they were denoted as bilayer stabilisers or destabilisers, respectively, and their effects were

correlated with molecular shapes of A and L helices (Figure 1.2.3.1) and their effects on intrinsic monolayer curvature. On a weight basis 18L and Ac-18A-NH_2 peptides were found to cause the largest shift of T_H among other natural and model peptides. Thus they were chosen for further studies.

While easily observed with biological membranes, reciprocal effects of the A- and L- helices are not ubiquitous. Membrane permeabilization, the major activity of lytic peptides is usually modelled by the vesicles aqueous content leakage assays. Comparing leakage inducing activities of 18L and Ac-18A-NH_2, we found that these peptides had a pronounced reciprocal effect on the contents leakage from Me-DOPE vesicles. However, effects of simultaneous peptide addition were approximately additive for other lipids. We decided to study this more thoroughly, considering that understanding the lipid requirements for observation of reciprocal effects in model membranes can shed some light on the physical properties of biological membranes. Reciprocal effects of 18L and Ac-18A-NH_2 on the leakage of LUV aqueous content, on 18L-induced vesicle fusion, and 18L-induced conductance activities in planar bilayer membranes were studied in model systems of varied lipid composition.

Equilibrium and kinetic peptide membrane binding studies were performed as a prerequisite for the study of reciprocal effects in order to better understand the molecular events in the course of peptide-lipid interactions. Parallel studies of the binding behaviour of two peptides with both similar and distinctly different properties also added to a fundamental understanding of the kinetics and thermodynamics of peptide-lipid interactions. Possible biological implications of the described features of peptide-membrane interactions are discussed.

The study of reciprocal peptide activities also necessitates in depth study of mechanism of these activities. Generally membrane interactions of class A helices are better characterised better, so we focused more on detailed studies of the mechanism of 18L-induced membrane permeabilization.

1.2.4 Mechanism of membrane permeabilization by class L peptides

Basic modes of amphipathic peptide-membrane interactions have been described in Epand et al. (1995). Two major modes have been discussed regarding the mode of membrane permeabilization by L class amphipathic peptides: pore formation of helical clusters or increasing the negative intrinsic monolayer curvature strain. Roughly this distinction correlates with a primarily aggregated (transmembrane "barrel" state) or a mostly monomeric (parallel to the surface) state of the membrane bound peptide. The concept of peptide oligomerization for the pore formation is useful to explain membrane permeabilization observed at extremely low peptide - lipid ratios, in the range of several peptide molecules per vesicle. Contrary to that, if peptide induces membrane permeabilization in the same range of peptide-lipid ratios as it affects the lipid phase behavior, then one can not ignore the effect of peptide monomers. In practice, distinction between these two alternatives is complicated as both mechanisms can contribute to membrane permeabilization.

The proposal of peptide oligomerization as the main mechanism of membrane permeabilization by cationic L-class amphipathic peptides is mostly based on conductance measurements of lipid membranes. However, there is some controversy about such an

arrangement of cationic peptides in the membrane. For example, channels formed by mastoparan were found to be weakly cation selective, which was surprising for a helix bundle with a cationic interior [Mellor and Sansom, 1990]. Similar findings were observed with other peptides [for review Duclohier, 1994]. In the case of magainin 2, Cruciani et al. (1992), speculate about various alternative discrete arrangements, including lipid headgroups in the channel lining. Conductance measurements in bilayer membranes require a very stable bilayer and membrane potential and thus they do not necessary correlate with vesicle permeabilization experiments. Kerr et al. (1995), have recently shown that the haemolytic activity of a series of analogous peptides does not correlate with their channel-forming properties. Numerous studies of L-class peptides, such as magainin 1 and 2, reported that α-helices are oriented parallel to the surface of the membrane even at the leakage inducing peptide-lipid ratios [Matsuzaki et al., 1994; Bechinger et al., 1993]. Recently Matsuzaki et al. (1996) proposed that lipid molecules are incorporated in the peptidic pore, suggesting the importance of the lipid component of the membrane for permeabilization. Support for inclusion of lipid molecules in the pore formed by magainin also came from recent neutron scattering experiments [Ludtke et al., 1996]. Permeabilization induced by peptide membrane destabilisation ultimately will also occur through the aqueous pores across the membrane, however these pores are likely to be transient structures with flickering diameter and the necessary inclusion of lipid molecules in the pore structure. Naturally, peptide-induced membrane destabilisation defects are likely to include peptides in the pore lining. Pores induced by membrane destabilisation are likely to be strongly affected by intrinsic monolayer curvature strain and thus be highly dependent

on the lipid composition. However, intrinsic monolayer curvature strain, can also influence the activity of established peptidic pores, such as alamethicin (Keller et al., 1993). These considerations illustrate the complications in distinguishing pure peptidic pore formation and membrane destabilisation as modes of membrane permeabilization.

There have been relatively few systematic studies of lipid effects on the lytic activities and membrane binding properties of amphipathic helical peptides In this thesis we studied the mode of 18L-induced membrane permeabilization in various lipid systems and found it to be strongly lipid dependent. We discuss possible mechanisms of peptide-membrane permeabilization in various lipid systems.

1.2.5 Amphipathic peptides effects on lateral membrane organization

It is often supposed that lateral organization can be induced by membrane proteins or peptides [Chapter 1.1.3]. The greatest attention has been drawn to the possibility of domain formation by transmembrane hydrophobic α-helical segments via the hydrophobic mismatch or "mattress" mechanism [Davis et al, 1983; Mouritsen and Bloom, 1993]. Also there were several works on membrane segregation induced by peripheral proteins or by water soluble poly-L-lysin whose membrane association is primarily of an electrostatic nature. Less is known about peptides inserting parallel to the surface of the membrane which is often the case for amphipathic α-helical peptides.

In this thesis, there were studied effects on membrane lateral organization of two, described above [Chapter 1.2.2], model amphipathic peptides, 18L and Ac-18A-NH_2. Activities of these peptides are affected by membrane composition, namely by the presence

of acidic or nonbilayer forming lipids. While acidic lipids similarly increase activities of both peptides, the presence of nonbilayer forming lipids enhances the lytic activity of 18L and decreases that of Ac-18A-NH_2 [Chapter 3.4]. These properties, taken together with high membrane affinity, make these peptides an interesting choice for examining general peptide effects on the lateral organization of lipid membranes.

In studies of peptide effects on membrane organization we used anthrylvinyl- and perylenoyl-labelled lipid-specific fluorescent probes [Chapter 1.1.3.1].

We studied peptide effects on lipid mixing in a miscible fluid phase as well as peptide effects on preexisting domain structure as well as and peptide effects on the gel-to-liquid phase transition. Competition between charge-charge interactions, peptide preference for fluid phase lipid and/or effects of peptide geometric characteristics (shape) were evaluated. We discuss peptide effects on lateral membrane organization in the general context of peptide membrane interactions.

2. Materials and Methods

2.1 Materials

Details of the synthesis and characterization of the peptides have been described elsewhere [Tytler et al., 1993; Venkatachalapathi et al., 1993]. Peptides were synthesized by the solid phase method using t-BOC chemistry. Peptides were cleaved from the resin using anhydrous HF and purified by reverse phase HPLC [Anantharamaiah, 1986]. The following peptides were used in the work: 18L,

GIKKFLGSIWKFIKAFVG [Tytler et al., 1993]; K18L, KWLLKFYKLVAKLLLKAF [Epand et al. 1993]; 18A, DWLKAFYDKVAEKLKEAF; Ac-18A-NH_2, N-Acetyl-DWLKAFYDKVAEKLKEAF-amide [Venkatachalapathi et al., 1993].

DOPC, DOPE, DMPG, DOPG, Me-DOPE, diPhyPC, NBD-PE and NBD-PC were purchased from Avanti Polar Lipids (Alabaster, AL) and were used without further purification. 1-acyl-2-[*trans*-12-(9-anthryl)-11-dodecenoyl]-*sn*-3-glycerophosphocholine (APC) and 1-acyl-2-[9-(3-perylenoyl)nonanoyl]-*sn*-3-glycerophosphocholine (PPC) were synthesized as previously reported [Molotkovsky et al., 1979], and were kindly provided by Dr. Jul. Molotkovsky. Aminonaphthalene-3,6,8-trisulfonic acid (ANTS), *p*-xylenebis-(pyridinium bromide) (DPX), 3-3'-diethylthiacarbocyanine iodide (diSC_2(5)), terbium III chloride (Tb) and dipicolinic acid (DPA) were obtained from Molecular Probes (Junction City, OR). Fluoresceinisothiocyanate-labelled dextran (FITC-dextran) M.W. 20,000, 10,000 and 3,000 and valinomycin were purchased from Sigma Chemical Co (St. Louis, MO). Lubrol and Triton X-100 were purchased from Calbiochem (San Diego, CA). All other reagents were of analytical grade. Buffers were prepared in double distilled deionized water.

2.2 Liposome preparation

Multilamellar vesicles (MLV) were made from vacuum dried lipid films by suspending them in an appropriate buffer (20 mM Tris-HCl, 1 mM EDTA, 0.02% NaN_3, pH 7.4, unless otherwise stated) followed by shaking and less than 20 seconds of low power sonication. Large unilamellar vesicles were made by multiple extrusion of MLV through

two stacked 100 nm pore polycarbonate filters (Nucleopore Corp., Pleasanton, CA). Lipid concentration of the vesicles was determined using a phosphate assay [Ames, 1966].

2.3 Fluorescent measurements

2.3.1 Hardware

Fluorescence experiments were done on an SLM AB-2 fluorometer (Urbana, IL). Unless otherwise stated, measurements were done in 3 ml quartz cuvettes with stirring and thermostated at 25°C. Temperature of the sample was monitored by a thermistor probe inserted in the cuvette. In temperature scanning expertiments, heating and cooling was performed linearly with time with simultaneous recording of temeperature and fluorescence data. Anisotropy of fluorescence of APC, APE and APG probes was measured in the L-format with excitation at 365 nm and emission at 435 nm. Positions of polarizers were changed automatically using the AB-2 SLM Aminco software.

To avoid light-scattering artifacts appropriate photofilters have been used both on the excitation and emission whenever fluorescence signal had been monitored at fixed wavelengths. This correction was essential at the conditions of low fluorescence intensity and in the measurements of anisotropy of fluorescence.

For resolution of fast kinetic processes we used a stopped-flow accessory for the SLM-Aminco AB-2, with a time resolution of up to 1 ms, and a time delay of 2 ms.

2.3.2 Fluorescence spectra acquisition

A number of fluorophors have been used in this work. Peptide tryptophan fluorescence was used to monitor association of peptides with membranes, peptide

self-association in buffers and peptide effects on lateral membrane organization. Tryptophan fluorescence spectra were recorded in the range of 310-480 nm with excitation at 280 nm and bandwidths of 4 nm for both excitation and emission. Excitation at 280 nm was chosen to reduce overlap with the water Raman sctattering peak. Perylenoyl spectra have been used for estimates of water permeability and/or water content of the bilayer [Molotkovsky et al., 1987]. Perylenoyl fluorescence was excited at 435 nm and recorded from 470 to 600 nm. Anthrylvinyl fluorescence was excited at 365 nm and recorded from 390 to 480 nm. Background was routinely subtracted. More complex correction of spectra was unnecessary since lipid concentrations used in the experiments were below 0.2 mM in order to reduce scattering artifacts.

Fluorescent spectra of other fluorophors (ANTS, Tb^{3+}/DPA, FITC, $diSC_2(5)$ and NBD) were used only for the control of positions of corresponding maximums of excitation and emission.

2.4 Fluorescence resonance energy transfer (FRET)

2.4.1 FRET determination and efficiency calculations

The conventional method of presenting data on fluorescence resonance energy transfer is via calculating transfer efficiency (E). According to Lakowicz (1983) $E = (I_o - I)/I_o$ where I_o is the fluorescence intensity of donor in the absence of acceptor and I - intensity in the presence of acceptor. This formula can be applied directly, if it is possible to measure fluorescence intensity of donor in the absence of acceptor. This approach was used for the

calculation of efficiency of FRET from anthrylvinyl- to perylenoyl-labelled phospholipid in the peptide titration experiments. To eliminate FRET, we added the detergent Triton X-100 to dilute the phospholipids. The control experiments show that solubilization with Triton X-100 does not significantly change the integral intensity of the unquenched anthrylvinyl-labelled fluorophor. For the calculation of fluorescence resonance energy transfer from the anthrylvinyl probe to the perylenoyl probe fluorescence emission spectra were excited at 365 nm and recorded in the range from 390 nm to 600 nm. Background due to scattering and direct excitation of perylenoyl probe was routinely subtracted.

The approach described above was not suitable for the studies of FRET from peptide tryptophan to the anthrylvinyl probe (APC, APE, or APG) as tryptophan fluorescence is more sensitive to the polarity of the environment and also at 280 nm commercially available detergents have a high background fluorescence and/or absorption. Efficiency of FRET from the peptide to the anthrylvinyl probe was calculated from consecutive fluorescence emission spectra, excited at 280 nm and recorded in the range from 310 nm to 480 nm. These spectra were then fitted with the sum of peptide and probe fluorescence components and the transfer efficiency was calculated as:

$$E = (I_a/Q_a)/(I_t + I_a/Q_a)$$

where I_a is integral intensity of anthrylvinyl fluorescence, Q_a - quantum yield of anthrylvinyl fluorescence and I_t integral intensity of peptide fluorescence. The quantum yield of anthrylvinyl fluorescence is ~ 0.59 as reported by Johansson et al. (1990).

In the temperature scanning experiments, changes in FRET from peptide tryptophan to the anthrylvinyl probe were monitored by measuring fluorescence intensity with excitation at 280 nm and emission at 435 nm using 4 nm monochromator slits.

The temperature dependence of peptide induced lateral organisation was calculated from the efficiency of APL/PPC FRET in the experiments which simultaneously monitored fluorescence intensities with excitation at 365 nm and emission at 510 nm and 435 nm using 4 nm monochromator slits. Efficiency was determined as

$$E=(I_p/Q_p)/(I_a+I_p/Q_p)$$

where I_a intensity of anthrylvinyl fluorescence (435 nm), Q_p- quantum yield of perylenoyl fluorescence (~ 0.65, according to Molotkovsky et al., 1984) and I_p intensity of perylenoyl fluorescence (510 nm).

2.4.2 Surface increase calculation

As had been shown by Fung and Stryer (1978) in the case of randomly distributed donor and acceptor in one plane, FRET efficiency is defined as

$$E = 1 - \frac{1}{\tau_o} \cdot \int_0^\infty \exp\left(\frac{-t}{\tau_o}\right) \cdot \exp\left(-\sigma_a \int_a^\infty \left[1 - \exp\left(-\left(\frac{t}{\tau_o}\right)\left(\frac{R_o}{r}\right)\right)^6\right] 2\pi r dr\right) dt$$

where R_o is the Foerster radius for the donor-acceptor pair, σ_a is the surface density of the acceptor, τ_o is the fluorescence lifetime of donor in the absence of acceptor and **a** is the distance of the closest approach of donor and acceptor. The second exponent in the equation is the energy transfer term. Efficiency is independent of the surface density of the donor, and it is not very sensitive to **a**. Quantitative integration [Fung and Stryer, 1978] shows that for a Foerster radius (R_o) within 20-60 Å, up to E ~ 0.4, efficiency is

approximately proportional to the surface density of acceptor (σ_a), that is $E \propto \sigma_a$. This also can be shown more rigorously. Taking into account following relationships:

$$\sigma_a = s_l \times (n_a/n_l)$$

$$\Delta S = s_p \times p \quad \text{and} \quad S_o = s_l \times l$$

where s_l is the surface area of one lipid molecule, s_p - surface increase due to membrane incorporation of one peptide molecule, n_a/n_l - molar fraction of acceptor molecules in the membrane, ΔS - change in membrane surface (S_o), p - peptide concentration, l - lipid concentration, ΔE - change in FRET efficiency (E_o). We have at linear approximation:

$$\Delta E/E_o = -\Delta S/S_o = -s_p/s_l \times p/l$$

That is the slope of the initial linear part of the plot of $\Delta E/E_o(p/l)$ will give the ratio of surface increase due to one peptide compared to that produced by one lipid molecule.

2.5 Kinetics of peptide binding to liposomes

The time course of binding was monitored by the increase in peptide tryptophan fluorescence at 330 nm upon membrane binding. Fluorescence was measured using a stopped-flow accessory for the SLM-Aminco AB-2, with a time resolution of up to 1 ms, and a time delay of 2 ms. To improve signal-to-noise ratio we averaged at least five consecutive runs. Fluorescence was measured at excitation and emission wavelengths of 280 and 330 nm respectively, and 4 and 8 nm slits.

Alternatively, binding kinetics was monitored using fluorescence energy transfer from the peptide tryptophan to anthrylvinyl fluorophor embedded in the hydrophobic

core of the bilayer. Liposomes (LUV) for this assay contained 2 mol % of 1-acyl-2-[*trans*-12-(9-anthryl)-11-dodecenoyl]-*sn*-3-glycero-phosphocholine (APC). Measurements were done with the same stopped-flow accessory. Fluorescence was measured at excitation and emission wavelengths of 295 and 435 nm respectively, and 4 and 16 nm slits and using a 390 nm cut-off filter in the emission beam to reduce light scattering effects.

2.6 Membrane permeability assays

2.6.1 Leakage of aqueous content. ANTS/DPX assay

The ANTS/DPX assay [Ellens et al., 1984], dequenching of ANTS released into the medium, was used to monitor leakage induced by peptide interaction with vesicles. Multilamellar vesicles (MLV) were made in buffer (20 mM Tris-HCl, 1 mM EDTA, 0.02% NaN_3, pH 7.4) containing 12.5 mM ANTS and 45 mM DPX. The pH of the buffer was adjusted after dissolution of ANTS and DPX. LUV were prepared by extrusion as described above. Vesicles with encapsulated contents were separated from the media on a Sephadex G-75 column equilibrated with buffer containing 25 mM NaCl for osmotic strength compensation. Vesicles were used within 1-2 days, however, no spontaneous leakage was observed within at least one week of storage of the vesicles at 4°C. Leakage was monitored by following the increase of fluorescence intensity at 530 nm using 360 nm excitation and bandwidths of 2 and 16 nm for excitation and emission, respectively. A UV bandpass filter was used on the excitation side, and a 390 nm cut-off filter on the emission

side were used to diminish scattered light. Leakage was initiated by injection of 100-200 μl of a vesicle suspension of desired lipid concentration into a cell with 2 ml of a dilute peptide solution. Injection of peptide into vesicles was found to be less reproducible because of fast peptide binding to the membrane and transient high local peptide concentrations [Polozov et al., 1994b]. The 100% leakage level was determined by vesicle disruption after the addition of 50 μl of 10% Lubrol. Fluorescence increase from background to 100% leakage was more than 10-fold.

2.6.2 Dissipation of membrane electrical potential

An assay for the presence of an electrical membrane potential [Loew et al., 1985] was used in order to determine if there is any loss of potential at peptide/lipid ratios below those at which ANTS leakage occurs. The typical experiment was performed as follows: LUV were prepared by extrusion of MLV made in buffer containing 100 mM KCl, 20 mM Tris-HCl, pH 7.4. 3 μl of vesicle suspension was diluted into 2.50 ml of isosmotic, K^+-free buffer containing 3 μM of carbocyanine dye $diSC_2(5)$, at a total lipid concentration of 20 μM. A membrane potential was established by the addition of 1 nM valinomycin. Fluorescence was monitored with excitation at 620 nm and emission at 670 nm. Addition of valinomycin results in 98% fluorescence quenching in about three minutes, which is stable for about 2 hours and which can be reversed by the disruption of vesicles with detergent. Potential release was initiated by injection of a constant volume (500 μl) of dilute peptide solutions in K^+-free buffer. This mode of mixing was found important for reproducibility of the assay. The percent of fluorescence restored, at the probe and lipid

concentrations used, corresponds to the percent of vesicles with completely released potential.

2.6.3 Leakage of aqueous content. FITC-Dextran assay

FITC-Dextran, of molecular weight 3,000, 10,000 and 20,000 (Sigma, MO) was encapsulated into vesicles at self-quenching concentrations - 4 mM for M.W. 20,000, 8 mM for M.W. 10,000 and 25mM for M.W. 3,000. Vesicles were separated from unencapsulated material by passing vesicles through a Sephacryl S-300 HR column equilibrated with buffer containing 40 mM NaCl. Internal and external media were isosmotic. Increase of fluorescence upon release of FITC-dextran into the media was used for an estimate of the size of the defects formed by peptides. In order to compare results with the potential release assay, the mode of peptide vesicle mixing was the same as that used in the potential release assay. Initial vesicle fluorescence intensity, corrected for dilution, was taken as zero leakage. 100% leakage was obtained by disruption of vesicles with detergent, 30 μl 10% (w/v) Lubrol. The increase of fluorescence intensity from 0% to 100% leakage was approximately 3-fold. According to the supplier's data the average Stokes radius of the FITC-Dextrans is 3.3 nm, 2.3 nm and 1.4 nm for molecular weights 20,000, 10,000 and 3,000, respectively.

2.6.4 Membrane permeability assay. NBD-PC/DT

We used the following assay to assess the permeability of the membrane a long time after peptide addition. LUV labelled inside only with NBD-PC (~ 0.5%) were prepared from symmetrically labelled LUV (1% NBD-PC) by short time (2 min) incubation of LUV with 10 mM sodium dithionite (DT) followed by vesicle separation from the media

by gel filtration or by 200 times dilution with subsequent overnight storage at 4 °C for total dithionite deactivation (modified from McIntyre and Sleight (1991)). Dithionite solution was used freshly prepared and stored on ice, the pH of the solution was adjusted with NaOH to 7.4. For analysis of membrane permeability vesicles were mixed with peptide at a certain peptide/lipid ratio. After preincubation with peptide for a fixed time, 10 mM DT is added. Membrane permeability to dithionite was monitored by reduction of NBD-fluorescence measured with excitation at 468 nm and emission at 535 nm using 4 nm monochromator slits. Percent of NBD fluorescence reduction was determined at 10 minutes after dithionite addition. Permeability values have been corrected for lipid (NBD-PC) translocation to the outside of the membrane [Chapter 2.11]. Values for lipid translocation had been obtained by determination of percentage of reduction of NBD-PC in vesicles which were preincubated with trypsin before DT addition. Percent of NBD fluorescence reduction depends on the percent of permeable vesicles. Both ANTS/DPX and NBD-PC/Dithionite assays would report similarly for the all-or-none mechanism of leakage, but in the case of gradual leakage, then slow leakage of all of the vesicles would not result in complete dequenching of ANTS. In contrast it would still result in complete reduction of NBD-PC, although with lower rate.

2.7 Fusion assays

2.7.1 Lipid mixing fusion assay

The APC/PPC donor-acceptor pair was used for monitoring lipid mixing. Vesicles were labelled by APC and PPC by mixing stock solutions of lipid in chloroform. APC and

PPC do not transfer spontaneously between vesicles; they do not segregate in separate phases in fluid lipid bilayers and they do not have a charged fluorophor which can affect peptide- membrane interactions [Bergelson et al., 1985; Polozov et al., 1994a]. All of the above makes this pair convenient for monitoring membrane fusion. Vesicles labelled with 2% APC and 1% PPC were mixed with unlabelled vesicles at a ratio of 1:10. Fusion was initiated by injection of a vesicle suspension into the peptide solution in the fluorescence cell, with stirring. Lipid mixing results in dequenching of APC fluorescence. Fusion was monitored by the increase of fluorescence emission at 434 nm using an excitation wavelength of 370 nm (slits 8 nm and 4 nm, respectively). To reduce scattering effects an ultraviolet bandpass filter was used in the excitation beam and a yellow cut-off filter (390 nm) was used on emission. Complete dequenching of APC fluorescence was obtained by the addition of excess detergent (50 µl 10% Triton X-100). Control experiments showed that disruption of APC-labelled vesicles did not affect APC fluorescence.

2.7.2 Aqueous content mixing fusion assays

Both the ANTS/DPX quenching assay [Ellens et al., 1985] and the Tb/DPA complex formation assay [Wilschut et al., 1980] have been used to measure membrane fusion by the mixing of aqueous contents. We employed the Tb/DPA assay to avoid artefacts caused by vesicle aggregation. LUV were prepared by the extrusion procedure. The vesicles were made either in 2.5 mM $TbCl_3$ and 50 mM sodium citrate or in 50 mM DPA (sodium salt) and 20 mM NaCl. In addition the media contained 2 mM L-histidine and 2 mM TES adjusted to pH 7.4. Vesicles were separated from unencapsulated material by gel filtration on a Sephadex G-75 column eluted with 100 mM NaCl, 2 mM L-histidine, 2

mM TES, pH 7.4. Fusion was initiated by injection of LUV into the fluorescence cell containing the peptide solution. The sample was excited at 276 nm and the fluorescence emission was measured at 545 nm. Tb^{3+} itself does not fluoresce significantly. An increase in fluorescence occurs upon Tb/DPA complex formation due to intermolecular energy transfer. Vesicle aqueous contents mixing was followed as an increase in fluorescence.

For the ANTS/DPX aqueous contents mixing assay, LUV containing either 25 mM ANTS or 90 mM DPX were prepared separately by the extrusion procedure. Both solutions were buffered with 20 mM Tris-HCl, pH 7.4. Vesicles were separated from the unencapsulated material on a Sephadex G-75 column, equilibrated with the Tris buffer containing 25 mM NaCl added for osmotic compensation. Fluorescence measurements were conducted with the same settings as for the ANTS/DPX leakage assay. Fusion was monitored by the decrease in ANTS fluorescence. DPX is capable of significantly quenching ANTS fluorescence only in the millimolar range of concentrations, i.e. at conditions of vesicle aqueous contents mixing. DPX released into the media did not affect ANTS fluorescence, as was confirmed by detergent disruption.

2.8 Electron microscopy

Vesicles and peptide-lipid complexes were visualised using the electron microscope. For freeze-fracture electron microscopy 20% glycerol had been added to vesicle suspensions to ensure amorphous freezing. The lipid concentration was 15 mM. Samples (4 µl) were quenched on gold alloy planchets in a slurry of ethane cooled with liquid nitrogen. Freeze-fracture replicas were prepared by platinum shadowing in a Balzers

BAF 301 apparatus equipped with electron beam guns. Replicas with traces of lipids removed were picked up on the grids and viewed in a JEOL electron microscope.

2.9 Bilayer conductance measurements

Planar lipid bilayers were formed across a hole in a Teflon film sandwiched between Teflon blocs containing 2-ml reservoirs, according to Mueller and Rudin, 1968. Lipid bilayers were formed by painting a solution of lipid in hexadecane onto a 0.1 mm diameter hole, pre-treated with hexadecane, and waiting for the solution to thin as was determined electrically by an increase in capacitance. The lipid used for the formation of bilayers was diphytanoylphosphatidylcholine (diPhyPC) which is known for its ability to form stable BLMs [Redwood et al., 1971] free of 'channel-like' artefacts. The buffer employed was 2 M KCl, 10 mM Tes, pH 7.4. Peptide solution in distilled water (0.1 mg/ml) was added to one side only (designated as *cis*). Currents were detected and amplified with an Axopatch amplifier and were recorded on the computer. Current records were filtered at 2 kHz.

2.10 Titration calorimetry

Isothermal heats of reaction of were measured using the Omega cell of a Microcal titration calorimeter [Wiseman et al., 1989]. Solutions were degassed under vacuum prior to use. LUV (200 μM) were placed in the 1.3 ml reaction cell and thermally equilibrated prior to use. A 0.5 mM solution of peptide was made in the same buffer as the LUV (20 mM Tris-HCl, 1 mM EDTA, 0.02% NaN_3, pH 7.4). Peptide was delivered in 10 μl aliquots from a 100 μl motor-driven syringe. Injections were made

at 4 min intervals with continuous stirring (350 rpm). The observed enthalpies were corrected for the heat of dilution of buffer into the vesicle suspension. The calorimeter was calibrated electrically.

2.11 Assay on lipid flip-flop and membrane asymmetry

To assess peptide effects on lipid flip-flop and bilayer asymmetry we used dithionite reduction of NBD-PC fluorescence modified from McIntyre and Sleight (1991). The assay is based on incorporation of NBD-labelled phospholipids into the membrane and reduction of NBD by dithionite, which results in formation of nonfluorescent ABD on the surface accessible for dithionite. Both lipids labelled by the head group or by the acyl chains can be used. It is possible to prepare vesicles labelled symmetrically, inside only or outside only. Change in probe distribution is indicative of the flip-flop rates in the membrane. LUV labelled inside only with NBD-PC (~ 0.5%) were prepared as described above [Chapter 2.6.4]. Vesicles were mixed with peptide at the certain peptide/lipid ratio, after preincubation with peptide for a fixed time trypsin was added to stop peptide-induced membrane permeabilization. After approximately 3 minutes incubation of vesicles with trypsin 10 mM sodium dithionite (DT) is added. NBD-fluorescence was measured with excitation at 468 nm and emission at 535 nm using 4 nm monochromator slits. Percent of NBD fluorescence reduction, determined at 10 minutes after dithionite addition, was considered to correspond to the percent of lipid probe translocation to the outer leaflet of the bilayer. Lipid redistribution from the outer to the inner monolayer was assessed using LUV outside only labelled with NBD-PC. This LUV

were prepared by incubation of unlabelled vesicles with NBD-PC dissolved in ethanol. Injection of lipid ethanol solution in buffer has long been known to result in fast spontaneous formation of vesicles [Batzri and Korn, 1973]. This spontaneous formation of NBD-PC only vesicles was reduced by fast stirring condition and by usage of relatively dilute NBD solution and high residual concentrations of ethanol up to 10%. Vesicles were then incubated overnight and subsequently dialyzed to remove ethanol. More than 95% of NBD was restricted to the outer leaflet. Since fluorescence in probe-only vesicles is strongly self-quenched, we used the absence of a fluorescence increase upon vesicles disruption with excess detergent as a control of the absence of probe-only vesicles.

2.12 Osmotic strength measurements

Osmotic strength of buffers was measured using a freezing point depression micro-osmometer, Avanced Micro-Osmometer 3MO Plus (Advanced Instruments, Norwood, MA). Relatively low osmotic strengths have been used in this work. Thus osmotic strength was linearly dependent on solute concentrations. Empirical calibration curves have been used for conversions of concentration to osmotic strength in titration experiments.

3. Results and Discussion

3.1 Membrane Binding Properties of Amphipathic Peptides

3.1.1 Peptides in water and solvents

Fluorescence spectra of the peptides, Ac-18A-NH_2 and 18L, in water were found to be the same with a fluorescence maximum at 351 nm. The total intensity of fluorescence was found to be proportional to peptide concentration up to 200 μM, and higher if corrected for inner filter effects both in water and methanol (Figure 3.1.1.1). This is indicative that these peptides do not undergo aggregation in this range of concentration and exist as monomers in water as well as in methanol. This is consistent with the previous CD studies of Ac-18A-NH_2 which showed that the peptide in buffer exists essentially as a random coil [Venkatachalapathi et al., 1993].

While soluble in water, both 18L and Ac-18A-NH_2 peptides are poorly soluble in hydrophobic organic solvents such as hexane. Binding of peptides to membranes is accompanied by a blue shift of tryptophan fluorescence emission. The spectra of membrane-bound peptides were shifted to the blue compared with n-octanol, dioxane or ethyl acetate (Figure 3.1.1.2). While it is difficult to evaluate the hydrophobicity of the peptide tryptophan membrane environment, it can be concluded that it is quite hydrophobic.

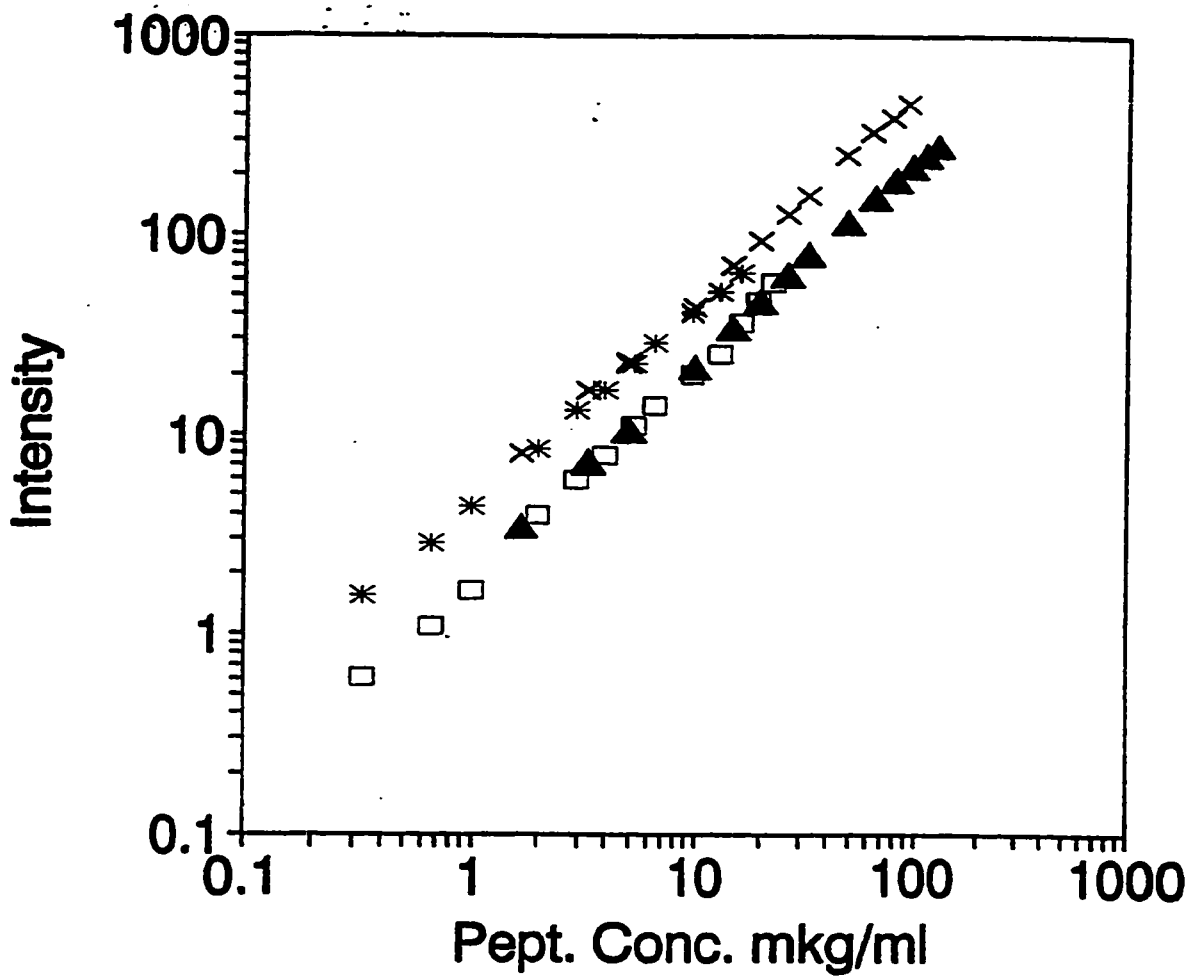

Figure 3.1.1.1. Concentrational dependence of intensity of tryptophan fluorescence of 18L and Ac-18A-NH_2 peptides in water (18L (□); Ac-18A-NH_2 (▲)) and in methanol (18L (*) and Ac-18A-NH_2 (×)). Logarithmic scale was chosen to illustrate linearity of dependence in the wide range of concentrations. (Linear character of the dependence is evident from the slope of the logarithmic dependence). Fluorescence was corrected for inner filter effects.

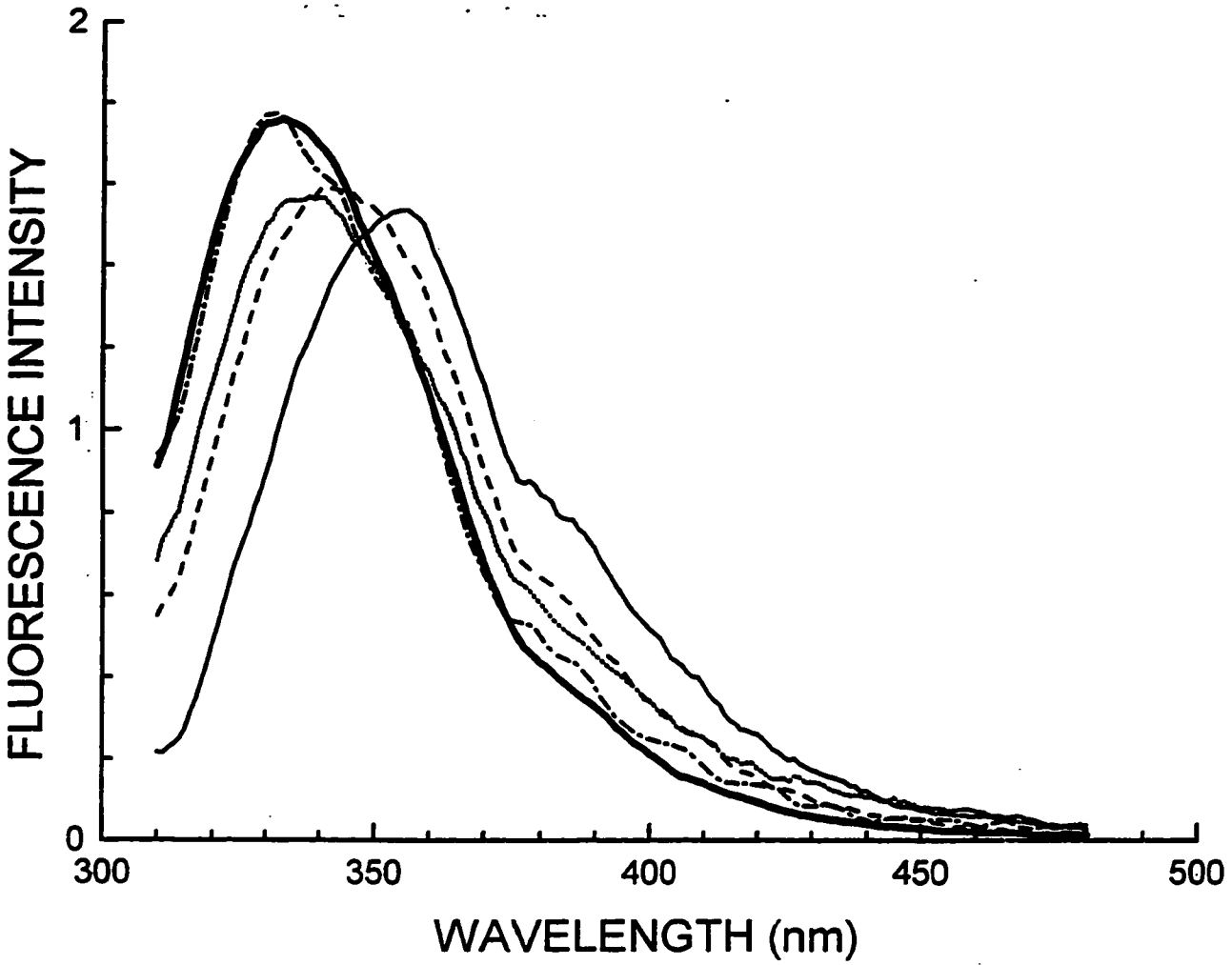

Figure 3.1.1.2. Tryptophan fluorescence spectra of peptide 18L in solvents and in membrane environment (DOPC:DOPE, 1:1). Spectra scaled to the same integral intensity. Fluorescence background subtracted. Bold solid line - spectrum of 18L in membrane environment, solid line - 18L in water, dashed line - 18L in ethanol, dotted line - 18L in octyl alcohol, dash-dotted line - 18L in hexane, spectrum in hexane had much less intensity due to poor peptide solubility.

3.1.2 Equilibrium binding studies

Previously membrane binding constants have been estimated from the half-shift of the tryptophan emission spectrum [Segrest et al., 1983; Pownall et al., 1984] or from the increase of fluorescence intensity at fixed wavelength [Epand and Epand, 1980; Matsuzaki et al., 1994]. We found intensity changes at one particular wavelength susceptible to large error. In addition, the fluorescence of peptides with a high affinity for membranes may be self quenched at a high peptide/lipid ratio as a consequence of peptide association in the membrane. We suggest quantitating the binding from the deconvolution of the spectra into membrane-bound and free components. Peptide-membrane association *a priori* is not a one step process, as a number of peptide arrangements within the bilayer are possible. It is not straightforward how these different arrangements would affect the fluorescence spectrum of tryptophan. However, our data support the idea that at relatively low peptide/lipid ratio there exists only one bound state corresponding to the most blue-shifted tryptophan fluorescence spectrum. In the course of the titration of the peptide solution with liposomes (for typical titration experiment, see Fig. 3.1.2.1), a final intensity increase and fluorescence shift are obtained. A further increase in liposome concentration did not give any additional change, after background subtraction. At very high lipid concentration, a decrease in fluorescence intensity, due to a scattering effect, was observed without shift in the wavelength of maximal emission. The same reproducible blueshifted shape of tryptophan spectra was observed in the experiments on the titration of LUV (at sufficiently high lipid concentration) with peptides. In this experiments, tryptophan fluorescence intensity was linear with peptide concentration and after background

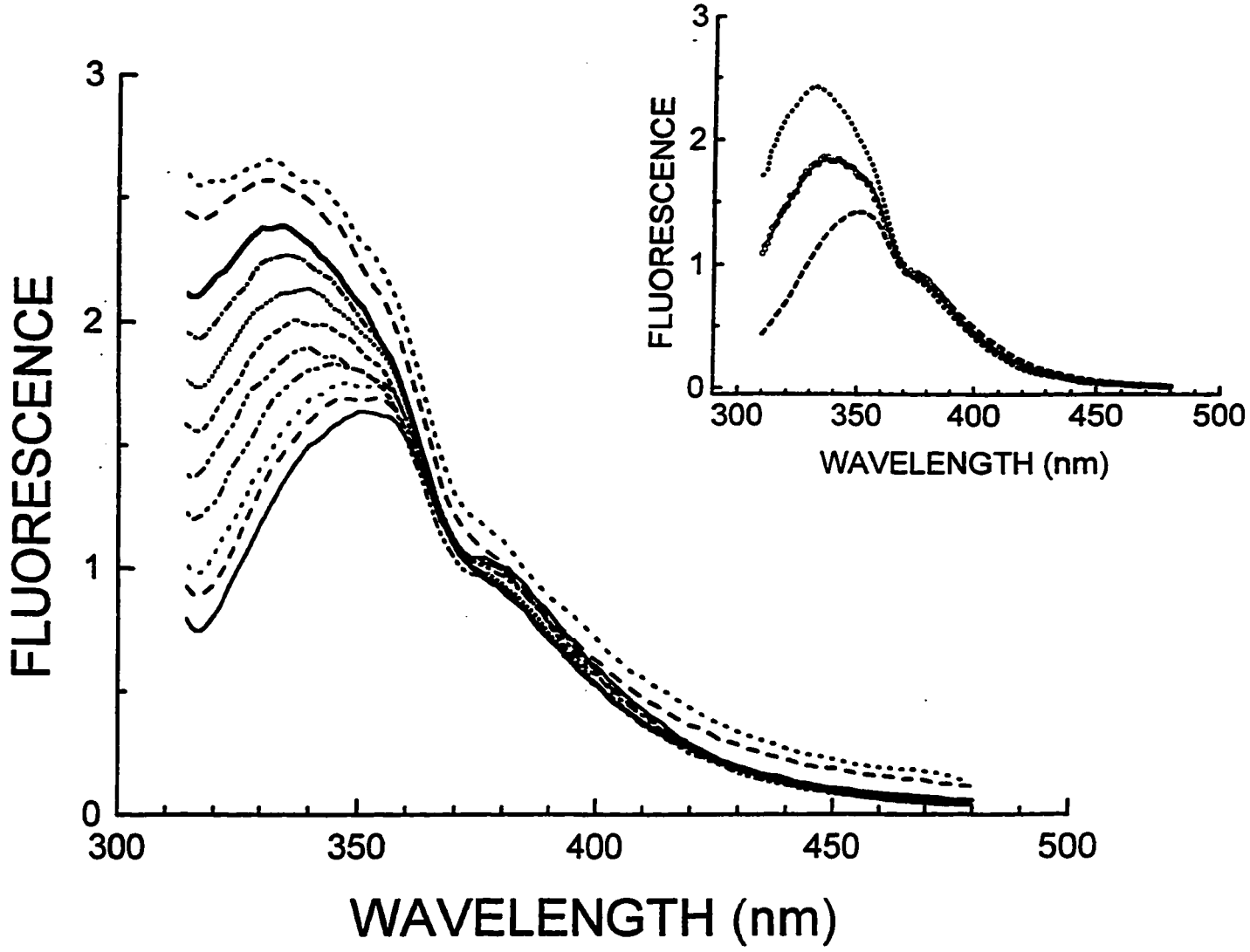

Figure 3.1.2.1. Typical change in peptide (Ac-18A-NH_2, 12.5 μM) fluorescence spectra upon titration with vesicles (DOPC:DOPE, 1:1). From bottom to the top, lipid concentration is 0 μM, 6 μM, 12 μM, 25 μM, 38 μM, 50 μM, 62 μM, 87 μM, 145 μM, 290 μM, 460 μM. Background not subtracted. Difference between 145 μM, 290 μM and 460 μM spectra is only due to an increase in background fluorescence. Inset shows the fit of intermediate spectra by the sum of two components from bound and free peptide. Dashed and dotted lines are respectively the spectra of free and membrane bound peptide. Example of experimentally determined spectrum (lipid concentration 50 μM) is shown by open circles. Solid line shows the fit of the spectra by a linear combination of free and membrane bound spectra. Background signal was subtracted from all of the spectra.

subtraction the shape of the spectrum was independent of the peptide concentration, provided that the peptide/lipid ratio was sufficiently low. We found that for every particular peptide and lipid system, the shape of the membrane-bound peptide spectrum was different, although reproducible. Spectra of 18L bound to membranes were generally more blue-shifted than those of Ac-18A-NH_2 under identical conditions. The tryptophan environment of peptides bound to membranes containing acidic lipids was less hydrophobic than it was in zwitterionic membranes.

Knowledge of the peptide tryptophan spectrum, both in solution and in the membrane bound state, makes it possible to determine the peptide distribution between aqueous and membrane environments. Each spectrum in the course of the titration can be fitted by the superposition of the spectrum of the membrane-bound and of the free peptide (Fig. 3.1.2.1, inset). That is, in the course of the titration of peptide of concentration P_0, for every lipid concentration L, the fluorescence intensity at a particular wavelength λ, $I_\lambda(L)$, can be represented as:

$$I_\lambda(L) = P_f(L) \cdot I_{\lambda 0} + P_b(L) \cdot I_{\lambda \infty} \qquad (3.1.2.1)$$

$$\text{where } P_0 = P_f(L) + P_b(L) \text{ for all L} \qquad (3.1.2.2)$$

$I_{\lambda 0}$ and $I_{\lambda \infty}$ are the specific intensities for the peptide in water and in membrane respectively, at wavelength λ. $P_f(L)$ and $P_b(L)$ are the peptide concentrations in water and in membrane. For every L value, $P_f(L)$ and $P_b(L)$ can be found numerically by least square optimisation. The standard deviation between the experimental points and the curve fit was comparable to the deviation between consecutive spectra of the same sample and usually was within 2%, but was higher (5%) when close to the sensitivity

limit of the technique at low peptide concentrations. Knowledge of the amounts of bound and free peptide at every lipid concentration makes it possible to reconstruct binding isotherms ($r(P_f)$) i.e., a plot of bound peptide/lipid ratio ($r=P_b/L$) versus free peptide concentration P_f. This approach allows for the quantitative analysis, not only the titration of peptide by liposomes, but also the titration of liposomes with peptide, as well as a dilution assay [Pownall et al., 1984] where binding is determined by the red shift of peptide fluorescence in a series of dilutions of peptide-liposome mixtures. The description of binding was considered valid if the binding isotherms, derived by titration of peptide with LUV or of LUV with peptide, from several concentrations, coincided.

There was a significant difference between lipid and peptide titration assays. Values of bound peptide/lipid ratios at the same free peptide concentrations deduced from titration of liposomes with peptides were exactly two-fold less than those from the titration of peptide with vesicles. This can be explained by the different lipid accessibility in the two assays. In the course of titration of peptide with vesicles the initially high free peptide concentrations led to the permeabilization of the first vesicles added, resulting in the accessibility of both sides of the membrane bilayer. Thus the bound peptide/lipid ratio is twice as high as in the titration of liposomes with peptide where the experiment starts with a low peptide-to-lipid ratio which is insufficient for vesicle disruption and thus only the outer vesicle surface is accessible.

We derived binding isotherms for 18L or Ac-18A-NH_2 with DOPC, DOPC:DOPE(1:1) or DOPG (Fig. 3.1.2.2). Binding studies were restricted to lipids in

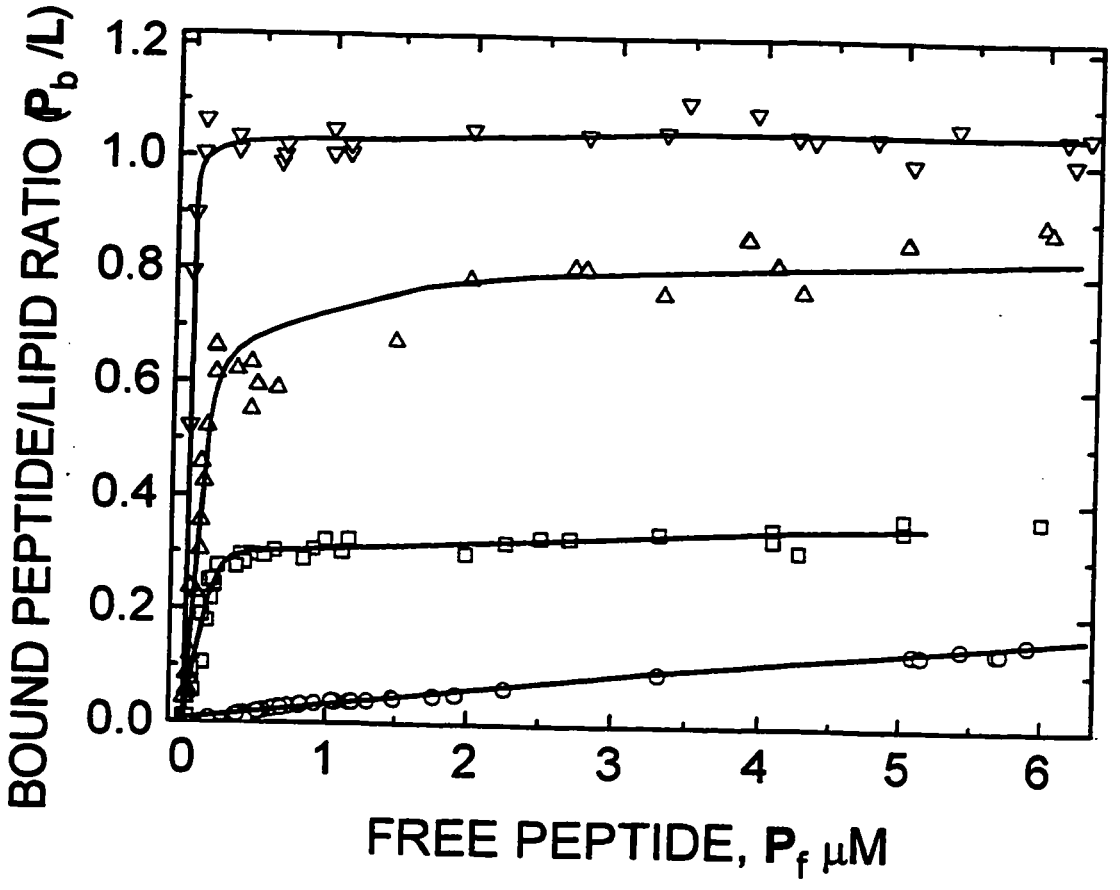

Figure 3.1.2.2. Binding isotherms for 18L and Ac-18A-NH_2 peptides. The isotherm of binding of 18L to DOPG (▽), of Ac-18A-NH_2 for DOPG (△), of 18L to DOPC:DOPE (1:1) (□) and of Ac-18A-NH_2 to DOPC:DOPE (1:1) (o). Each binding isotherm was derived form several titration experiments as described in the text.

the fluid phase since both Ac-18A-NH_2 and 18L were found unable to penetrate into the gel phase [Chapter 3.2.1, Polozov et al., 1995; Polozov et al., 1997a]. The binding isotherm for 18L with all types of lipids appears linear until saturation at micromolar concentrations of free peptide. For Ac-18A-NH_2, such a pattern was observed only for acidic lipids. In the case of zwitterionic DOPC and DOPC:DOPE, no apparent saturation was observed. From the linear part of the binding isotherm, partition coefficients of peptide between water and the membrane phase, as well as the corresponding free energies of peptide-membrane association (ΔG_b), were determined (Table 3.1.2.1). Binding isotherms for DOPC and Ac-18A-NH_2 or 18L are not shown as they were similar to those of DOPC:DOPE. With less precision Ac-18A-NH_2 or 18L binding to DMPC (at 37°C) and DOPC:Chol (7:3) was also estimated and found similar to other zwitterionic lipids.

The proper resolution of the initial linear part of binding isotherm and determination of binding constant requires titration of low peptide concentrations, such that P_0 is within the linear range of the isotherm $r(P_f)$. In practice this is limited by the need to have the sufficient fluorescence signal above the background of the liposome suspensions, that is P_0 must be above ~0.05 μM. This requirement corresponds to an upper limit of the binding constants (K) resolved by this assay $K \sim 1/(5\times10^{-8}\ M)=2\times10^{7}\ M^{-1}$ or a free energy of binding $\Delta G_b = -RT\ln(55.5\times K)= -12.3$ kcal/mole. For the stronger binding only saturation part of the binding isotherm can be resolved. The range of K which can be determined by this assay is actually higher than that of a centrifugation assay [Spuhler et al., 1994], or a circular dichroism titration

Table 3.1.2.1. Equilibrium and dynamic parameters of the 18L and Ac-18A-NH_2 peptide binding with various types of lipids: association constants (K), free energy of association (ΔG_b), and association and dissociation rate constants (k_a and k_d).

PEPTIDE	LIPID	Association constant, K, M^{-1}	[a]Free energy of association, - ΔG_b, kcal/mol	[b]Association rate constant k_a, $M^{-1}\cdot s^{-1}$	[c]Dissociation rate constant k_d, s^{-1}
18L	DOPC:DOPE (1:1)	$1.35\cdot10^6$	10.7	$1.9\cdot10^5$	0.15
	DOPC	$1.2\cdot10^6$	10.6	--	--
	DOPG	$4.5\cdot10^7$	12.8	--	--
Ac-18A-NH_2	DOPC:DOPE (1:1)	$3.2\cdot10^4$	8.5	$1.3\cdot10^5$	3.9, 3.6[d]
	DOPC	$4.0\cdot10^4$	8.6	--	--
	DOPG	$3.5\cdot10^6$	11.3	$2.8\cdot10^5$	0.075

[a] Free energy of peptide lipid association is calculated from the association constant K, as $\Delta G = -RT\cdot\ln(K\cdot55.5)$.

[b] Association rate constants k_a were derived from the slope of the concentration dependence of association rate (Fig. 3.1.3.2).

[c] Dissociation rate constants k_d were calculated as $k_d=k_a/K$, except for [d] which was determined from concentration dependence of the association rate extrapolated to zero concentration.

[Schwarz and Blochman, 1993]. Measurement of the higher **K** can be achieved using fluorescently modified peptides.

The deconvolution procedure was modified for the quantitation of binding for peptides with very high membrane affinity, e.g. 18L:DOPG. If $\mathbf{P_0}$ in the titration experiment is higher than the linear range of the binding isotherm for that peptide/lipid system than first liposomes addition will lead to peptide binding with saturating peptide/lipid ratios and self-quenching of tryptophan fluorescence. Increase in the total intensity is observed only when all peptide is already bound and further titration results in a decrease of the bound peptide/lipid ratio which occurrs without a significant change in the shape of the spectra. Eventually the fluorescence intensity reaches a maximum and a further addition of vesicles does not induce any changes after background subtraction. For quantitation of the peptide-membrane binding for these systems the quenched bound peptide spectrum was used as a reference for the bound peptide and the the same deconvolution procedure was applied. Comparing isotherms derived from several peptide concentrations we were able to resolve the saturation part of the binding isotherm. Only minimal estimates of **K** and ΔG_b are presented in Table 3.1.2.1. for the 18L:DOPG binding.

In order to examine the reciprocal effect of Ac-18A-NH_2 and 18L on peptide membrane binding we preincubated vesicles with 18L at peptide-lipid ratios 1:40 and 1:20 and then titrated vesicles with Ac-18A-NH_2 and derived binding isotherms, subtracting initial 18L fluorescence as a background. Within experimental error binding isotherms of Ac-18A-NH_2 coincided with that of lipid without peptide

preincubation. We determined this for DOPC:DOPE (1:1) and DOPC LUV. Thus we conclude that the two peptides bind to a membrane independently.

Titration calorimetry was used for the determination of the enthalpy of peptide-membrane binding. Experiments on titration of LUV of DOPC:DOPE (1:1) or DOPG with Ac-18A-NH_2 or 18L peptides were conducted. At particular experimental conditions (200 μM phospholipid), all peptide injected binds to the membrane. We observed enthalpy changes only slightly above the enthalpies of peptide dilution, in the range of 0.2-0.5 kcal/mol peptide. This indicates that the largest part of the free energy of peptide-membrane binding ΔG_b comes from an entropic contribution.

3.1.3 Kinetics of peptide binding

Increase in tryptophan fluorescence intensity (emission at 330 nm) was used to monitor the kinetics of peptide-membrane association. Association of both Ac-18A-NH_2 and 18L was found to be a fast process and to take place in tens of milliseconds. Typical time traces of peptide binding are presented (Fig. 3.1.3.1). The final extent of fluorescence increase depended on the lipid concentration for the Ac-18A-NH_2 peptide but was practically independent of lipid concentration for 18L. This was expected, since at the lipid concentrations used, according to the binding constants for DOPC:DOPE, the percentage of bound Ac-18A-NH_2 should depend on lipid concentration while 18L must always be essentially bound.

We fitted the time course of Ac-18A-NH_2 binding with a single first order rate constant. The plot of the binding rate constant versus lipid concentration is shown in

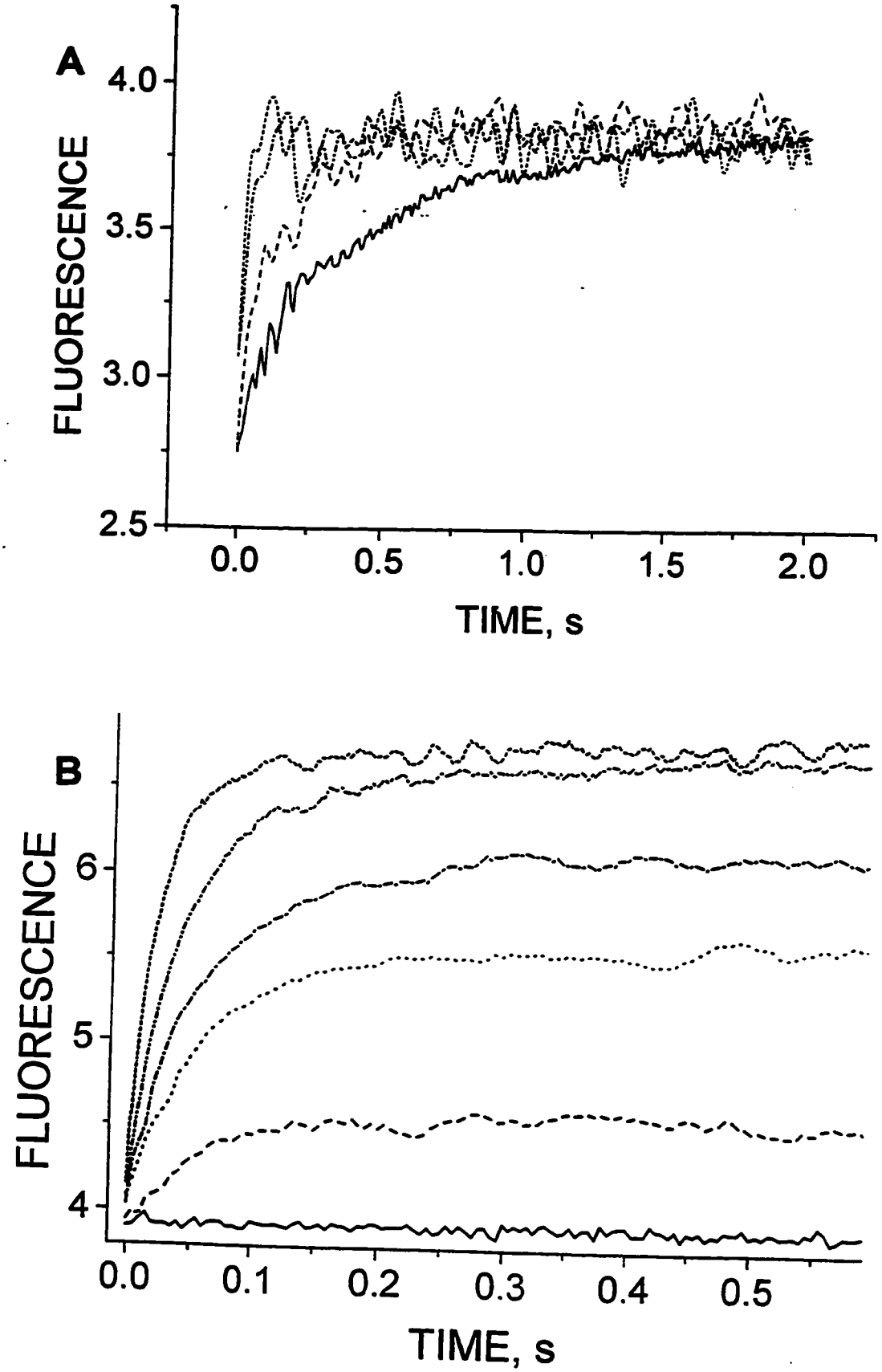

Figure 3.1.3.1. Typical time course of peptide binding to membrane monitored by the increase of tryptophan fluorescence at 335 nm. **A.** Kinetics of 18L (5 μM) binding to DOPC:DOPE (1:1) LUV of the following concentrations: (from the left to the right) 250 μM, 200 μM, 50 μM, 32 μM. **B.** Kinetics of Ac-18A-NH_2 (5 μM) binding to DOPC:DOPE (1:1) LUV of the following concentrations: from the top to the bottom 340 μM, 170 μM, 85 μM, 50 μM, 25 μM, 0 μM. Experimental conditions are as described in Materials and Methods.

Fig. 3.1.3.2. Such a distinct linear dependence is characteristic of a one step association-dissociation equilibrium:

$$P_f + L \underset{k_d}{\overset{k_a}{\leftrightarrow}} P_b \qquad (3.1.3.1)$$

Where P_f represents peptide in water, P_b the peptide associated with an aggregate of lipid molecules, L is an aggregate of lipid molecules, k_a - the rate constant of association and k_d - the rate constant of dissociation. In the case of excess lipid, the formally second order binding process follows pseudo first order kinetics, that is the amount of the membrane bound peptide (P_b) approaches an equilibrium value (P_{be}) following a single exponential time course with a rate constant R linearly dependent on lipid concentration (L):

$$P_b(t) = P_{be} \times (1-\exp[-R \times t]) \qquad (3.1.3.2)$$

$$\text{where } R = k_a \times L + k_d \qquad (3.1.3.3)$$

For Ac-18A-NH_2 binding to DOPC:DOPE (Fig. 3.1.3.2.) we calculate an association rate constant $k_a=1.3\times10^5$ $M^{-1}s^{-1}$ and a dissociation rate constant $k_d=3.6\pm0.3$ s^{-1}, which corresponds to a half-time of peptide dissociation $t_{1/2}=\ln2/k_d=0.19\pm0.03$ s. Hence the corresponding equilibrium binding constant, $K=k_a/k_d=(3.5\pm0.3)\times10^4$ M^{-1}, is very close to the value of $K=3.2\times10^4$ M^{-1} derived from the titration experiments (Table 3.1.2.1). To confirm the fast dynamic character of the Ac-18A-NH_2-membrane association equilibrium, we directly monitored the process of peptide dissociation from the membrane. Upon two fold dilution of the vesicle suspension preincubated with Ac-18A-NH_2, we observed partial peptide

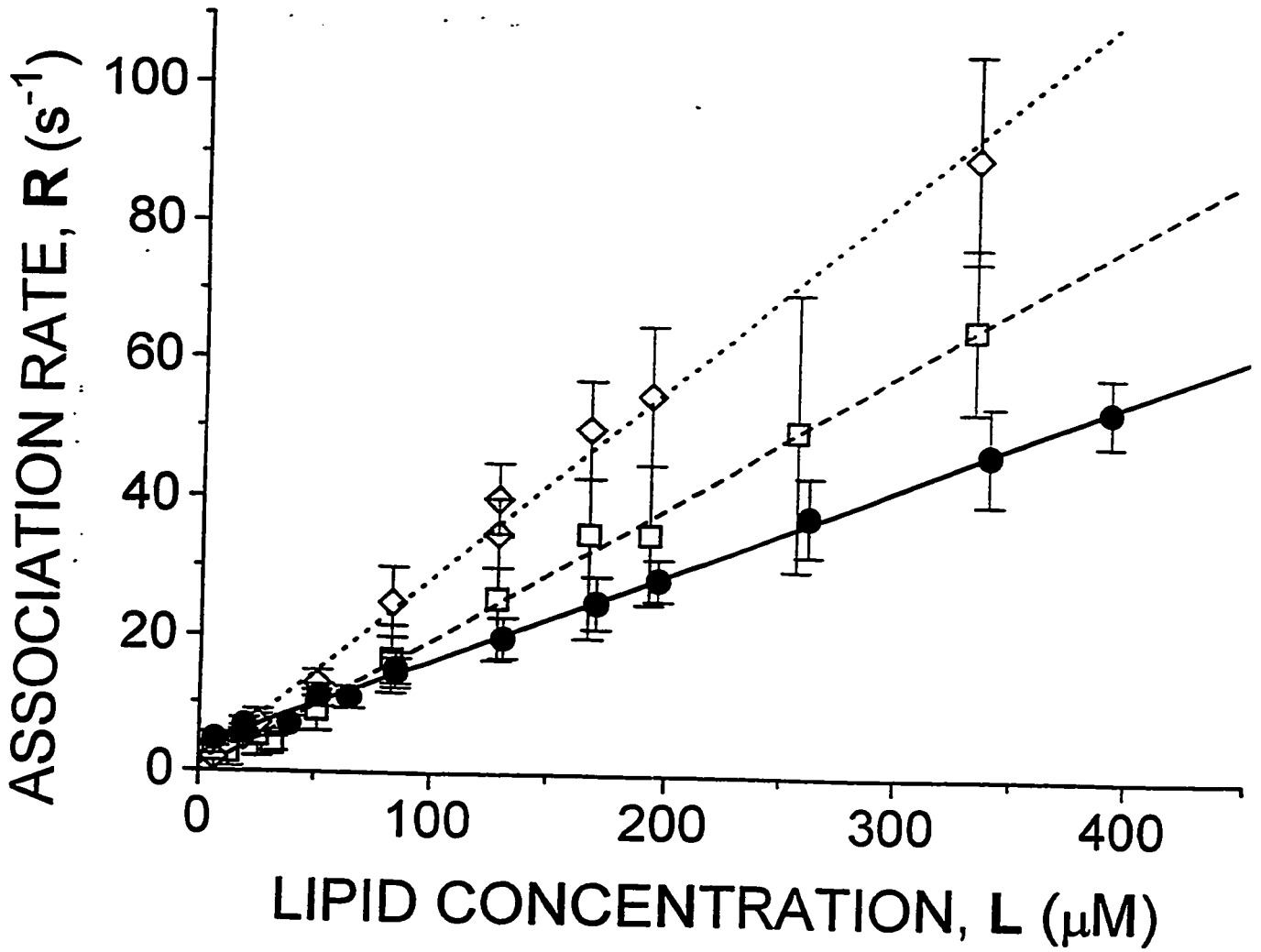

Figure 3.1.3.2. Dependence of peptide binding rate constant (R), determined by monoexponential fit of the time traces, on lipid concentration (L). Straight lines are derived by linear regression. Circles and solid line - Ac-18A-NH_2 binding to DOPC:DOPE (1:1). Squares and dashed line - 18L binding to DOPC:DOPE (1:1). Diamonds and dotted line - Ac-18A-NH_2 binding to DOPG.

dissociation which was completed within 0.1-0.2 s (Fig. 3.1.3.3). In the case of high peptide/lipid ratios (>1:20), the Ac-18A-NH_2 binding kinetics becomes more complicated. The initial rate increases above that expected from a linear dependence on concentration and the overall kinetics apparently becomes non-monoexponential and dependent both on peptide and lipid concentrations.

For the binding of 18L to the membrane, as well as Ac-18A-NH_2:DOPG binding, we were able to determine the peptide-membrane association rate constant k_a, but there was a large uncertainty in the determination of k_d. In addition to a monoexponential fit, association rates for these cases were analysed using an analytical expression for the kinetics of sequential binding [Bentz et al., 1988 (eq. II.6); Nir et al., 1994] which takes into account saturation of binding. The values of the association rate constants derived by both approaches coincided within experimental error. Association rate constants are presented in Table 3.1.2.1.

Due to the high peptide-membrane affinity we were unable to directly determine the dissociation rate of 18L from DOPC:DOPE membranes, but we were able to confirm the dynamic character of the peptide-membrane equilibrium indirectly using the ANTS/DPX leakage assay (Fig. 3.1.3.4). A small aliquot of DOPG vesicles was added to 18L, which had been prebound to DOPC:DOPE vesicles at a non-leaky peptide/lipid ratio. The much higher affinity of 18L for acidic lipids results in the redistribution of 18L to acidic lipids and the induction of leakage. The pattern of leakage curves observed is similar to the one in the absence of zwitterionic liposomes

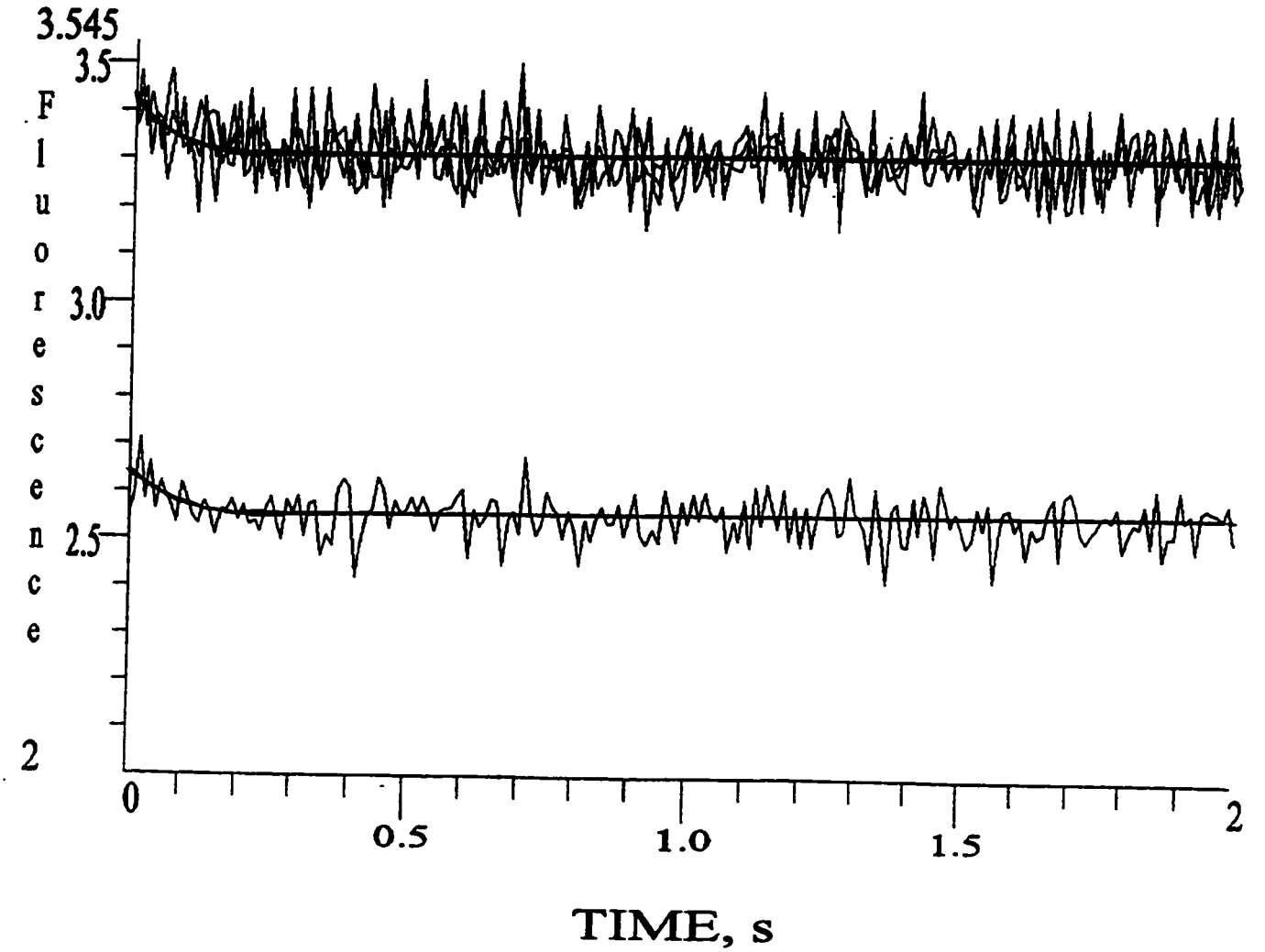

Figure 3.1.3.3 Typical time traces of dissociation of Ac-18A-NH_2 from DOPC:DOPE (1:1) membranes upon dilution twice of peptide-vesicle suspension. Stopped flow experiments monitoring decrease in tryptophan fluorescence intensity at 335 nm. The low signal to noise ratio is related to only a small shift of peptide-membrane equilibrium upon this dilution. The upper time trace is the dilution of 65 μM of lipid. The relaxation time in this system is expected to be 0.123 s according to values from Table. 3.1.2.1. The lower time trace is for starting with 40 μM lipid and corresponding expected relaxation time is 0.16 s. Reasonable correspondence between theory and experiment is illustrated by the drawn solid lines.

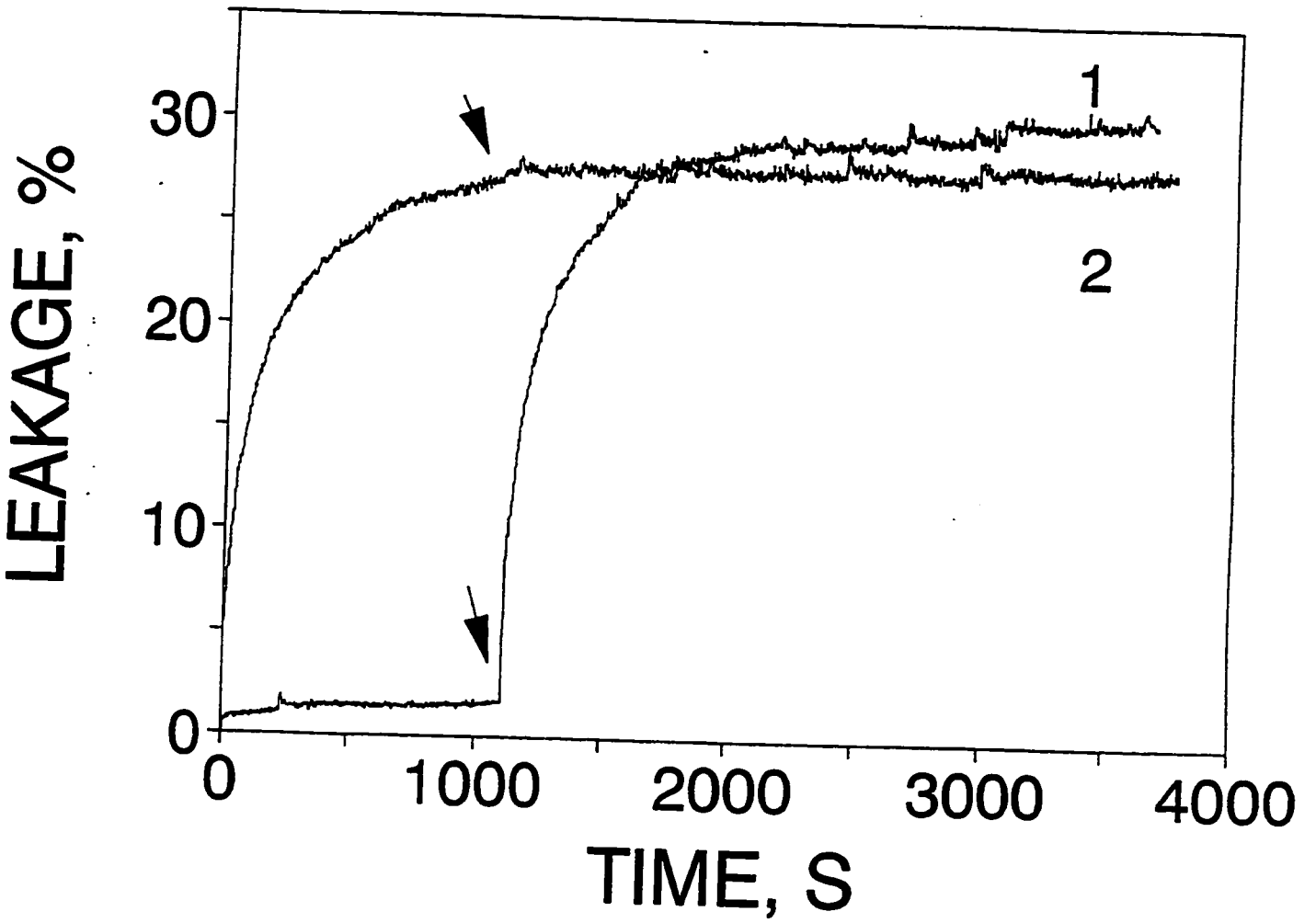

Figure 3.1.3.4. Leakage experiment confirming the dynamic character of 18L partitioning between membranes. Curve 1: DOPC:DOPE (1:1) LUV (65 μM) were added to a solution of 3 μM 18L, causing relatively low leakage at this peptide/lipid ratio. At the arrow 15 μM of DOPC:DOPG (1:1) LUV were injected into the cell. Redistribution of 18L into these vesicles caused fast leakage. Curve 2: Control experiment , 15 μM of DOPC:DOPG LUV were injected into the cell with 5 μM 18L solution. The initial leakage rate is exactly the same as after DOPC:DOPG LUV injection in the Curve 1. At the arrow an additional 45 μM DOPC:DOPG LUV were injected which resulted in inhibition of leakage due to peptide redistribution and decrease of bound peptide/lipid ratios. 100% of leakage was determined by vesicle disruption with detergent and thus corresponds to the leakage of both DOPC:DOPE and DOPC:DOPG LUV in curve 1, and all DOPC:DOPG LUV in curve 2.

(peptide in buffer), thus indicative of the peptide dissociation rate being faster than the leakage rate.

Another assay on binding kinetics used fluorescence energy transfer from tryptophan to APC, a fluorescent lipid analog with the fluorophor attached at the C_{12} position of the C-2 fatty acid and thus located deep within the bilayer. Using this assay, a rapid component was observed for both Ac-18A-NH_2 and 18L peptides, similar to the one observed by tryptophan fluorescence increase. In addition, however, for both Ac-18A-NH_2 and 18L there were observed slow components, in the range of seconds to tens seconds, which were not observed using the tryptophan assay. Efficiency of fluorescence energy transfer from peptide to probe is dependent not only on the incorporation of tryptophan into the hydrophobic region of the membrane, but also to the rearrangement of peptide relative to fluorescent probe, and thus we suppose that the slow component corresponds to peptide redistribution within the membrane subsequent to initial binding.

3.1.4 DISCUSSION (Membrane partitioning)

Binding isotherms $r(P_f)$ for both peptides, with all lipids studied, had a linear portion at low peptide/lipid ratios (Fig. 3.1.2.2). This linear part of the $r(P_f)$ corresponds to the peptide monomer partitioning into the membrane without subsequent aggregation [Schwarz, 1989]. Binding constants (K) have been derived from the slope of the linear part of the binding isotherms (Table 3.1.2.1). Binding constants of 18L are higher than those reported previously for similar peptides such as mastoparan ($K_{DOPC}=1.65x10^3$

M^{-1}, Schwarz and Blochmann, 1993) or magainin 1 and 2 (K_{DOPG}=0.26x10^6 M^{-1}; 3.0x10^6 M^{-1}, Matsuzaki et al., 1991). Values of the binding constant for the Ac-18A-NH_2 peptide are also high compared to other data on membrane binding of analogs of A-type amphipathic peptides. In a recent paper, Spuhler et al. (1994) report binding constants for the 18A (not the N-acetyl peptide-amide, which we used in the present work), derived from a centrifugation assay, of 170 M^{-1} for DOPC and 900 M^{-1} for DOPC:DOPG, 1:1. The lower binding affinities of 18A compared to the Ac-18A-NH_2 are in accordance with the previously published observation that end group blockage of 18A significantly increases it's membrane affinity [Venkatachalapathi et al., 1993].

Binding isotherms show that the analysis using a partitioning model is valid only within a limited range of free peptide concentrations. With increased peptide-lipid ratios, the binding isotherm starts flattening and eventually goes to saturation. High membrane activity of peptides necessitates the introduction of a coefficient of 0.5 for comparison of the vesicle and peptide titration experiments. The reasonable assumption that only the external leaflet of the membranes is available for peptide binding [Beschiashchvili and Seelig, 1990] appeared to be valid only for Ac-18A-NH_2/DOPC:DOPE partitioning. The saturating shape of binding isotherms corresponds to the mutual repulsion of bound peptides and is indicative of the absence of in plane aggregation of peptides [Schwarz, 1989]. The saturation part of the binding isotherm makes it possible to estimate the limiting number of peptides capable of binding to a vesicle, or alternatively the size of the lipid binding cluster. In acidic membranes, where peptide charges are neutralised, the size of the peptide binding

cluster probably is determined by steric considerations as well as by decreased electrostatic attraction, while in zwitterionic membranes the limiting factor will be electrostatic repulsion of charged peptides. The very high saturation levels observed are indicative of vesicle disruption during the process of titration. This disruption could be monitored visually. At sufficiently large peptide/lipid ratios, 18L peptide increased the turbidity of both zwitterionic and acidic LUVs, while the Ac-18A-NH_2 peptide clarifies the MLV suspensions.

Binding of cationic peptides to zwitterionic and acidic membranes was previously described in terms of the Gouy-Chapman theory [Kuchinka and Seelig, 1989; Beschiashchvili and Seelig, 1990; Mosior and McLaughlin, 1992]. According to this description, negative charge on the acidic membrane creates a membrane potential which causes charged peptides to redistribute to the membrane. This passive accumulation of peptides near an anionic membrane surface results in a high apparent binding constant. This aspect is important for the binding of cationic 18L. However, Ac-18A-NH_2 also had a much higher affinity for anionic membranes than for zwitterionic lipids (almost two orders of magnitude from DOPC to DOPG, Table 3.1.2.1). Titration calorimetry experiments show that the free energy of binding is of entropic origin both for 18L and Ac-18A-NH_2 and for both zwitterionic and acidic membranes. Recently, it was found that the binding of the 18A peptide to the membrane does not change the overall surface charge of membranes [Spuhler et al., 1994], that is 18A is indeed zwitterionic in the membrane bound state. The ratio of bound peptide to lipid for both 18L and Ac-18A-NH_2 at saturation was found to be

higher for acidic lipids than for zwitterionic ones (Fig. 3.1.2.2). This also can not be explained only as a response to membrane potential. Rather, high peptide/lipid ratios at saturation are favoured by mutual repulsion of negatively charged lipid headgroups and also by reduction of peptide-peptide repulsion which may take place for the cationic 18L peptide. There also may be an input from the direct interaction of charged aminoacids with a charged lipid headgroups. Spuhler et al. (1994) showed that 18A affects the conformation of lipid headgroups in a manner expected for positively charged peptides. This is consistent with the "snorkel" conformation adopted by 18A in a bilayer [Venkatachalapathi et al., 1993].

The monomer partitioning model is successful in describing the peptide binding kinetics as well as the equilibrium binding data. Peptides were found to be in dynamic equilibrium with membranes having an association time in the millisecond range and a dissociation speed which depended on the peptide affinity for membranes and ranged from hundreds of milliseconds to tens of seconds. The dynamic character of the binding equilibrium is highly lipid and peptide dependent. As it is shown in the Chapter 3.1.3, we derived an equilibrium binding constant, **K**, from experimentally determined association and dissociation rates of Ac-18A-NH_2 with DOPC:DOPE membranes and found it to coincide with the **K** derived from equilibrium studies. In accordance with the binding isotherm, we were not able to experimentally determine the dissociation rates for the 18L peptide or the Ac-18A-NH_2 peptide with acidic membranes. However, a knowledge of the association rate constant k_a, and the binding constant, **K**, are sufficient to completely describe the dynamic character of peptide binding.

Variation in k_a was much less than that found for the equilibrium binding constant K. For example, k_a of Ac-18A-NH_2 for DOPG was only approximately two times higher than that for DOPC:DOPE, while the difference in K was three orders of magnitude. This shows that difference in peptide affinity for membranes, at least in the present case, is largely determined by the dissociation rate constant k_d as $k_d = k_a / K$. The upper boundary for the association rate constant is the diffusion limited rate constant, r_d. It was shown theoretically [Schwarz, 1987] that

$$r_d = b \times N_A \times D_0 \times (A_L / R_a)$$

involving b, the fraction of lipid molecules that are in the outer leaflet of the bilayer; N_A, Avogadro's number; D_0, the diffusion coefficient of the free peptide; A_L, the area per lipid headgroup on the bilayer surface; and R_a, the outer radius of a vesicle. For the DOPC:DOPE system we may estimate that A_L=0.7 nm^2, R_a=50 nm and b=0.5. The D_0 calculated for a peptide of about 2,000 MW at 25°C is 3×10^{-6} cm^2/s [Schwarz, 1987]. Thus $r_d = 1.25 \times 10^6$ $M^{-1}s^{-1}$ and the ratio k_a/r_d=0.104 for association of Ac-18A-NH_2 with DOPC:DOPE. This shows that the measured association rates are relatively close to the diffusion limit, i.e. there is no large barrier for the entrance of a peptide molecule into the bilayer. It is thus understandable why variation in the binding constant occurs via the modulation of the dissociation rate constant. We can conclude that strong binding correlates with a slower exchange of peptide between water and membranes.

As we discuss below we found that fusion and leakage-inducing activities of 18L and Ac-18A-NH_2 peptides depend strongly on the membrane composition, namely, on

the presence of nonbilayer forming lipids and presence of acidic lipids [Chapter 3.4, Polozov et al., 1997b]. Our current binding studies show that membrane charge strongly affects binding behavior of both cationic 18L and zwitterionic Ac-18A-NH_2. However, peptide binding was essentially not affected by the presence of nonbilayer forming lipids, that is, it was similar for several zwitterionic membranes studied.

3.2 Amphipathic Peptide Effects on The Lateral Domain Organization of Lipid Bilayers

3.2.1 Metastability of peptide association with gel state membranes

We found that while both peptides bind with high affinity to fluid lipid membranes, peptides were unable to penetrate into the membrane in the gel state. Figure 3.2.1.1 shows the temperature dependence of the fluorescence energy transfer from peptide tryptophan to an anthrylvinyl fluorophor attached to the acyl chain of a phospholipid (APC). Fluorescence was excited at 295 nm (peptide) and measured at 435 nm (probe). Fluorescence intensity is dependent on the average distance between the peptide tryptophan and the fluorophor embedded in the bilayer. Ac-18A-NH_2 (5 μM) was added to DMPC:DMPE (1:1) MLV (50 μM) in the gel state at 6°C. The sample was heated up to 59°C. Increase in fluorescence at around 20°-30°C is due to peptide insertion into bilayer at the beginning of the gel phase melting. The main phase transition is accompanied by a reversible decrease in the fluorescence intensity. In control experiments peptide tryptophan fluorescence in unlabelled vesicles monotonously decreased with increasing temperature

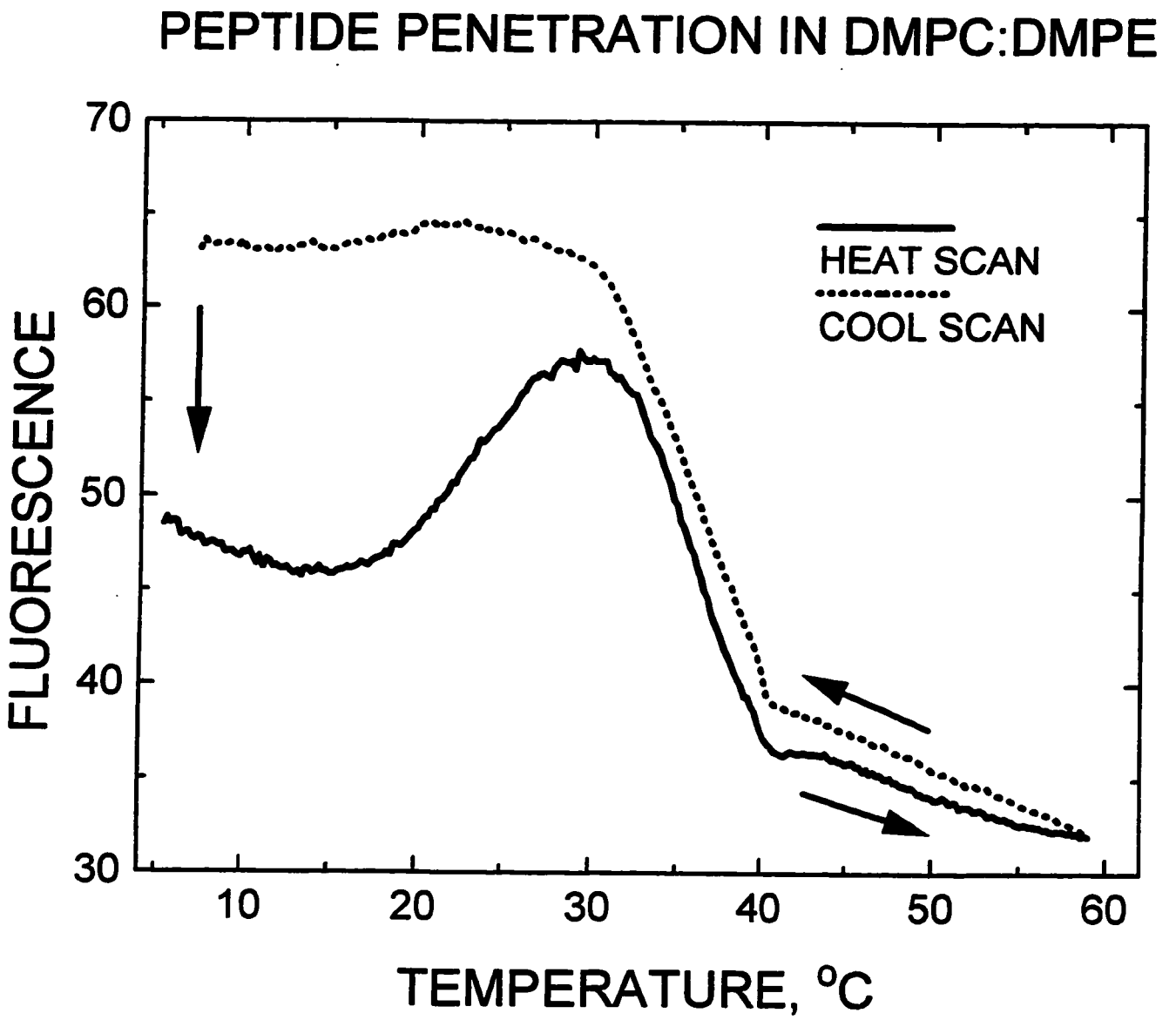

Figure 3.2.1.1. Temperature dependence of energy transfer from peptide to probe. Fluorescence was excited at 295 nm (peptide) and measured at 435 nm (probe). Ac-18A-NH_2 peptide (5 μM) was added to DMPC:DMPE (1:1) LUV (50 μM) in gel state at 6°C. The sample was heated up to 59°C. Increase in fluorescence at around 20°-30°C is due to peptide insertion into bilayer. Main phase transition is accompanied by a reversible decrease in fluorescence intensity due to increased water permeability of the bilayer and temperature-dependent quenching of the probe. Upon cooling, the peptide is kinetically trapped in the gel phase. Fluorescence intensity returned to the initial values after overnight storage of the sample at 4°C. Both heating and cooling was at a constant rate of 0.5°C/min.

but without abrupt changes in the area of the main phase transition. In the absence of peptide, probe fluorescence was monotonously decreasing with rising temperature with a steeper slope in the area of the phase transition, however these changes were less pronounced than those on Fig. 3.2.1.1. Considering this, we ascribe reversible change in fluorescence around the main phase transition to increased temperature quenching of the probe and lateral expansion of the bilayer increasing the average distance between peptides and probes. Upon cooling, peptides stayed in the membrane, however this peptide entrapment was kinetic rather than thermodynamic as peptides dissociated from the membranes on a timescale of hours. Fluorescence intensity returned to the initial values after overnight storage of the sample at 4°C. Decrease in energy transfer from peptide to probe can be also due to probe segregation into a separate phase. However, this should be accompanied by probe self-quenching, which was not observed.

Tryptophan fluorescence supports the energy transfer data. Addition of gel state liposomes to peptide solution resulted in the limited blue shift of tryptophan fluorescence. Melting the gel state results in significant blue shift of tryptophan fluorescence. Cooling below the main phase transition results in the small red shift, and subsequent overnight storage in the cold results in the further red shift to the spectra equivalent to those observed upon addition of liposomes to peptide solution. This sequence of events is illustrated in the Figure 3.2.1.2. for the case of 18L peptide and DMPC:DMPE liposomes. In principle, tryptophan spectra with maxima between 330 nm and 350 nm, may be the result of superposition of tryptophan spectra in different environments (membrane and buffer). If this was the case then peptide distribution between different environments would depend

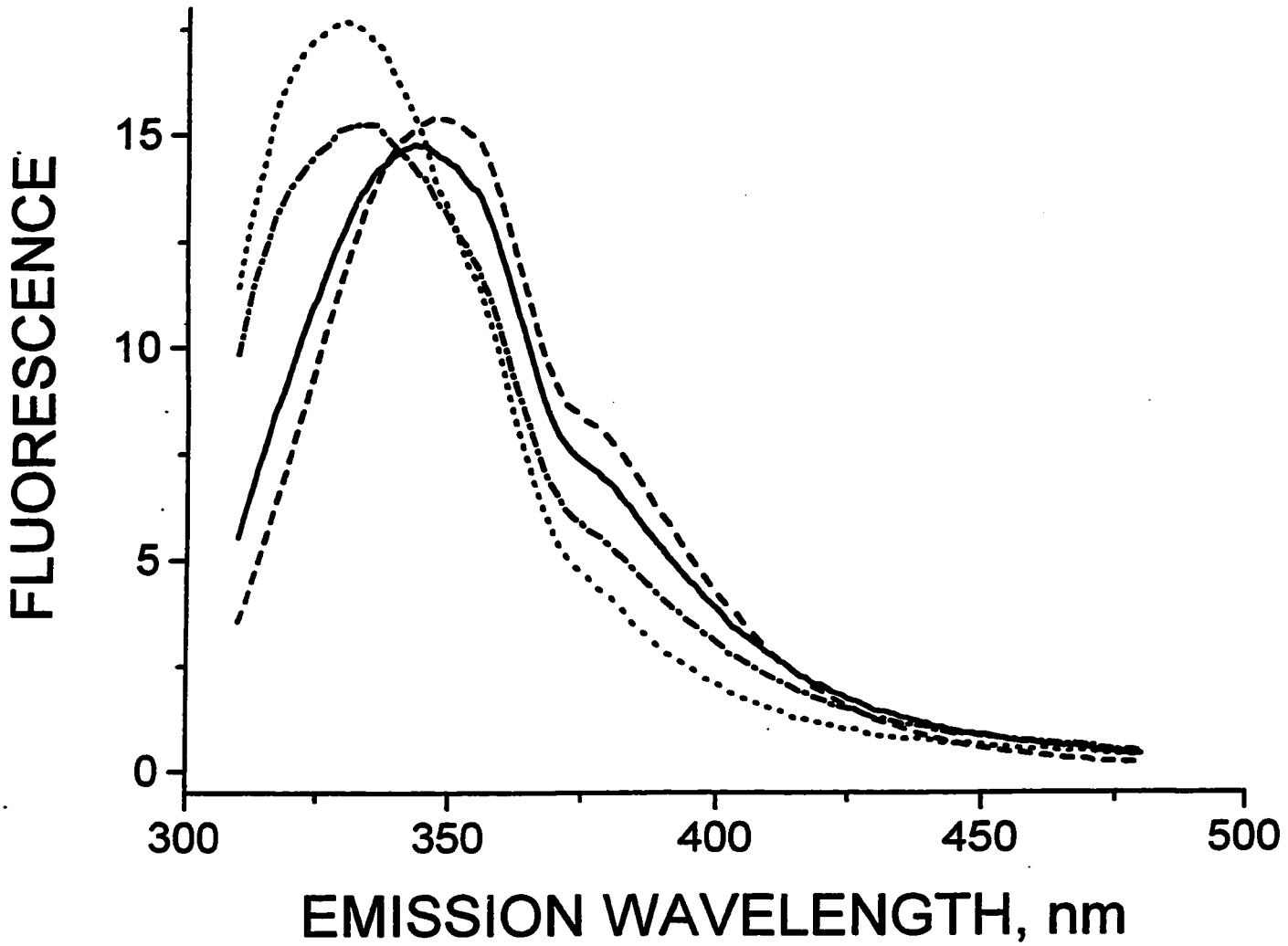

Figure 3.2.1.2. Tryptophan fluorescence of 18L (5 μM) in water (dashed line), after addition of 50 μM of DMPC:DMPE (1:1) LUV at 8°C (solid line), after heating to 42°C (short-dashed line) and after cooling to 4°C (dash-dotted line). Spectrum of the sample stored overnight at 4°C was the same as after lipid addition (solid line). All spectra were scaled to the same integral intensity.

on the lipid concentration and peptide/lipid ratio. However, the spectra were independent of lipid concentration for sufficiently low peptide/lipid ratios.

Metastability of peptide interactions with gel phase lipids had been reported previously [Epand, 1978; Epand, 1982]. Our data show that this metastability is observed even at low peptide/lipid ratios not accompanied with vesicle disruption. Similar behaviour was observed for both 18L and Ac-18A-NH_2 for several lipid systems (DMPC, DMPE, DMPC:DPPE). This suggests that such metastability may be a general feature of membrane-amphipathic peptide interactions. In single component lipid systems, the main phase transition occurs over a narrower temperature range which was also reflected by the temperature dependence of peptide incorporation. The fluorescence increase coincides not with the completion, but rather was close to the onset, of the phase transition. This can be explained taking into account the high affinity of 18L and Ac-18A-NH_2 peptides to membranes in the fluid phase [Chapter 3.1.2; Table 3.1.2.1]. Maximal fluorescence increase, associated with peptide incorporation, will be observed when there is enough surface for incorporation of all of the peptide, that is before complete melting of the gel phase. The exact temperature at which incorporation is achieved is expected to depend on the particular peptide/lipid ratio and peptide-fluid membrane binding constant. Peptides can also serve as a site for gel phase melting which will also result in peptide insertion in the membrane before completion of the phase transition.

3.2.2 Peptide effects on the lateral organization of the fluid phase

When the membrane consists of several molecular species, one can imagine that interaction of peptides with such a membrane occurs not with the membrane as a whole but

rather via association of peptides with particular lipid species. Geometric (Shape) factors were previously found to modulate many aspects of 18L and Ac-18A-NH_2 membrane interactions [Tytler et al., 1993; Chapter 3.4]. Correlation between the shape and the activities of peptides was especially pronounced for lipid systems with propensity for nonbilayer phase formation, such as Me-DOPE:DOPC and DOPC:DOPE mixtures. We decided to test if the geometric shape of peptides can induce lateral separation in membranes. A hypothetical "shape complementarity" mechanism is illustrated on Fig. 3.2.2.1A. Another tentative motif for lateral phase organization is illustrated on Fig. 3.2.2.1B. Charge-charge interactions also strongly modulate 18L and Ac-18A-NH_2 membrane interactions and it is natural to suppose that charge-charge association between acidic lipids and basic amino acid residues can lead to lateral separation of lipids. As an approach for the investigation of peptide-induced lateral organization of the membranes, we used energy transfer from membrane bound peptide tryptophan to the anthrylvinyl fluorophor of a lipid-specific probe. It was shown that deviation of the concentration dependence of energy transfer efficiency can be used as an indication of the non-random distribution of probe molecules [Fung and Stryer, 1978]. It has been shown that distribution of anthrylvinyl-labelled lipid-specific probes in the plane of membrane corresponds to that of their natural counterparts [Polozov et al., 1994a; Gromova et al.,

A

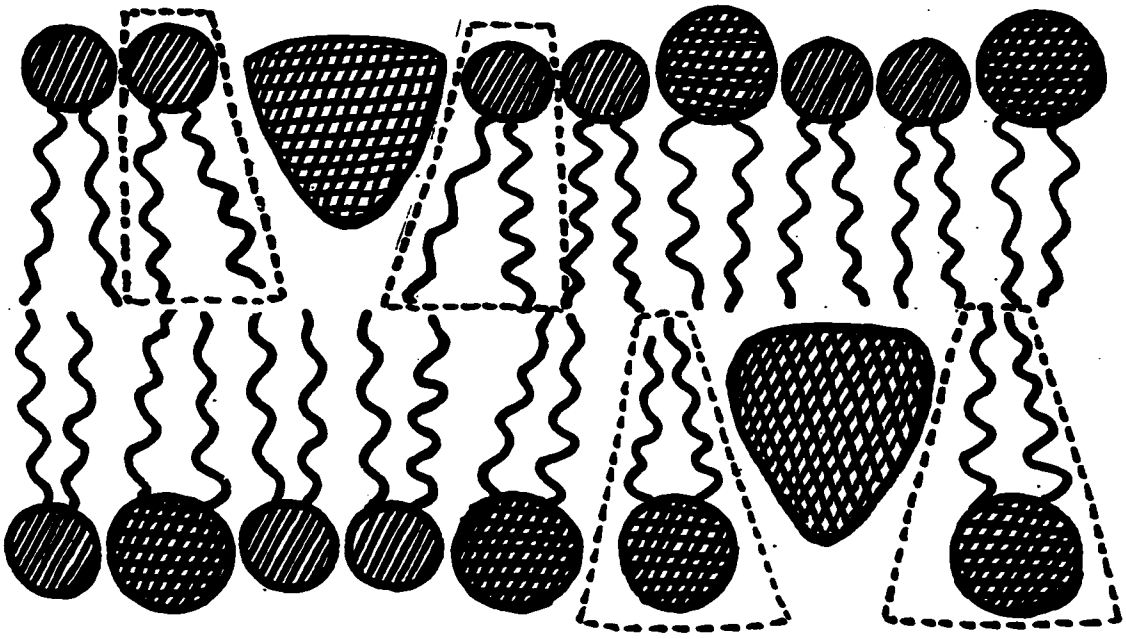

B

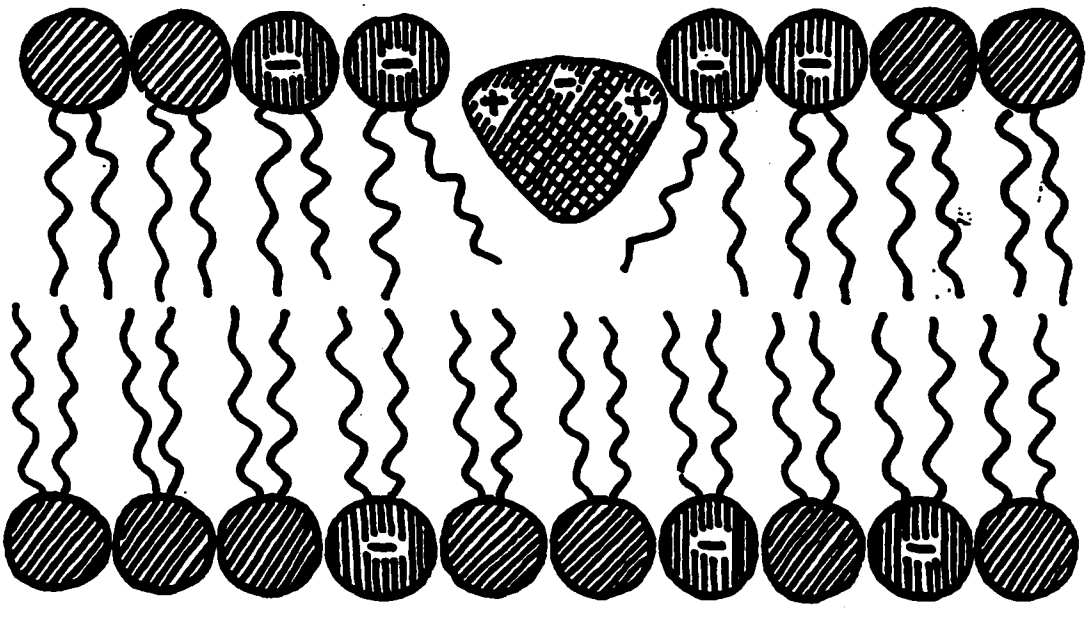

Figure 3.2.2.1. Possible mechanisms of peptide induced lateral lipid segregation. A. Shape complementarity. B. Charge-charge interactions. Vicinity of cationic amino acid residues is suggested to be enriched with anionic lipids relative to the rest of the membrane.

1992]. Comparing the efficiency of resonance energy transfer for different lipid types of probes, we can detect preferential association of peptides with particular lipid species.

The DMPC:DMPG (1:1) mixture had been studied as an example of an acidic lipid containing membrane. 18L is cationic and Ac-18A-NH_2 has positive charges at the peptide-lipid interface, although overall it is zwitterionic. For both peptides, the efficiency of transfer to APG was significantly higher than to APC, which is an indication of the preferential association of both peptides with acidic lipids (Fig. 3.2.2.2). Significant differences in the efficiency of energy transfer were also observed between Ac-18A-NH_2 and 18L, which we can attribute to the increased depth of incorporation of 18L into membranes. Originally peptides were added to the fluid membrane. If cooled down below phase transition, these peptides stayed kinetically trapped in the membrane. Energy transfer in the gel phase was larger than in the fluid state and the difference between two types of peptides and two types of probes was more pronounced than in the fluid phase.

We supposed that peptides can induce lateral lipid separation in the DOPC:DOPE (1:1) system as consequence of a shape compensation mechanism. However, coincidence of the efficiencies of transfer from peptide to APC or APE is indicative of complete mixing in this system (Fig. 3.2.2.3). Coincidence of the curves measured for two types of peptides indicates the similar depth of penetration of peptide tryptophan in the bilayer. This was also supported by the coincidence of tryptophan fluorescence spectra of both peptides associated with DOPC:DOPE (1:1) membranes. Since we have seen no evidence of preferential association of peptides with lipids according to a shape compensation mechanism, we conclude that effects of peptides on this membrane are mediated via

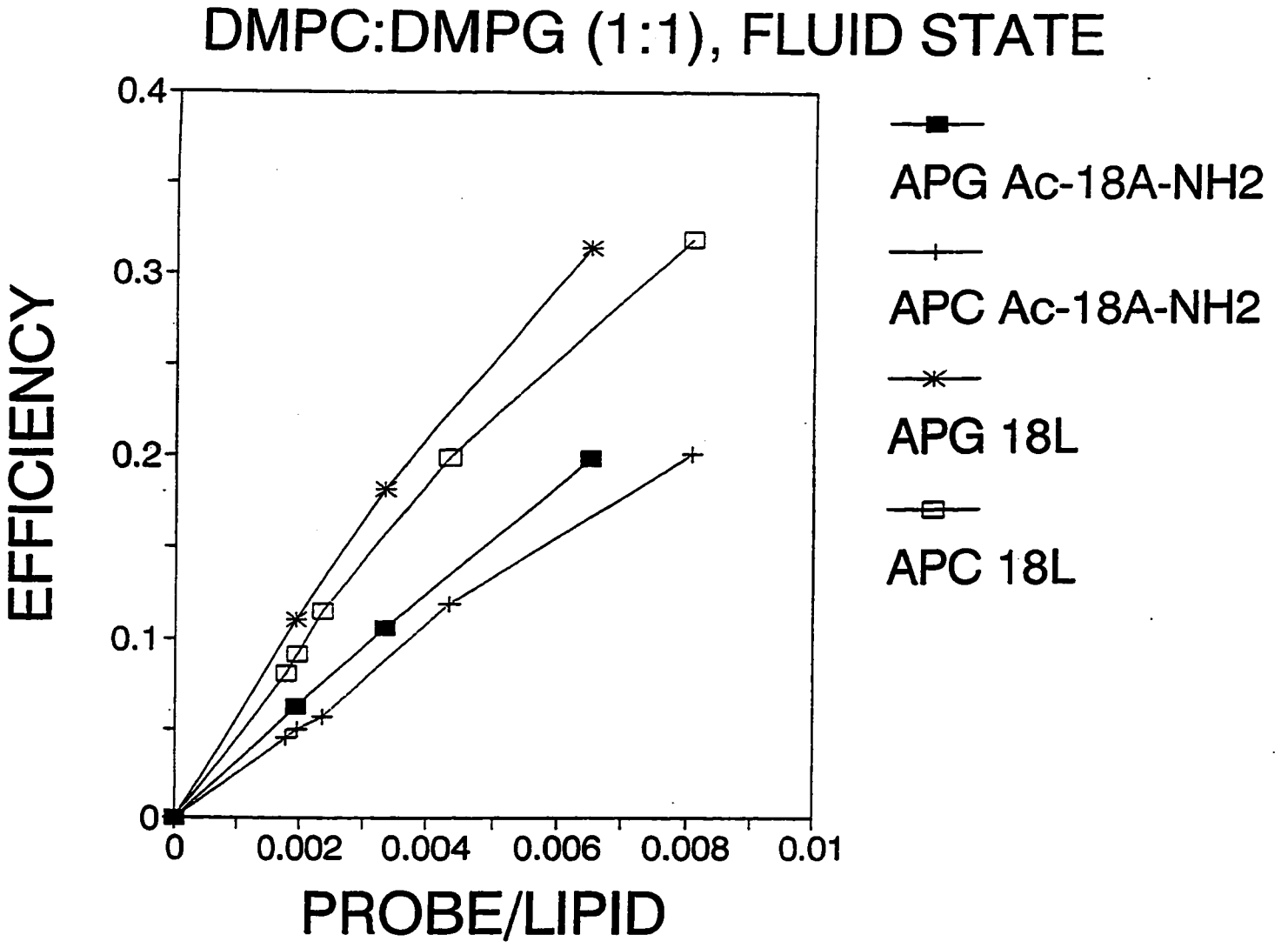

Figure 3.2.2.2. DMPC:DMPG (1:1) membrane, fluid state (37°C), peptide/lipid molar ratio - 1:10. Dependence of efficiency of fluorescence peptide to probe energy transfer on the molar fraction of probe in the membrane. Higher efficiency of energy transfer to the APG probe is indicative of the preferential association of both types of peptides with acidic lipids. Higher efficiencies observed for 18L are indicative of its deeper penetration into the bilayer.

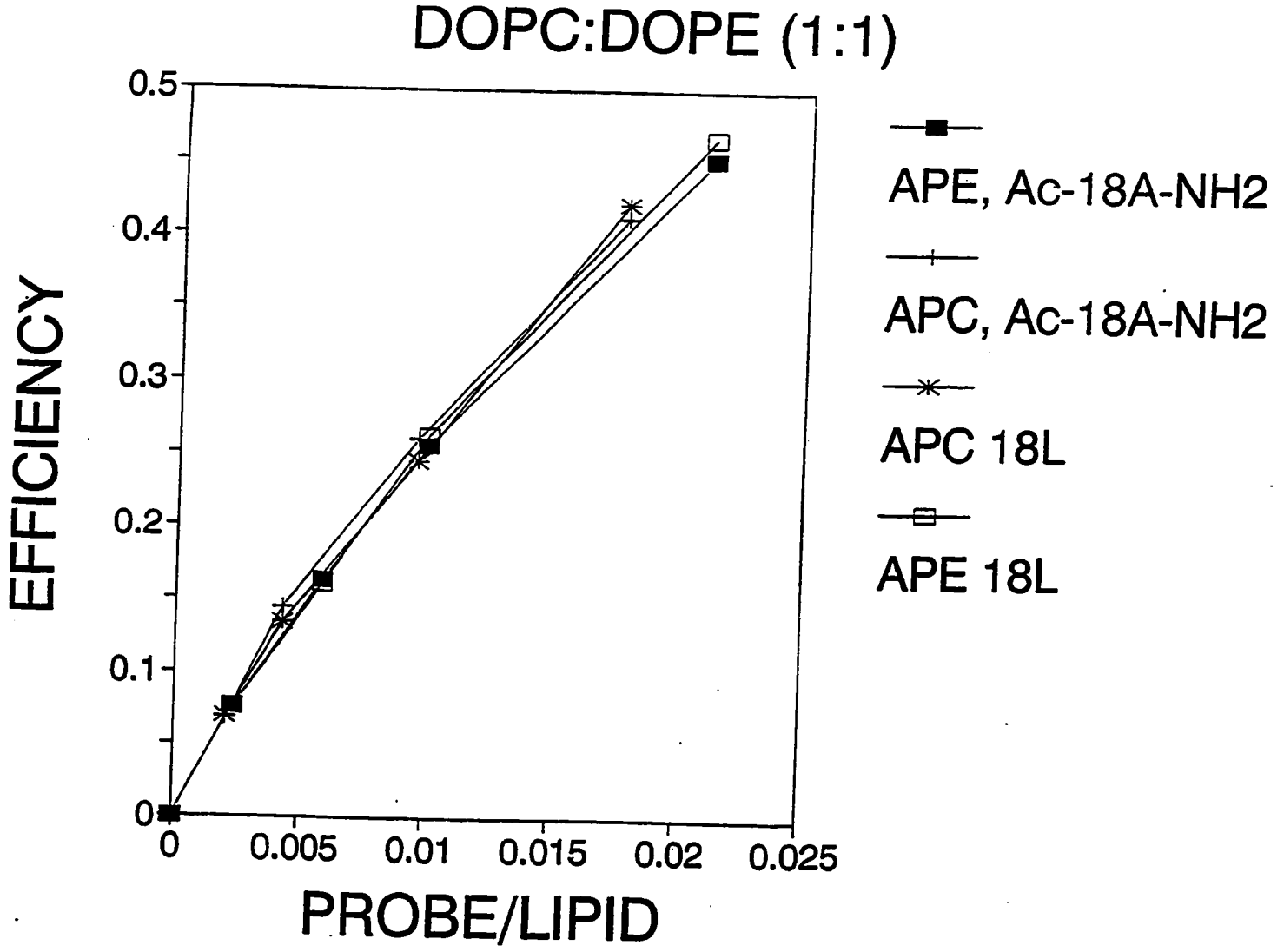

Figure 3.2.2.3. DOPC:DOPE (1:1) membrane, peptide/lipid ratio - 1:10. Dependence of efficiency of fluorescence peptide to probe energy transfer on the molar fraction of probe in the membrane. Coincidence of the efficiencies of transfer from peptide to APC or APE is indicative of the complete mixing in the system. Coincidence of the curves measured for two types of peptides indicates the similar depth of penetration of peptide tryptophan into the bilayer.

modulation of physical properties of the membrane as a whole rather than via membrane domain formation. A similar picture of the complete coincidence of energy transfer dependencies for APC and APE for 18L and Ac-18A-NH_2 was also observed with DMPC:DMPE (1:1) membranes.

To estimate the extent of demixing of lipid species in the presence of peptides, we used fluorescence energy transfer from anthrylvinyl-labelled to perylenoyl-labelled phospholipid probes. Efficiency of energy transfer is dependent on the average distance between donor and acceptor and thus is sensitive to deviations from the random distribution of probe. We titrated DOPC:DOPG (1:1) membranes with either APC/PPC or APG/PPC donor/acceptor pairs with peptides and monitored the change in energy transfer efficiencies in these systems (Fig. 3.2.2.4). We found that for both peptides, the relative decrease of transfer efficiency was the same for both pairs. Transfer efficiency is primarily sensitive to the surface density of acceptor (PPC in this case), which was the same for both donor acceptor pairs. However, transfer efficiency will be differently affected by separation or accumulation of donor or acceptor in the domains of the sizes of the Foerster radius (R_o). Thus the coincidence of the relative decrease in intensity suggests that there does not occur lateral separation on a scale larger than R_o, which is on the order of 44 Å for the anthrylvinyl/perylenoyl donor/acceptor pair [Smirnov et al., 1995]. Decrease in energy transfer efficiency between two lipid probes upon increase of membrane peptide content can be used to estimate the surface occupied by one peptide molecule upon membrane insertion as described in Materials and Methods. The relative decrease in transfer efficiency is plotted against the peptide/lipid ratio (Fig. 3.2.2.4). This gives the ratio of the surfaces

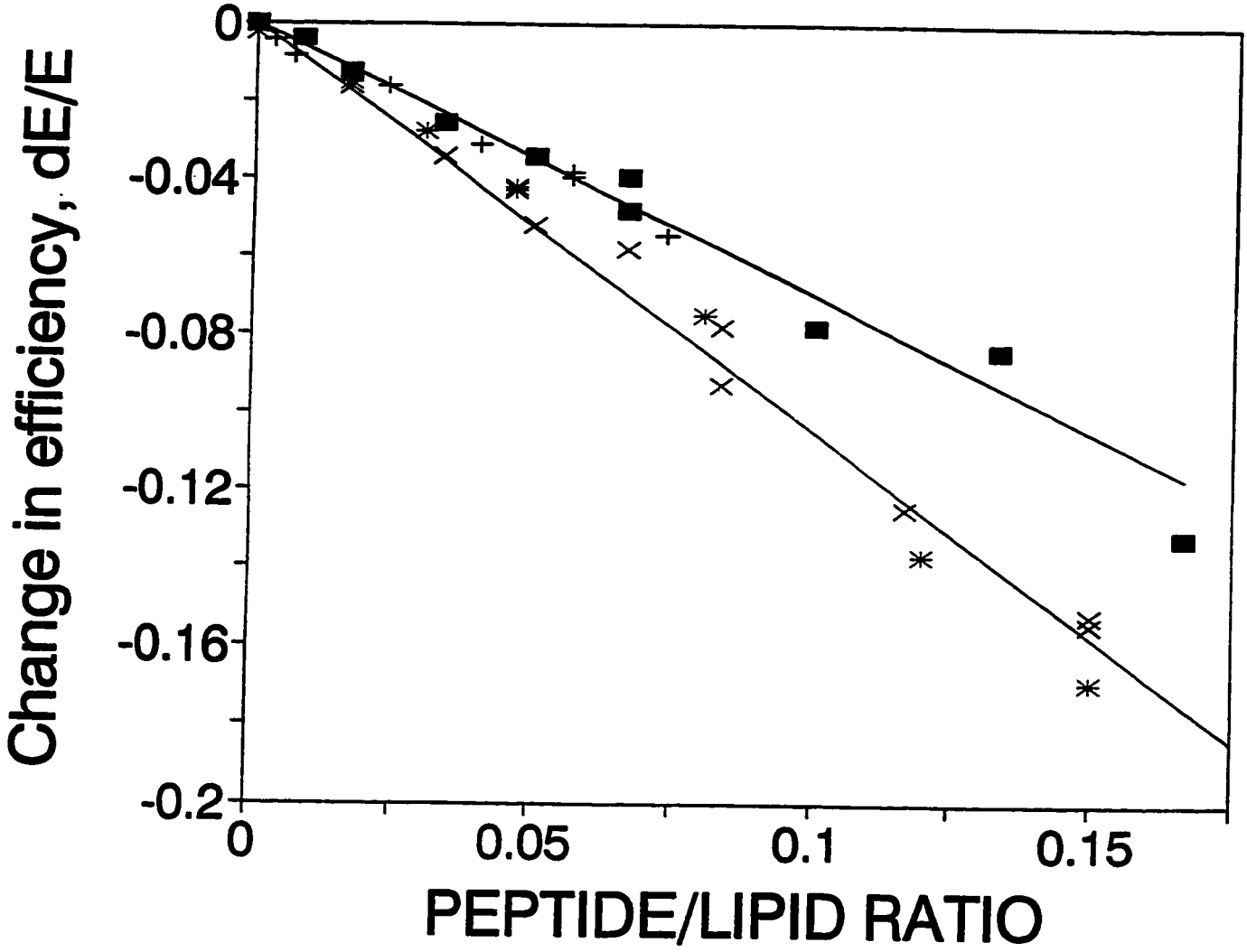

Figure 3.2.2.4. Changes in the efficiency of the fluorescence energy transfer from APC to PPC and from APG to PPC upon titration of DOPC:DOPG (1:1) LUV with amphipathic peptides. Decrease in efficiency is due to an increase in surface area of the bilayer upon peptide insertion. Titration with 18L: ■ - APC/PPC donor/acceptor pair, + - APG/PPC pair. Titration with Ac-18A-NH_2: ✳ - APC/PPC donor/acceptor pair, × - APG/PPC pair. Straight line were derived by linear regression, separate for 18L and Ac-18A-NH_2.

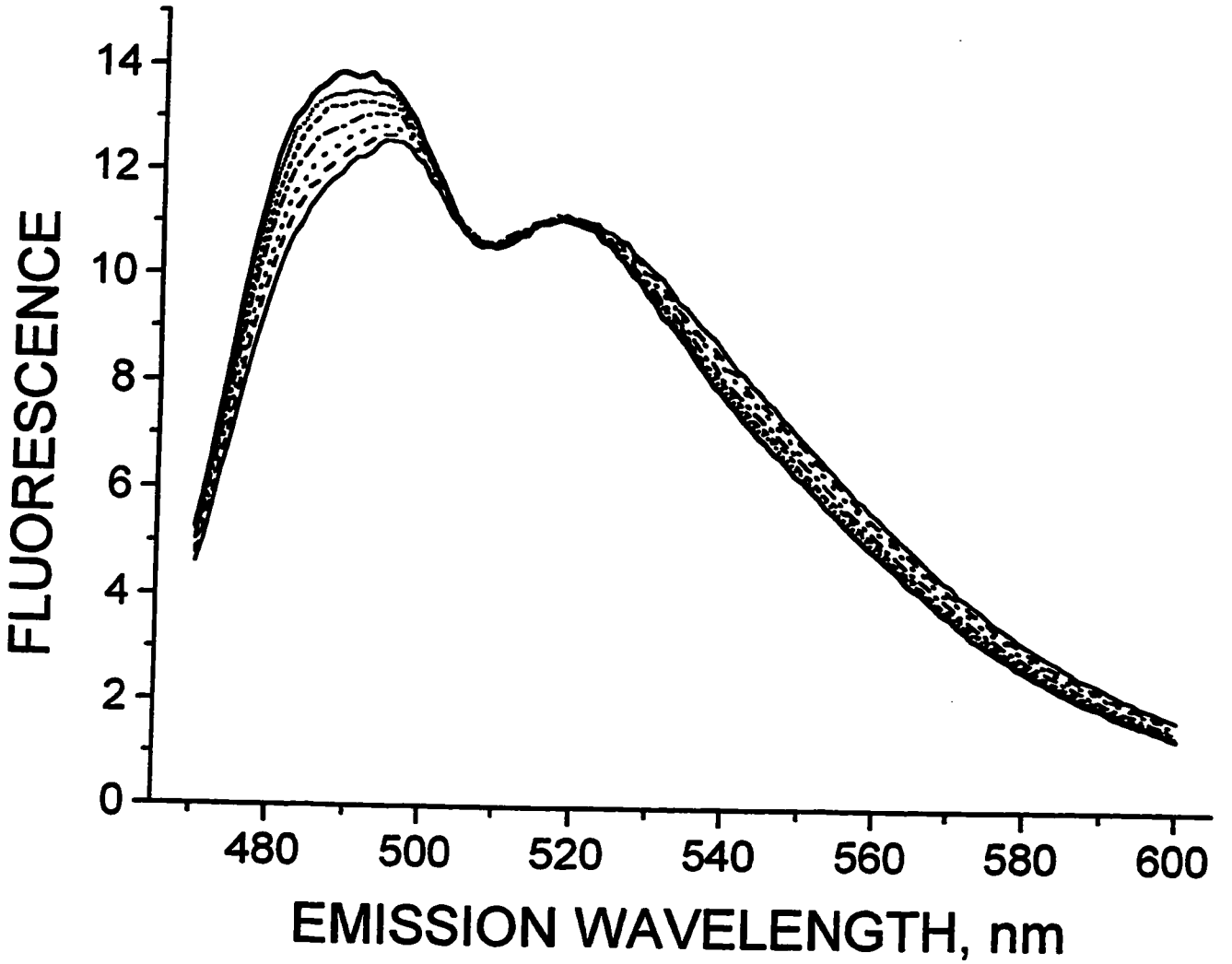

Figure 3.2.2.5. Changes in the shape of PPC fluorescence spectra in the process of titration of DOPC:DOPG (1:1) LUV with Ac-18A-NH_2 peptide. Curves correspond to the following peptide/lipid ratios: solid - 0, dashed - 1/60, dotted - 1/30 , dash-dotted - 1/20 , short-dashed - 1/15, short-dotted -1/12, heavy solid - 1/6.7. These spectral changes correspond to a decrease in polarity of the fluorophor environment.

occupied by one peptide and one lipid molecule. Both APC/PPC and APG/PPC donor acceptor pairs report a surface occupied by 18L $S_{18L} = 0.7\times S_l$ and by Ac-18A-NH_2 $S_{Ac\text{-}18A\text{-}NH2}=1.05\times S_l$ where S_l is the average surface per lipid molecule in this DOPC:DOPG (1:1) membrane. Values of 70±4 $Å^2$/lipid have been reported for DOPC in the L_α phase [Gruner et al., 1988]. There is no available data on the average surface per molecule in DOPG or DOPC:DOPG (1:1). For saturated PG (DPPG) in the gel phase, values of 48 $Å^2$ have been reported [Watts et al., 1981]. It is thus reasonable to estimate that the surface per lipid molecule in DOPC:DOPG (1:1) is within 50-70 $Å^2$.

An interesting related observation is that upon increase of peptide content in the membrane, changes in PPC fluorescence spectra (Fig. 3.2.2.5) indicated a decrease in the polarity of the environment of PPC. This is similar to the one that had been previously [Molotkovsky et al., 1987] interpreted as a decrease of water permeability and/or water content of the bilayer.

3.2.3 Peptide effects on the existing phase separation (gel-liquid crystal)

Preferential association of peptides with acidic lipids was capable of modulating a preexisting lateral organization of the membrane, that is in the course of the gel-liquid crystalline phase transition both peptides stabilized or destabilized the gel phase, depending on whether acidic lipids (PG) were the low or the high melting component (Fig. 3.2.3.1). Anisotropy of fluorescence of C_{12}- attached anthrylvinyl fluorophor has long been known to be sensitive to the phase state of the surrounding lipid [Bergelson et al., 1985; Polozov et al., 1994]. PC:PG vesicles labelled with APC or APG probes have been prepared.

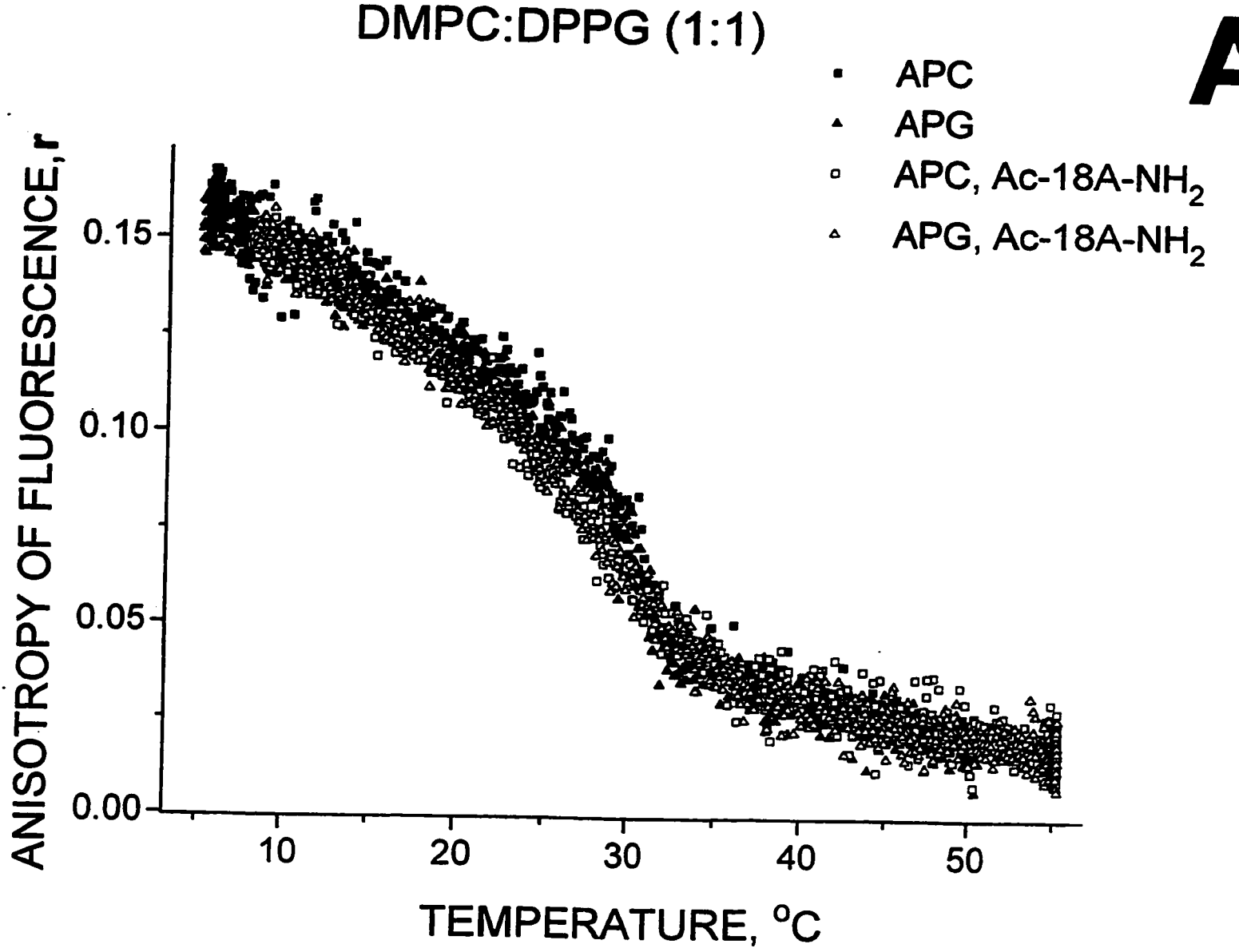

Figure 3.2.3.1. **A. DMPC:DPPG (1:1).** Temperature dependencies of anisotropy of fluorescence of probes APC and APG in DMPC:DPPG MLV in pure lipid membranes and in the presence Ac-18A-NH_2 (peptide/lipid molar ratio 1:10). Heat scans are shown.

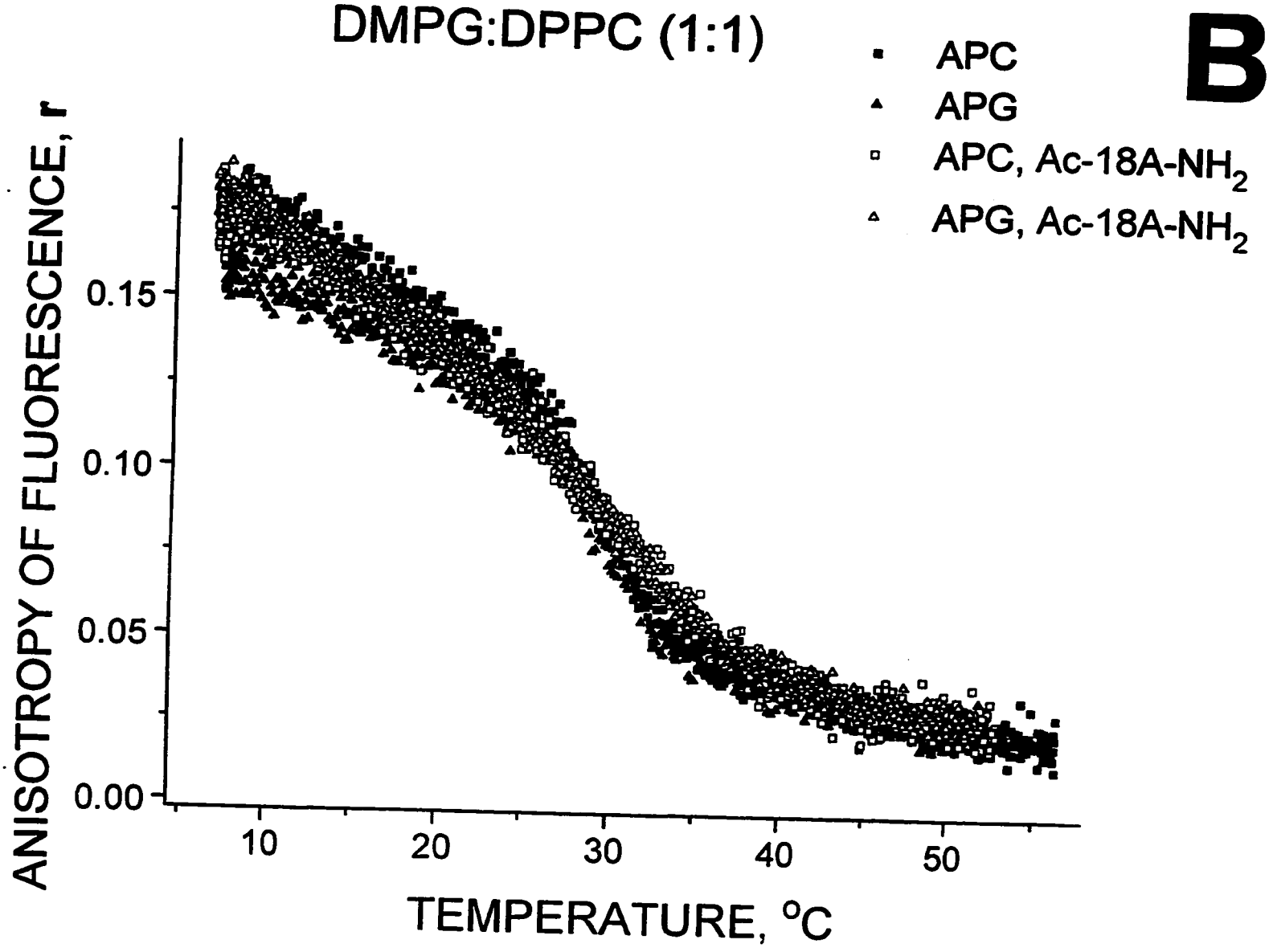

Figure 3.2.3.1. **B. DMPG:DPPC (1:1).** Temperature dependencies of anisotropy of fluorescence of probes APC and APG in DMPC:DPPG MLV in pure lipid membranes and in the presence Ac-18A-NH_2 (peptide/lipid molar ratio 1:10). Heat scans are shown.

PC:PG systems are often regarded as systems with almost ideal mixing. Thus phase transitions as reported by both APC and APG probes are essentially coincident. There was only a minor shift between cooling and heating scans. Addition of peptide similarly changed fluorescence anisotropy temperature dependencies reported by both probes, APC and APG. Ac-18A-NH_2 addition is shown in Fig. 3.2.3.1. Similar effects were observed upon addition of 18L. These findings are indicative of the very small size of domains formed by association of peptide with acidic lipids.

In the case when acidic lipids were the low temperature melting component (DMPG:DPPC, Fig. 3.2.3.1B), addition of peptide resulted in an increase of the temperature of completion of the phase transition. This can be explained as being due to depletion of the lower melting phase of acidic lipids because of specific peptide-lipid interactions.

In the case when acidic lipids were the higher melting component (DMPC:DPPG, Fig. 3.2.3.1A) or when both lipids had very close temperatures of the phase transition (DMPC:DMPG) the action of the peptide was similar to that of a general impurity. Namely, peptides cause a decrease in the cooperativity of the phase transition and decreased anisotropy values until the completion of the phase transition, the temperature of which was not affected significantly.

Contrary to what was found in acidic lipid-containing membranes, in the zwitterionic binary systems both peptides associated preferentially with the fluid phase. Both peptides affected the main phase transition of zwitterionic lipid systems (DMPC:DMPE, DMPC:DPPE) in the same way, decreasing both the temperatures of the

onset and the completion of the transition. DMPC:DMPE (1:1) has been long known as an example of non-ideal lipid mixing [Lee, 1975; Luna and McConnell, 1978; Polozov et al., 1994a]. Large hysteresis had been observed in this system. As expected for a non-ideal mixing system APC and APE probes report different phase transitions, shifted both in the onset and completion temperatures. Addition of peptide (18L on Fig. 3.2.3.2) decreases the difference in the anisotropy reported by different probes around the completion of the phase transition and it also broadens the phase transition and decreases the anisotropy values in the gel phase. On the whole, this is behaviour typical for impurities with preference for the fluid phase.

Besides anisotropy as an approach to study the temperature dependence of peptide-effects on membrane lateral organization, we used fluorescence energy transfer from APC or APG to PPC. The complexity of this approach is that the fluorescence properties of probes are temperature dependent and this dependence is also related to the phase state of the membrane. Thus external standards such as dilution with detergent are not so useful. Calculation of efficiency in this approach is also more approximate because instead of deconvoluting spectra we only measured intensity at two particular wavelengths, corresponding to anthryl (435 nm) and perylenoyl (510 nm) fluorescence. We neglect the dependence of quantum yield of perylenoyl fluorescence on temperature and medium polarity, which is not strictly correct. To get insight into the molecular organization of the membranes, we suggest comparing temperature dependencies of FRET efficiencies in the presence and in the absence of peptides. In DMPC:DMPG (1:1) vesicles, in the absence of peptides, the temperature dependencies of FRET efficiencies were similar for APC/PPC

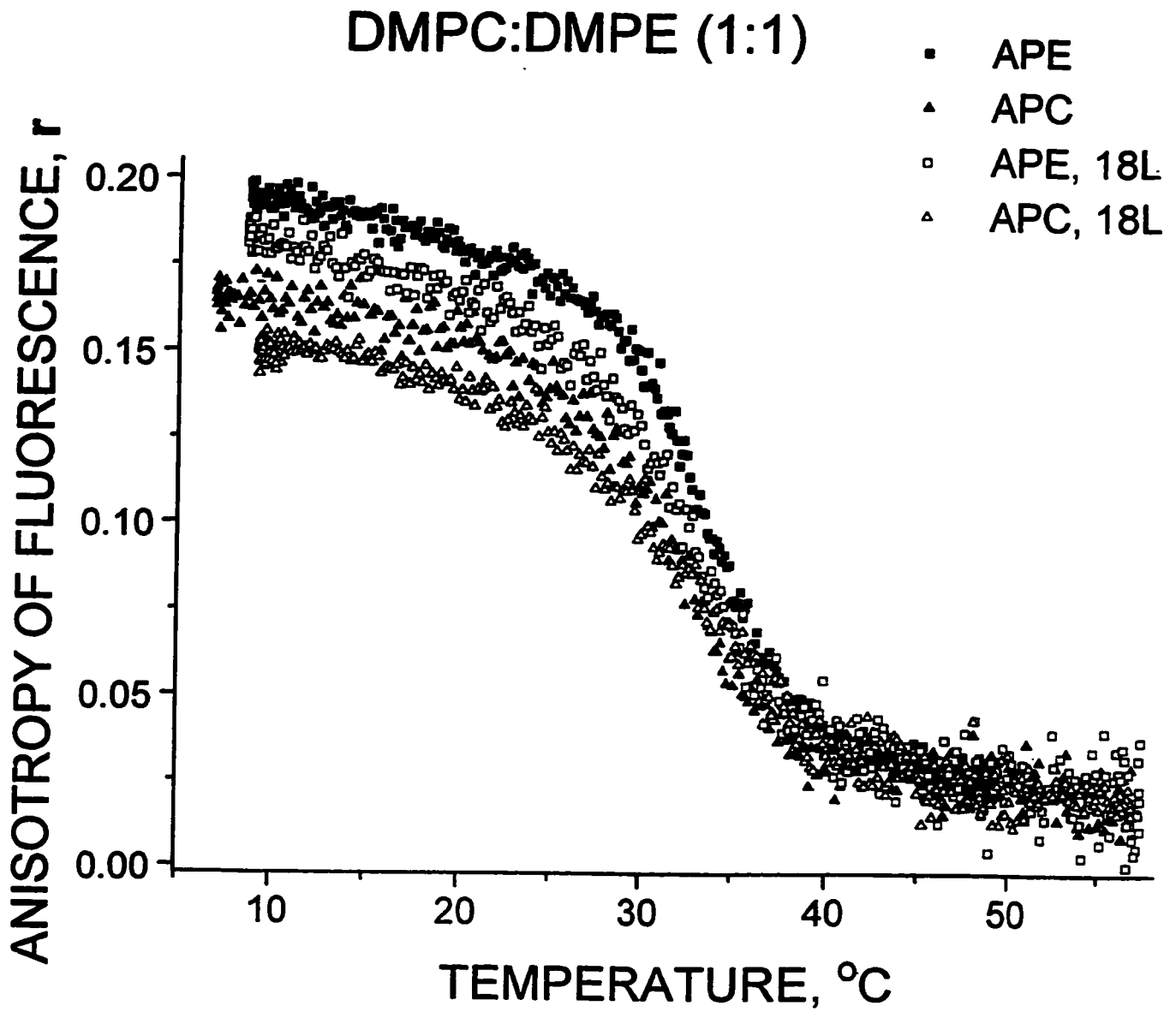

Figure 3.2.3.2 **DMPC:DMPE (1:1).** Temperature dependencies of anisotropy of fluorescence of probes APE and APC in DMPC:DMPE MLV in pure lipid membranes and in the presence 18L (peptide/lipid molar ratio 1:10). Heating scans are shown.

and APG/PPC donor/acceptor pairs (Fig. 3.2.3.3). However, 18L addition changed these dependencies in opposite ways. Upon heating without peptide, the efficiency was increasing several degrees below the main phase transition and decreasing with the onset of the phase transition. This decrease was essentially complete before the completion of the phase transition. After melting, the efficiency decreased slowly over a wide range of temperatures. There was very little hysteresis in this system, heating and cooling scans were nearly superimposable. In the fluid phase, addition of 18L (Fig. 3.2.3.3) decreased transfer efficiency due to the surface increase upon peptide incorporation in accordance with Fig 3.2.2.4. However, increase in transfer efficiency below the lipid phase transition was smoothed out for APC/PPC, while it was enhanced for APG/PPC. The temperature of maximum emission also shifted in different directions: from 17° to 18.5°C for APG/PPC, and from 18° to 16°C for APC/PPC. Difference between heating and cooling scans became more pronounced for APG/PPC, although it was shifted only 1°C. Similar changes were observed for the addition of Ac-18A-NH_2. These data are in agreement with anisotropy experiments (Fig. 3.2.3.1), which suggest that in this system peptide serves as a nucleation site for gel phase melting, and also with peptide-to-probe FRET experiments (Fig. 3.2.2.2) which suggest that the peptide environment is enriched in acidic lipids. Previously, we found that the PPC probe has some preference for the fluid phase [Polozov et al., 1994a]. Thus, the beginning of membrane melting in the presence of peptide, for the APG/PPC pair, results in the increased accumulation of both probes in the fluid phase (peptide vicinity) and consequently in the increase of E, relative to the one in the absence of peptide. Contrary to that, peptide domain formation will contribute to the demixing of donor and

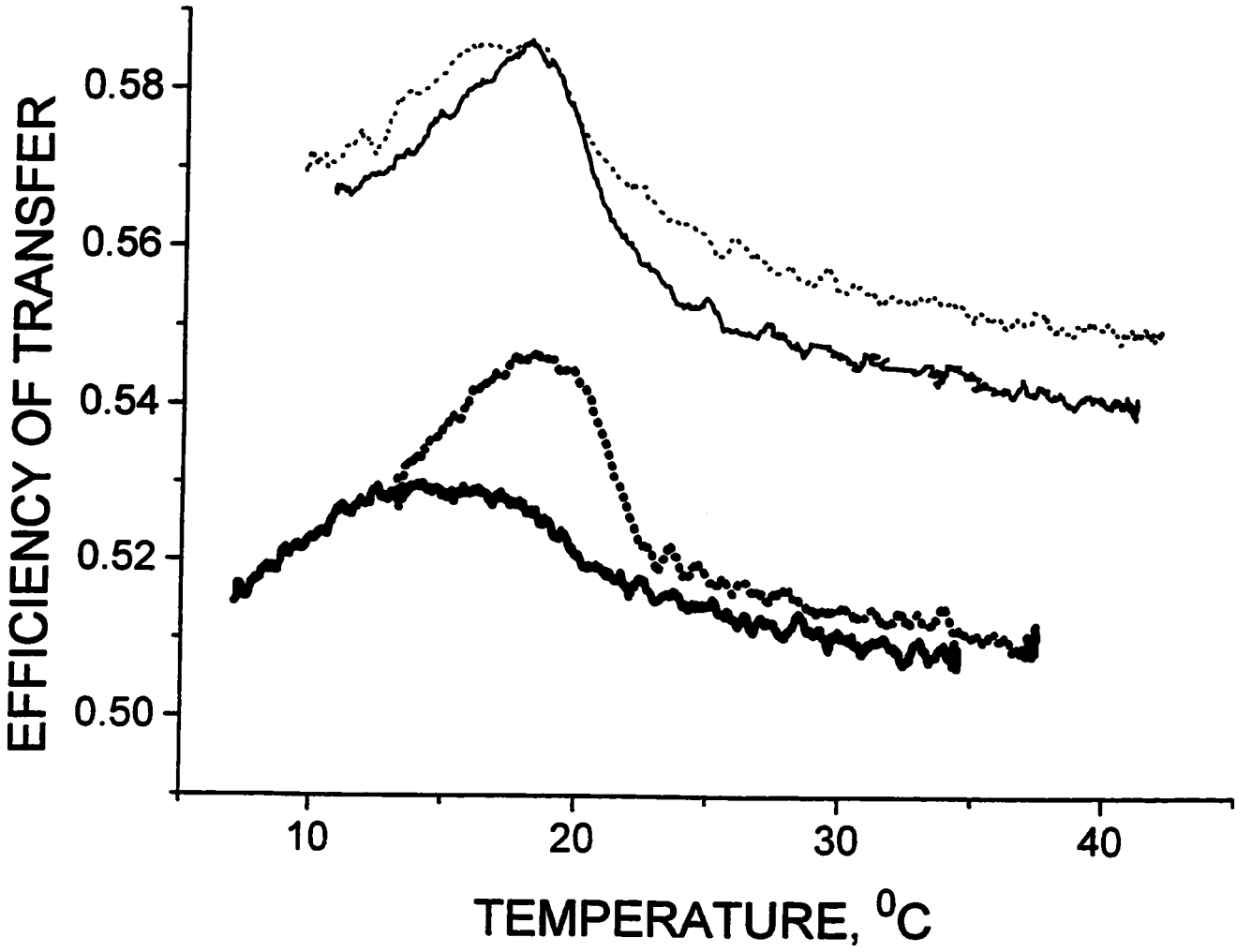

Figure 3.2.3.3 Temperature dependencies of the efficiency of the fluorescence energy transfer between two types of fluorescent lipid specific probes (APC (2 molar %) to PPC (1 molar %) (dotted lines) or APG (2 molar %) to PPC(1molar %) (solid lines) in the course of the main phase transition of DMPC:DMPG (1:1) LUV, lipid only systems (thin lines) or with molar 5% of 18L (bold lines). Heating scans are shown.

acceptor for the APC/PPC pair and thus to decrease of E(T), taking as a reference point the temperature dependence in the absence of peptide.

3.2.4 DISCUSSION (Lateral membrane organization)

Several fluorescence approaches were used to show that amphipathic peptides can induce lateral lipid separation in lipid membranes as well as modulate existing lateral organization in the membrane. Fluorescence detection is very sensitive to domain formation in the sense that the minimum domain lifetime to be detected is about the lifetime of the fluorophor excited state, that is on the scale of 10^{-8}s. Spacial resolution is about equal to the Foerster radius, that is 24 Å for the Trp-anthrylvinyl pair and 44 Å for the AV-perylenoyl pair. This means that the fluorescence method is sensitive to everything from membrane dynamic heterogeneity to stable domain formation on the scale of parts of the whole cell, although discrimination among the possibilities would require imaging methods. Our studies of binary lipid mixtures in the fluid phase thus indicate complete mixing of membrane components, both zwitterionic and anionic, in the absence of peptides. One can imagine three types of lateral organization: segregated, random and regular. In binary lipid mixtures, this approximately corresponds to preferences in like-like interactions, absence of preference, or preference of dislike interactions. Naturally, situations intermediate between described extremes are of biological relevance. Discussion of lateral organization in PE:PC systems usually centers around the possibility of segregation due to like-like association via the intermolecular hydrogen bond formation between PE headgroups. In the fluid phase of PE:PC mixtures we did not see any evidence of this type of association. Our data also rule

out any heterogeneity in DOPC:DOPE and DMPC:DMPE mixtures in the presence of peptides. The effects of L- and A-type amphipathic peptides on biological membranes and on model membranes with propensity for nonbilayer phase formation had been shown to correlate with the peptide modulation of intrinsic monolayer curvature (IMC) of the membrane [Tytler et al., 1993; Chapter 3.4]. Application of the IMC concept to a multicomponent system has to deal with the possible difference between short range order (local) and long range order (global) IMC, due to the lateral lipid domain formation. Our data on the complete lipid miscibility shows that a description in terms of global IMC can be applied, not only for single component systems (like Me-DOPE), but for binary and possibly multicomponent zwitterionic membranes.

Contrary to the case of zwitterionic PC:PE systems, in anionic PC:PG membranes both Ac-18A-NH_2 and 18L peptides affected membrane lateral organization. PC:PG membranes with identical or similar hydrophobic chains are usually discussed in terms of complete mixing [Findlay and Barton, 1978; Van Dijck et al., 1978] or regular lateral organization [De Bony and Tocanne, 1984]. It should be noted that macroscopic methods, like DSC, often used for analysis of lipid phase behavior are not easily discriminating these two types of organization [Raudino, 1995]. Electrostatic repulsion between anionic PG headgroup is a natural reason why these membranes have this motif of regular lateral membrane organization. Both Ac-18A-NH_2 and 18L have basic residues (lysines). In the membrane associated state, electrostatic interactions of peptide lysines with anionic lipids would result in accumulation of acidic lipids in peptide vicinity. The size of these domains enriched in acidic lipids is not larger than the Foerster radius for the

anthrylvinyl-perylenoyl donor-acceptor pair, as we had not seen significant lipid demixing in peptide titration experiments. Enrichment of the vicinity of the peptide with acidic lipids can be estimated from the data in Fig. 12. The efficiency of FRET from tryptophan to APL is primarily dependent on the surface density of APL in the vicinity of the peptide molecules, namely within R_o (~24 Å) distance around the peptide tryptophan. $E \approx \sigma_{local}$, is different from σ_o in the absence of peptide. As long as APL follows the distribution of the host PL, $\sigma_{local} = \sigma_o \cdot c_l / c_o$ where c_l is the concentration of host lipid in the vicinity of the peptide and c_o - host lipid concentration in the absence of peptide. From this we can conclude that the ratio of the FRET efficiencies derived by different probes directly corresponds to the ratio of two types of host lipids in the vicinity of the peptide: $E_{APC}/E_{APG} = (c_{l,PC}/c_{o,PC})/(c_{l,PG}/c_{o,PG}) = c_{l,PC}/c_{l,PG}$ since $c_{o,PC} = c_{o,PG}$ in this DMPC:DMPG (1:1) system. Comparing the slopes of $E(\sigma)$ dependencies (Fig. 3.2.2.2) we get $c_{l,PC}/c_{l,PG}=0.75$ for Ac-18A-NH_2 and 0.7 for 18L. This estimate is only a minimum for the case in which the actual domain arrangement is restricted to the area of less than the Foerster radius, that is if the actual organization is close to the stoichiometric association of acidic lipids with cationic residues of the peptide. Indication that peptide effects are pronounced at larger distances comes from data on bilayer expansion on peptide insertion. In this case, relatively low enrichment of acidic lipids suggests the dynamic character of this lateral domain structure.

Low values of bilayer surface expansion upon peptide insertion are indicative that peptide insertion is accompanied by more dense packing of the bilayer. In the absence of peptides, besides just steric considerations, charge-charge repulsions between charged lipid

molecules affect the surface area per molecule. Insertion of the peptide reduces lipid-lipid repulsion in the vicinity of the peptide and thus reduces the surface area per lipid molecule around the peptide. This results in apparent reduction of the measured surface occupied by one peptide molecule. More dense packing of the bilayer is also reflected in the spectra of the perylenoyl probe which corresponds to a less polar environment (Fig. 3.2.2.5). Bilayer thinning upon the insertion of amphipathic peptides into the membrane had been previously reported [Ludtke et al., 1995; Wu et al., 1995]. In the case of our peptides, the nominal ratio of total molar weight to total membrane surface increases even without thinning. This consideration suggests an increase in the packing density in the hydrophobic part of the bilayer.

The larger surface increase by Ac-18A-NH_2 is predictable since its hydrophilic surface is larger than that of 18L; there are 8 charged residues in this peptide compared with 4 in 18L. Also, the zwitterionic peptide Ac-18A-NH_2 is less potent than cationic 18L in screening anionic lipids. The small surface area occupied by the peptide also confirms the "snorkel hypothesis" of Venkatachalapathi et al. (1993) that the long hydrophobic part of the lysine side chain contributes to the insertion of the peptide.

Creation of domains is entropically unfavorable. Strong interactions, such as charge-charge interactions are required to cause preferential peptide-lipid association. More pronounced peptide effects are observed around the main phase transition of the bilayer, a state which is intrinsically susceptible to large fluctuations. Generally, peptide insertion reduces transition cooperativity. However, in other respects peptide effects are dependent on the lipid system. In zwitterionic PC:PE systems known for nonideality of

mixing, peptide addition reduces the difference in the PC and PE probes environments (Fig. 3.2.3.2), that is the peptide increases mixing in this system. Peptide preference for the fluid phase is expected since peptides can not stabily incorporate into the gel phase (Fig. 3.2.1.1 and 3.2.1.2). Along with this general fluid phase preference, peptide-lipid charge-charge interactions affected lateral membrane organization in the course of the main phase transition. When acidic lipids were the low melting component of the lipid mixture, peptide-acidic lipid interactions resulted in depletion the low melting component from the gel phase and thus shifting the completion of the phase transition to the higher temperatures. When acidic lipids were the high melting component of the binary mixture, peptide addition resulted in the broadening and shifting to lower temperatures of the onset and T_m of the transition. Contrary to the PC:PE system, in the PC:PG systems anisotropy values of the APC and APG probes essentially coincided, and there was only very small differences between heating and cooling scans. This also indicates a high miscibility in this system. While peptide affected the phase transition in these systems there was no detectable difference between the anisotropy measured by APC and by APG. This also indicates the nanoscopic scale of lateral organization, that is, there was no area within separated domains which is screened from lipids in other domains and thus maintain different motional order.

Despite belonging to different classes of amphipathic helices and opposing activities on biological, or model zwitterionic membranes, both 18L and Ac-18A-NH_2 peptides have similar effects on membrane lateral organization. Charge-charge peptide-lipid interactions are capable of modulating lateral membrane organization both in the fluid state and in the course of the main phase transition. While the size of hydrophobic and hydrophilic domains

of amphipathic peptides determine peptide activities, these geometrical factors alone, contrary to electrostatic interactions, are unable to induce demixing of membrane lipid components. Peptides were actually found to increase lipid mixing in membranes known for nonideality of mixing (DMPC:DMPE). Absence of complex lateral organization in zwitterionic fluid binary lipid mixtures supports the validity of a description of peptide-membrane interactions in terms of affecting parameters of the membrane as a whole, such as intrinsic monolayer curvature modulation.

3.3 Mechanism of Membrane Permeabilization by 18L Peptide

High membrane affinity of 18L [Chapter 3.1.2, Table 3.1.2.1] makes possible a choice of conditions for membrane permeabilization studies, such that the peptide is essentially all bound to the membrane, i.e. the total peptide/lipid ratio is the same as the bound peptide/lipid ratio.

3.3.1 18L-induced vesicle contents leakage

An insight into the mechanism of action of lytic peptide can be derived from the analysis of peptide-induced vesicle content leakage [Parente et al., 1990]. The most important feature is the range of leakage-inducing peptide/lipid ratios, as well as if leakage is gradual or follows an all-or-none mechanism. Also characteristic is the dependence of leakage on vesicles size and on lipid concentration.

We studied 18L-induced leakage for vesicles of different lipid composition [Chapter 3.4]. As a typical zwitterionic lipid system, where one can also observe a

reciprocal effect of 18L and Ac-18A-NH_2, we have chosen DOPC:DOPE 1:1 LUV for detailed studies. We found that high (~1:20) peptide/lipid molar ratios are required to observe a fast rate and a considerable extent of 18L-induced ANTS/DPX leakage from the DOPC:DOPE 1:1 LUV (Fig. 3.3.1.1). At lower bound peptide/lipid ratios, leakage proceeds slowly, on the scale of thousands of seconds. Leakage curves were found to be only modestly sensitive to the size of the vesicles at a constant peptide/lipid ratio and lipid concentration.

To discriminate between a gradual or an all-or-none vesicle leakage mechanism, we needed to stop leakage and separate partially leaked vesicles from the leaked content. We used peptide digestion by trypsin as a method to stop leakage and to seal vesicles. Trypsin was added to vesicles at various times after initiation of leakage. Vesicles were then separated from the media by gel filtration and analyzed for the degree of ANTS quenching [Table 3.3.1.1]. An all-or-none mechanism of leakage would result in the no change of quenching, unlike the case of the gradual leakage from all of the vesicles [Table 3.3.1.1]. Several factors contribute to the deviation of the experimental values from Stern-Volmer theory and increase the uncertainty in the determination of quenching. However, they are insignificant for the validity of a general conclusion that the mode of 18L-induced leakage is gradual.

A peculiar dependence on total lipid concentration was found for 18L-induced leakage (Fig. 3.3.1.1C). At constant peptide/lipid ratios, the extent and the rates of leakage at low lipid concentrations (Fig. 3.3.1.1A) were higher than those at high lipid concentration (Fig. 3.3.1.1B). In addition, the extent of leakage at a fixed long time

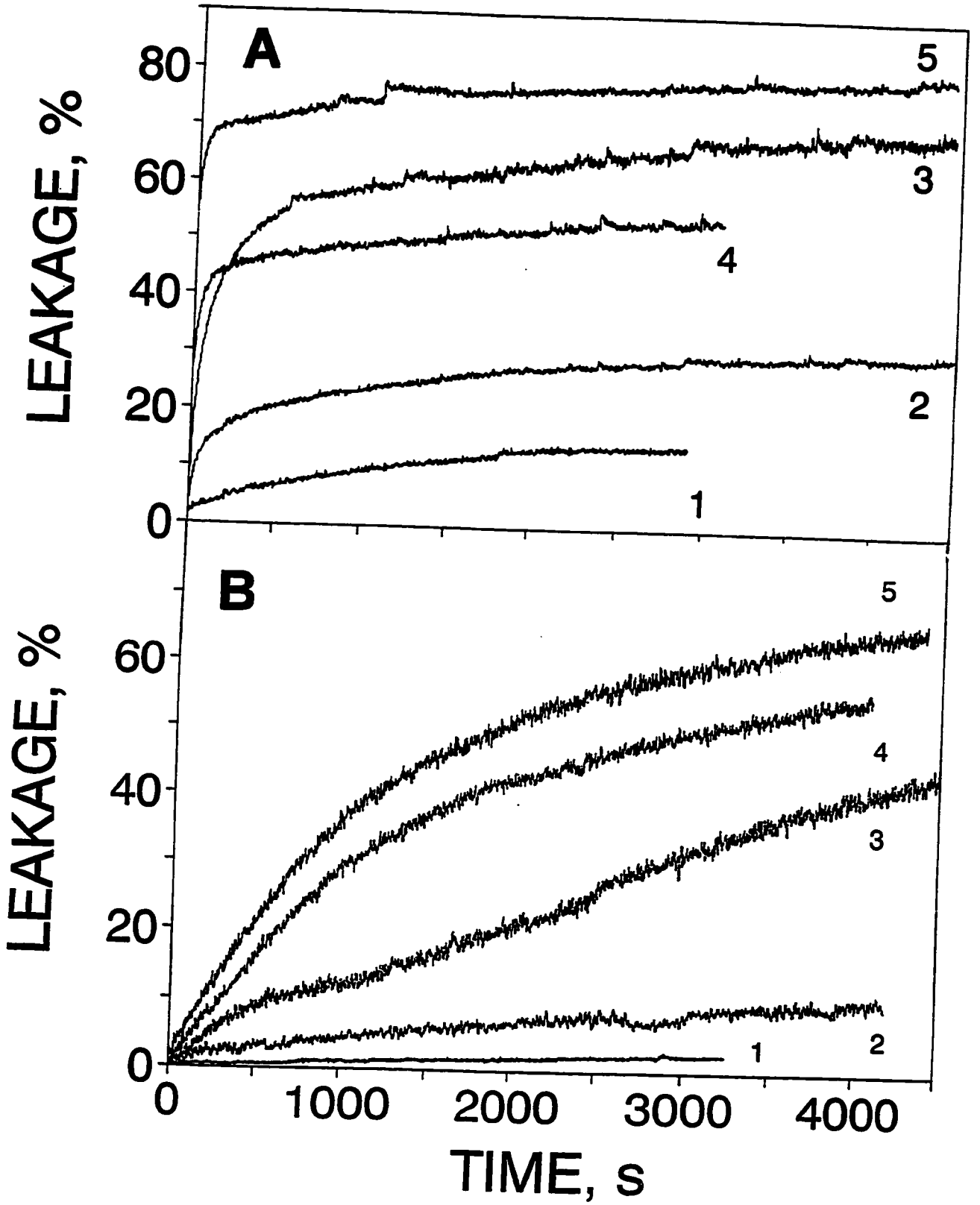

Figure 3.3.1.1 ANTS/DPX assay for 18L-induced aqueous contents leakage of DOPC:DOPE (1:1) large unilamellar vesicles for various peptide-lipid ratios. See next page for details.

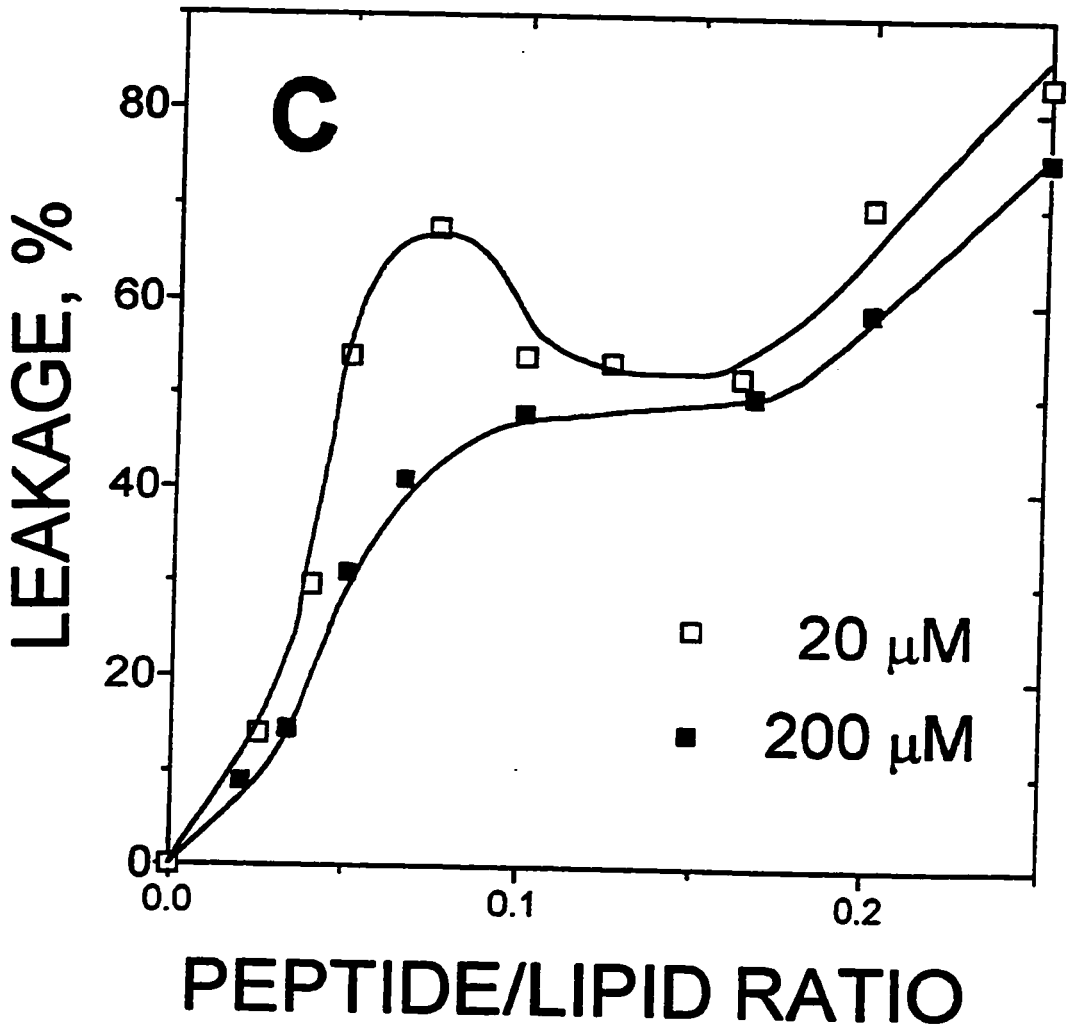

Figure 3.3.1.1 ANTS/DPX assay for 18L-induced aqueous contents leakage of DOPC:DOPE (1:1) large unilamellar vesicles for various peptide-lipid ratios. **A.** Lipid concentration 20 μM. Typical leakage time traces for various peptide concentrations. Peptide/lipid molar ratios were 0.025 for the curve 1, 0.04 for the curve 2, 0.075 for the curve 3, 0.125 for the curve 4 and 0.25 for the curve 5. **B.** Lipid concentration 200 μM. Typical leakage time traces for various peptide concentrations. Peptide/lipid molar ratios were 0.01 for the curve 1, 0.02 for the curve 2, 0.05 for the curve 3, 0.1 for the curve 4 and 0.2 for the curve 5. **C.** Dependence of percent of 18L-induced ANTS/DPX leakage observed at 3,000 s on peptide/lipid ratios. Lipid concentration 20 μM. (■), 200 μM (□). 18L is more than 95% bound under the experimental conditions. Thus the total peptide/lipid ratio coincides with bound peptide /lipid ratio.

Table 3.3.1.1 Mechanism of 18L-induced leakage. Predicted ANTS fluorescence quenching in vesicles leaking gradually or according to an all-or-none mode of leakage and comparison with experiment.

Percent of Leakage (%)	Expected degree of quenching[d]		
	Gradual mode[a]	All-or-none mode[b]	Experimental observation[c]
0	1:9.5	1:9.5	1:10 - 1:8
30	1:7.6	1:9.5	1:5-1:6
50	1:5.75	1:9.5	1:3-1:4
70	1:3.85	1:9.5	1:2-1:3
90	1:1.95	1:9.5	1:1.5-1:2

[a] Extent of quenching for the gradual mode of vesicle leakage was calculated using the Stern-Volmer equation, assuming dynamic quenching of ANTS by DPX, as determined by Smolarsky et al. (1977).

[b]No change is expected in the ANTS quenching, since vesicles are either intact or leaked completely

[c]Increase in the uncertainty of quenching arises from the additional background fluorescence from trypsin and from sample dilution on passage through the column as well as from possible incomplete termination of leakage by trypsin. Range of the observed values shown.

[d]Given as the ratio of fluorescence of vesicle contents before and after solubilization of the vesicles by Triton X-100. Measurements were made after termination of leakage by addition of tripsyn and removal of extravesicular probes by gel filtration

point at 2000 s was found to be nonmonotonic over the peptide-lipid ratios used (Fig. 3.3.1.1C). With an increase in the peptide/lipid ratio, leakage goes to about 50% and then passes through a plateau (for 200 μM) or minimum (for 20 μM) and then grows to 100% at bound peptide/lipid ratios around 1:5. (Fig. 3.3.1.1C). We thought that such a behaviour can be due to interference with other membrane effects induced by 18L such as with fusion. We hence studied fusion in more detail.

3.3.2 18L-induced vesicles fusion

Using the lipid mixing assay we found that, indeed, 18L causes membrane fusion at approximately the same peptide/lipid ratios as used for contents leakage. At constant peptide/lipid ratios the extent and the rate of fusion increased with an increase in lipid concentration. At 200 μM DOPC:DOPE, 1:1, the LUV fusion rate was comparable and somewhat faster than the rate of aqueous contents leakage (Fig. 3.3.2.1 and Fig. 3.3.1.1B).

To confirm the existence of fusion, and also to look at structures formed at high peptide-lipid ratios, we conducted electron microscopy studies. Micrographs of DOPC:DOPE LUV clearly show the fusion of vesicles in the presence of 18L (Fig. 3.3.1.2). It is remarkable that even at very high peptide to lipid molar ratios of up to 1:3 (which is close to 1:1 on a weight basis) there is an apparent retention of a vesicular morphology. No micelles or inverted phase formation were observed. Though, due to the time scale of sample preparation, we were unable to capture intermediate structures and show only final equilibrium structures.

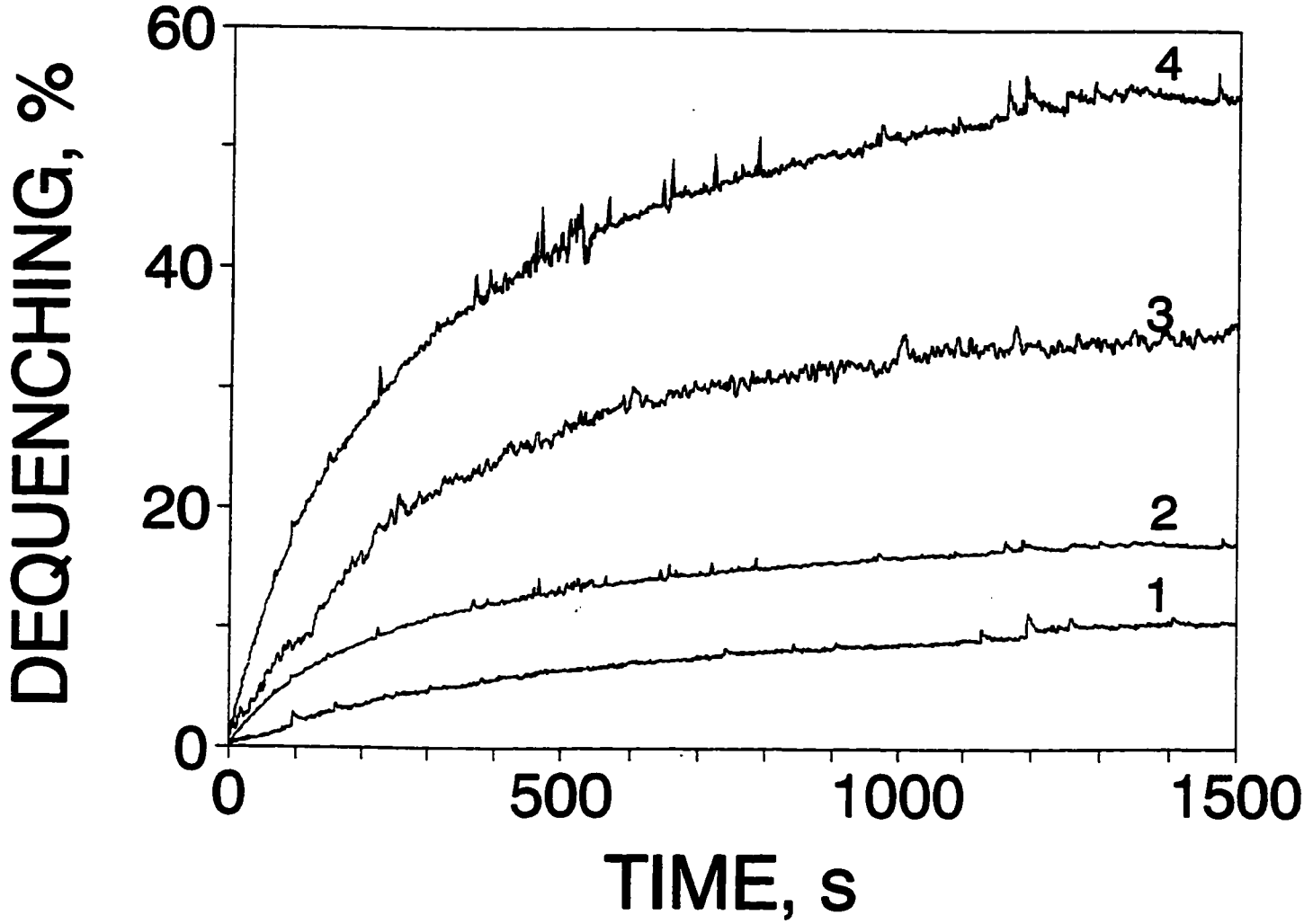

Figure 3.3.2.1 DOPC:DOPE (1:1) LUV fusion induced by 18L monitored by a lipid-mixing assay, based on dequenching of anthrylvinyl fluorescence from anthrylvinylphosphatidyl-choline (APC)-labelled liposomes upon fusion with unlabelled liposomes. Lipid concentration 200 μM, Peptide/lipid ratios were 0.004 for curve 1, 0.01 for curve 2, 0.04 for curve 3 and 0.09 for curve 4 (18L is more than 95% bound under the experimental conditions).

We also studied if 18L induces mixing of aqueous contents of fusing vesicles. The ANTS/DPX assay, based on the quenching of ANTS fluorescence by DPX upon vesicle fusion, showed 5%-10% fusion, despite the fact that 18L also causes vesicle leakage. To confirm that this decrease was not an artifact due to changes in light scattering upon vesicle aggregation and/or fusion, we employed the Tb-DPA aqueous contents mixing assay. Contrary to the ANTS/DPX assay, this assay is based on a fluorescence increase upon mixing of Tb^{3+} and DPA, initially encapsulated in separate vesicles. Formation of a Tb-DPA complex can occur both as a result of membrane fusion as well as a result of leakage, albeit with a much lower efficiency in the latter case. At constant lipid concentration the rate of fluorescence increase depended on the amount of peptide added (Fig. 3.3.1.3). At low ratios, a slow increase in fluorescence was observed. At ratios approximately corresponding to the plateau on the profile of the ANTS/leakage assay, we observed a fast increase in fluorescence followed by a subsequent decay. At higher ratios the decay was followed by a slow increase. At still higher ratios, the biphasic behavior changed to a fast increase without decay. While we can not distinguish between a monotonous increase due to leakage or due to fusion, we can definitely assign biphasic behavior to fast fusion followed by leakage. While it is difficult to quantitate the percent of fusion in this assay, it can be estimated as being close to 5-10%, similar to that reported by the ANTS/ DPX assay.

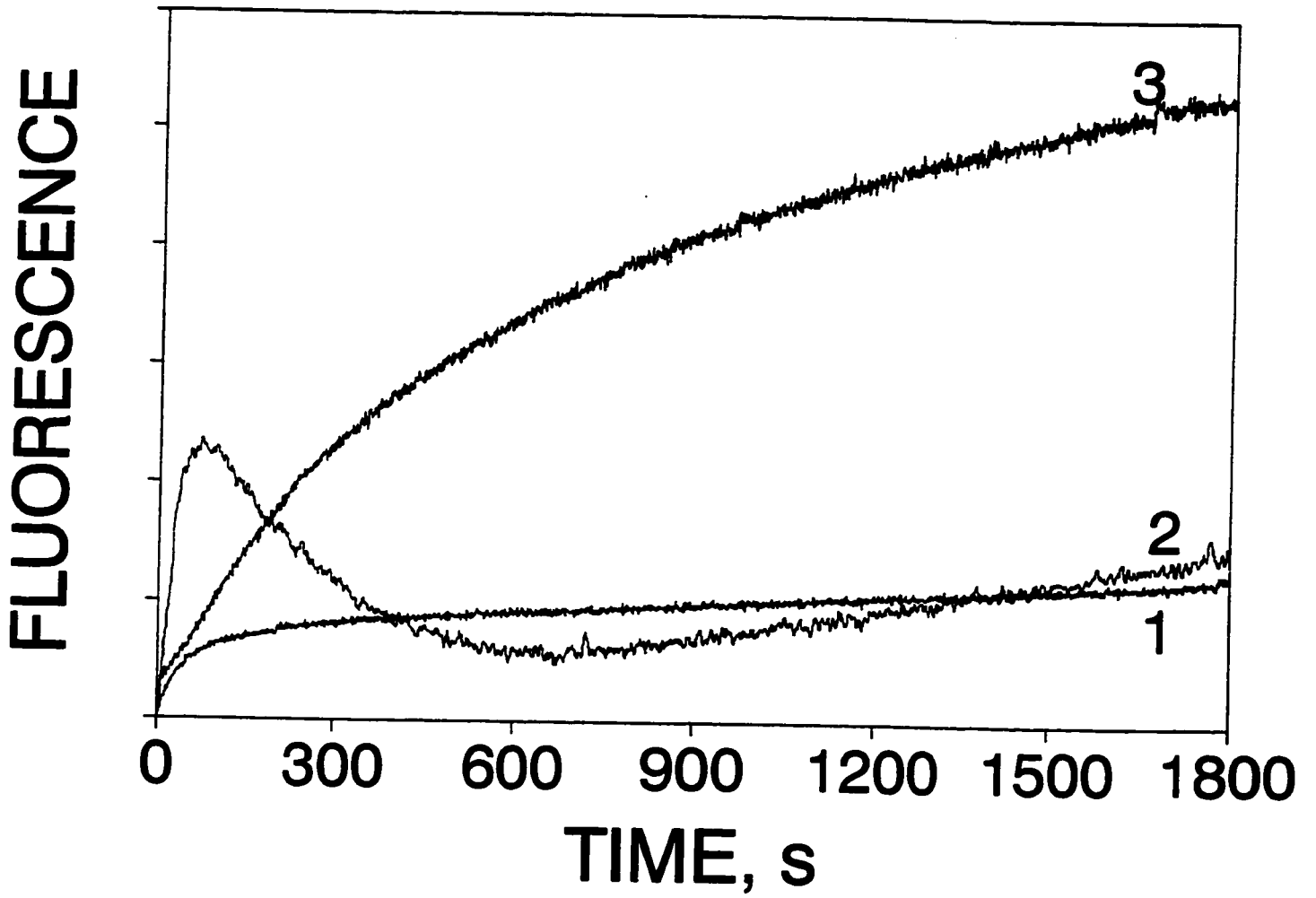

Figure 3.3.2.3 18L-induced vesicles aqueous contents mixing monitored by the Tb/DPA fusion assay. Lipid concentration 200 μM. Peptide/lipid ratios: 1 - 0.01; 2 - 0.05; 3 - 0.075. (see text)

3.3.3 The size of 18L-induced membrane defects

To estimate the size of 18L-induced membrane pores or bilayer defects we employed two additional assays - a potential release assay and the leakage of fluorescent dextrans. The potential release assay was used to see if there was any increase in ion permeability at peptide-lipid ratios less than those required for ANTS/DPX leakage. This assay requires the presence of a membrane potential in the vesicles prior to the addition of peptide. To diminish mixing artifacts, peptide was injected in a large volume of buffer (0.5 ml). The extent of potential release as a function of peptide/lipid ratio did not show any significant ionophoretic activity of 18L at peptide/lipid ratios below those required for ANTS/DPX leakage (Fig. 3.3.3.1). To estimate the upper boundary of the size of the 18L-induced defects we studied release of fluorescently modified dextrans (FITC-dextrans) of molecular weights of 3,000, 10,000 and 20,000. 18L was able to cause leakage of all of these molecules, which suggests that the size of the defects formed is sufficient for the release of at least 20,000 MW Dextrans. To ensure comparison with the potential release assay, we performed this assay at the same lipid concentrations and with the same peptide injection mode. The extent of dextran leakage (M.W. 20,000) as a function of peptide/lipid ratio essentially coincides with the plot for the potential release assay (Fig. 3.3.3.1). This coincidence, taken together with the similarity of leakage plots for dextrans of various sizes, suggests that 18L does not form small membrane pores, capable of releasing ions but not dextrans.

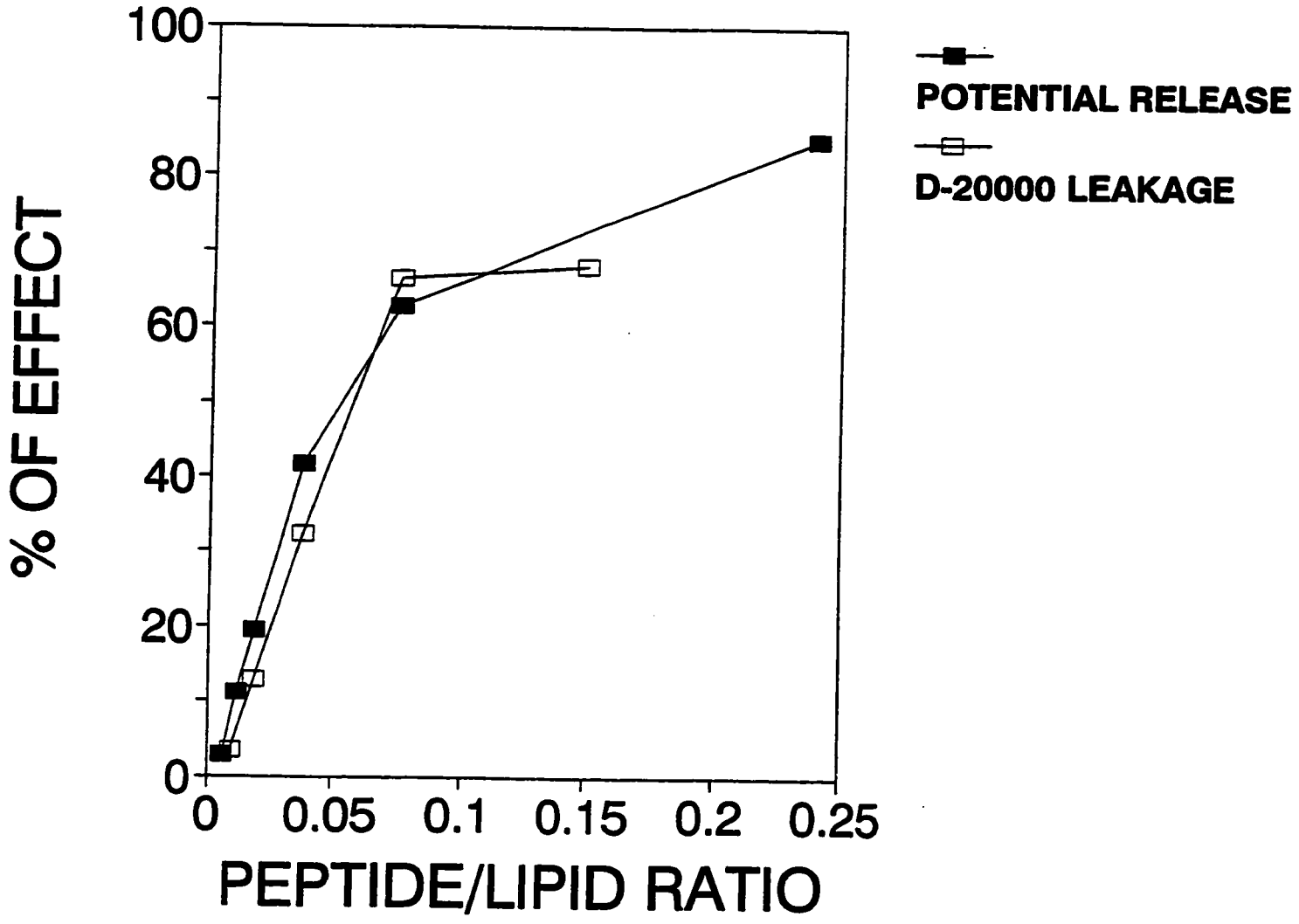

Figure 3.3.3.1. Percentage of FITC-dextran (D-20,000) leakage and of membrane potential release at 2,000 s after 18L addition for various peptide-lipid ratios. Time traces are not shown. Lipid concentration (20 μM) and the method for peptide-lipid mixing was the same in both assays (see Materials and Methods).

3.3.4 Long term permeabilization

As had been pointed out by Matsuzaki et al. (1995) leakage of entrapped aqueous contents of vesicles is a relaxation process. He proposed that leakage induced by magainin I occurs concomitantly with peptide translocation from the outer to the inner leaflet of the bilayer and equilibration of peptide content on the two leaflets results in reduction of leakage. The problem with the usual experimental procedures is that when the peptide/lipid ratio is high enough to cause large extents of leakage, once the vesicle content leaked out one can not easily judge the permeability state of the membrane. To address this question we used the following assay: LUV were labelled inside only with NBD-PC and mixed with the 18L peptide at a certain peptide/lipid ratio. After preincubation with peptide for a fixed time, 10 mM sodium dithionite is added, which results in reduction of NBD-fluorescence due to membrane permeability to dithionite. Results were corrected for the lipid translocation to the outer leaflet. Typical results are shown in Fig. 3.3.4.1. We can conclude that there occurs some deactivation of the peptide membrane permeabilizing activity, especially at low peptide/lipid ratios. However, with higher peptide/lipid ratios, even after very prolonged peptide-lipid preincubation, there was residual permeabilizing activity. The NBD-PC/Dithionite (Fig. 3.3.4.1) assay reports higher permeability values than the ANTS/DPX assay (Fig. 3.3.1.1C). The extent of reduction of NBD-PC fluorescence intensity depends on the fraction of vesicles permeable to dithionite, while for the ANTS/DPX assay leakage corresponds to the percentage of leaked DPX. Both the ANTS/DPX and the NBD-PC/Dithionite assays would report similarly for the all-or-none

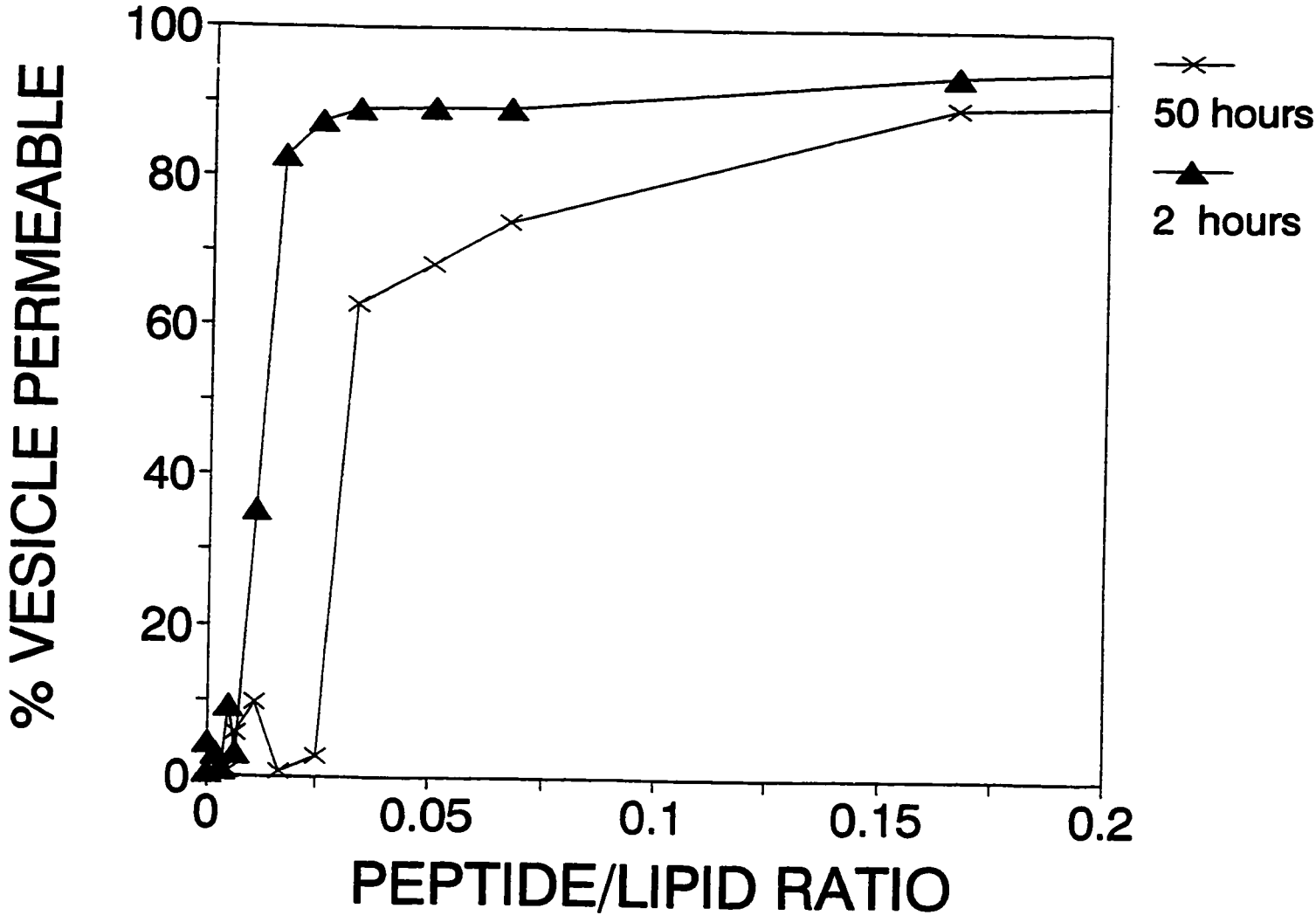

Figure 3.3.4.1. Percentage of vesicles permeable to sodium dithoinite after prolonged incubation of DOPC:DOPE (1:1) LUV with 18L with various peptide/lipid ratios. Lipid concentration 20 μM. Incubation for two days (50 hours) - ×, Incubation for 2 hours - ▲.

mechanism of leakage, but the NBD-PC/Dithionite assay is expected to give higher values in the case of gradual leakage. Therefore this results are consistent with the gradual mode of 18L -induced leakage (Table 3.3.1.1).

3.3.5 Bilayer conductance measurements

Bilayer conductance measurements are thought to be useful for the characterization of channel forming properties of membrane active peptides. We performed experiments to directly determine the channel forming properties of 18L using black lipid membranes. Injection of peptide into the reservoir, contrary to control buffer injections, often resulted in the collapse of the membrane. We also observed several types of conductance activities induced by 18L (Fig. 3.3.5.1). At the lowest peptide concentrations, conductance patterns similar to those of an ion channel were found in strongly polarized membranes (±145 mV). A single conductance level of about 250 pS was detected (Fig. 3.3.5.1A). With an increase in peptide concentration, depending on the history of the sample, transient increases in bilayer conductance ranged from 0.5 to 2 nS. Lower voltages (±45 mV) were required for observation of this type of conductance. Alternatively, at the same peptide concentrations, we occasionally also observed transient spikes in conductance (Fig. 3.3.5.1B), typical of those usually attributed to membrane defects. Further increase in peptide concentration resulted in the formation of a stable leaky state of the membrane with conductance in the range of 50-200 nS (Fig. 3.3.5.1C). Further increase in peptide concentration usually resulted in the collapse of the membrane. We also failed to detect channel

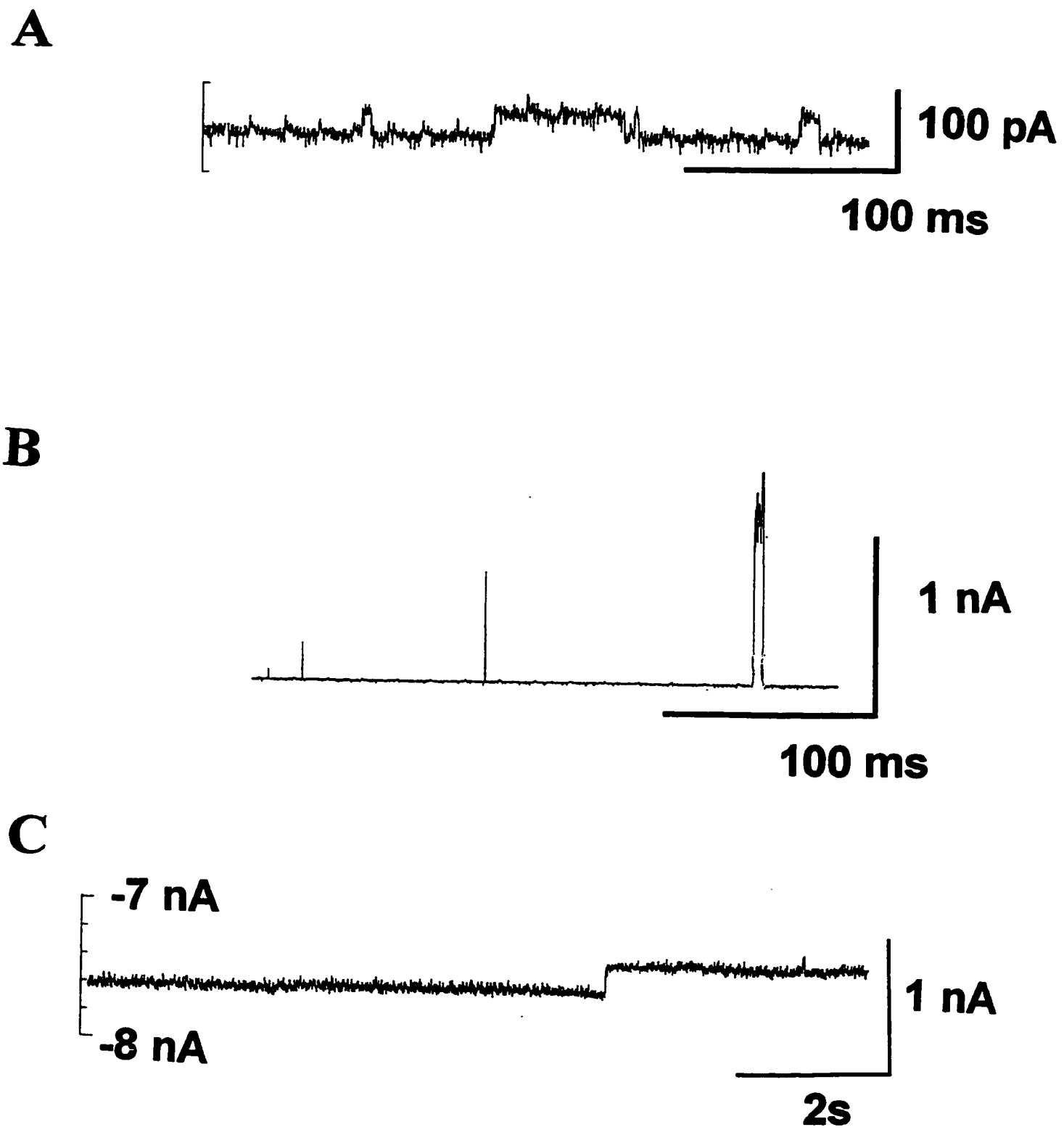

Figure 3.3.5.1. Types of bilayer conductance activities induced by 18L peptide. A. Channel-like activity. Single conductance level of 250 pS is seen. Peptide concentration 1μM. Membrane potential 45 mV. B. Transient spikes in the conductance with conductance levels in the range of several nS. Peptide concentration 2μM. Membrane potential 145 mV. C.. Stable leaky state with conductances about 50-200 nS. Peptide concentration 3μM. Membrane potential 45 mV.

forming properties of Ac-18A-NH_2 or the existence of reciprocal effects of Ac-18A-NH_2 and 18L in conductance activities.

3.4 Lipid Modulation of Peptide-Induced Leakage and Fusion and Reciprocal Effects of 18L And Ac-18A-NH_2

We studied 18L lytic activity in several binary lipid mixtures. We also paralleled this with studies of the lytic activity of Ac-18A-NH_2 and reciprocal effects of 18L and Ac-18A-NH_2. We restricted leakage studies to lipids in the fluid state as both 18L and Ac-18A-NH_2 peptides were unable to penetrate directly into the gel phase [Chapter 3.2.1; Polozov et al., 1995; 1997b] and partially due to technical reasons, i.e. the difficulty of obtaining stable, nonleaky ANTS/DPX-loaded vesicles from lipids in the gel phase or undergoing the main phase transition.

As we mentioned above, at the peptide and lipid concentrations used, the 18L peptide is essentially all membrane bound. However, incomplete binding of Ac-18A-NH_2 must be accounted for at low (20 μM) lipid concentrations. The binding constant for Ac-18A-NH_2 and DOPC:DOPE, 1:1, is 3.2 10^{-4} M^{-1} (Table 3.1.2.1). This corresponds to only about 40% of Ac-18A-NH_2 being actually membrane bound at 20 μM lipid concentrations. This correction for the efficiency of binding is insignificant for Ac-18A-NH_2 at 200 μM lipid concentration, when ~87% of peptide is in the membrane-bound state.

With zwitterionic lipids, DOPC:DOPE (1:0, 4:1, 3:2, 1:1, 2:3, Fig. 3.4.1A) and DOPC:ME-DOPE (1:0, 2:1, 1:1, 1:2, 0:1, not shown) the 18L lytic activity increased with increasing content of nonbilayer forming lipid while the opposite trend was observed for Ac-18A-NH_2. Addition of cholesterol (DOPC:Chol, 10:0, 9:1, 4:1) did not significantly affect the lytic activity of 18L or Ac-18A-NH_2. Both in DOPC:DOPE and DOPC:Me-DOPE binary mixtures, 18L fusogenic activity increased with the increasing content of nonbilayer forming lipid (not shown). In the case of membranes with a high content of nonbilayer forming lipid (DOPC:DOPE, 2:3, 1:1, 3:2 (Fig. 3.4.1B); DOPC:Me-DOPE, 1:1, 1:2, 0:1 (not shown)), simultaneous addition of 18L and Ac-18A-NH_2 resulted in less leakage than caused by the addition of 18L alone. In pure DOPC as well as in DOPC:DOPE, 4:1 (Fig. 3.4.1B) and DOPC:Me-DOPE, 2:1 (not shown), the reciprocal effect was not observed. On the contrary, the simultaneous addition of Ac-18A-NH_2 and 18L to DOPC caused leakage approximately equal to the sum of that observed with the independent addition of these peptides.

Addition of Ac-18A-NH_2 had a similar inhibitory effect regardless if it was added before (Fig. 3.4.2, curve 3), simultaneously (not shown), or after 18L addition (Fig. 3.4.2, curve 2), except that a higher extent of 18L-induced leakage was observed in the case of the delayed addition of Ac-18A-NH_2 due to the high initial leakage rate before Ac-18A-NH_2 addition. This independence on the order of addition is indicative that action of peptides is not mediated by peptide aggregation within the membrane or by direct 18L and Ac-18A-NH_2 interactions.

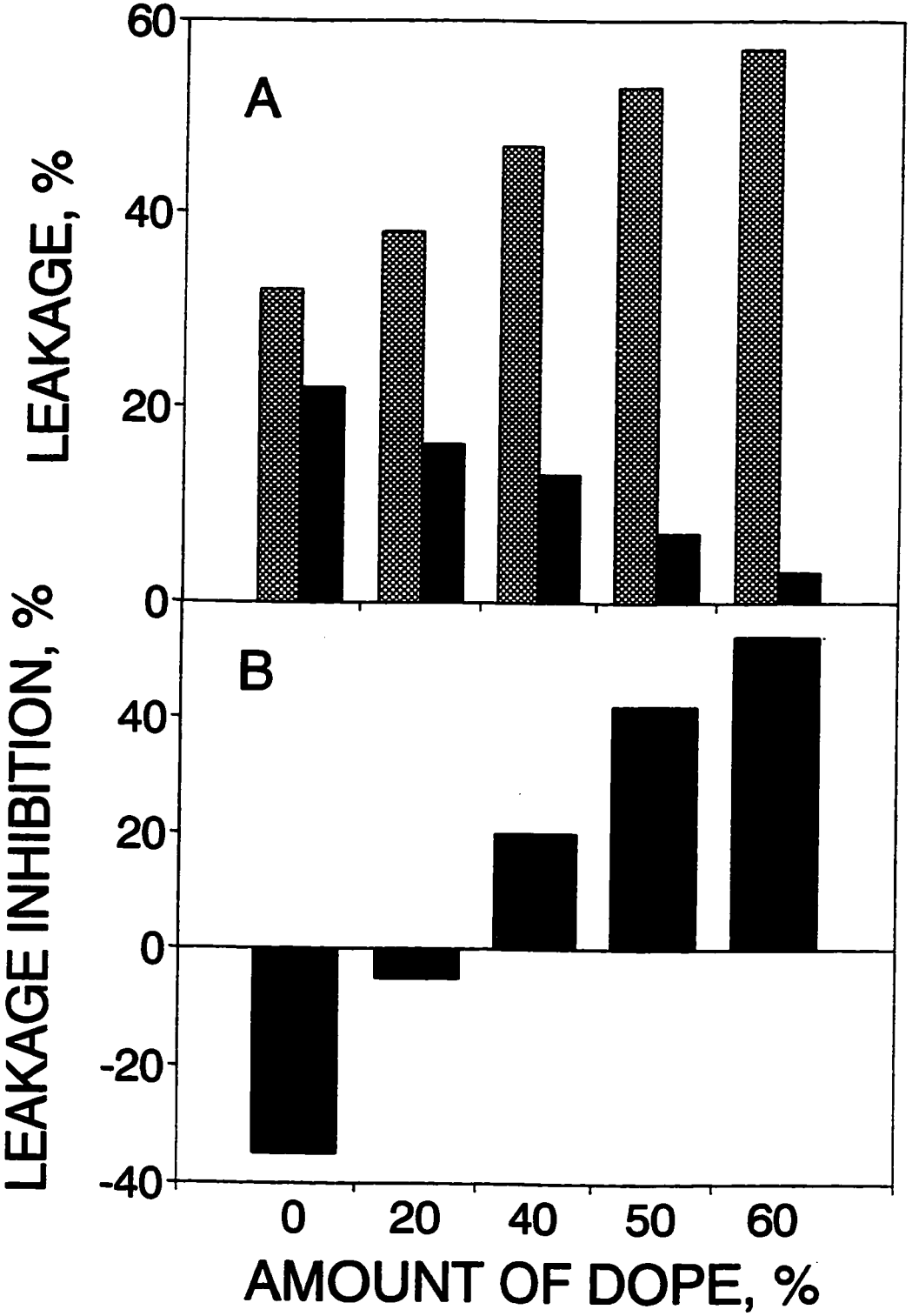

Figure 3.4.1. **A.** Vesicle leakage induced by 18L or Ac-18A-NH_2 from LUV composed of varying DOPC:DOPE mixtures as estimated by the extent of ANTS/DPX leakage. Leakage was initiated by injection of 20 μM DOPC:DOPE LUV of varied composition into the peptide solution. Percent leakage at 2,000 s was taken as a measure of leakage extent. Hatched bars - leakage induced by 1 μM 18L peptide. Solid bars - leakage induced by 2.5 μM Ac-18A-NH_2 peptide. **B.** Inhibition by Ac-18A-NH_2 of 18L-induced leakage depending on the ratio of DOPC:DOPE. Lipid concentration was 20 μM, 18L - 1 μM, Ac-18A-NH_2 - 1 μM. Leakage inhibition was calculated as a percent of the decrease of leakage caused by addition of Ac-18A-NH_2 to 18L compared to 18L alone. In both cases the extent of leakage was determined at 2,000 s.

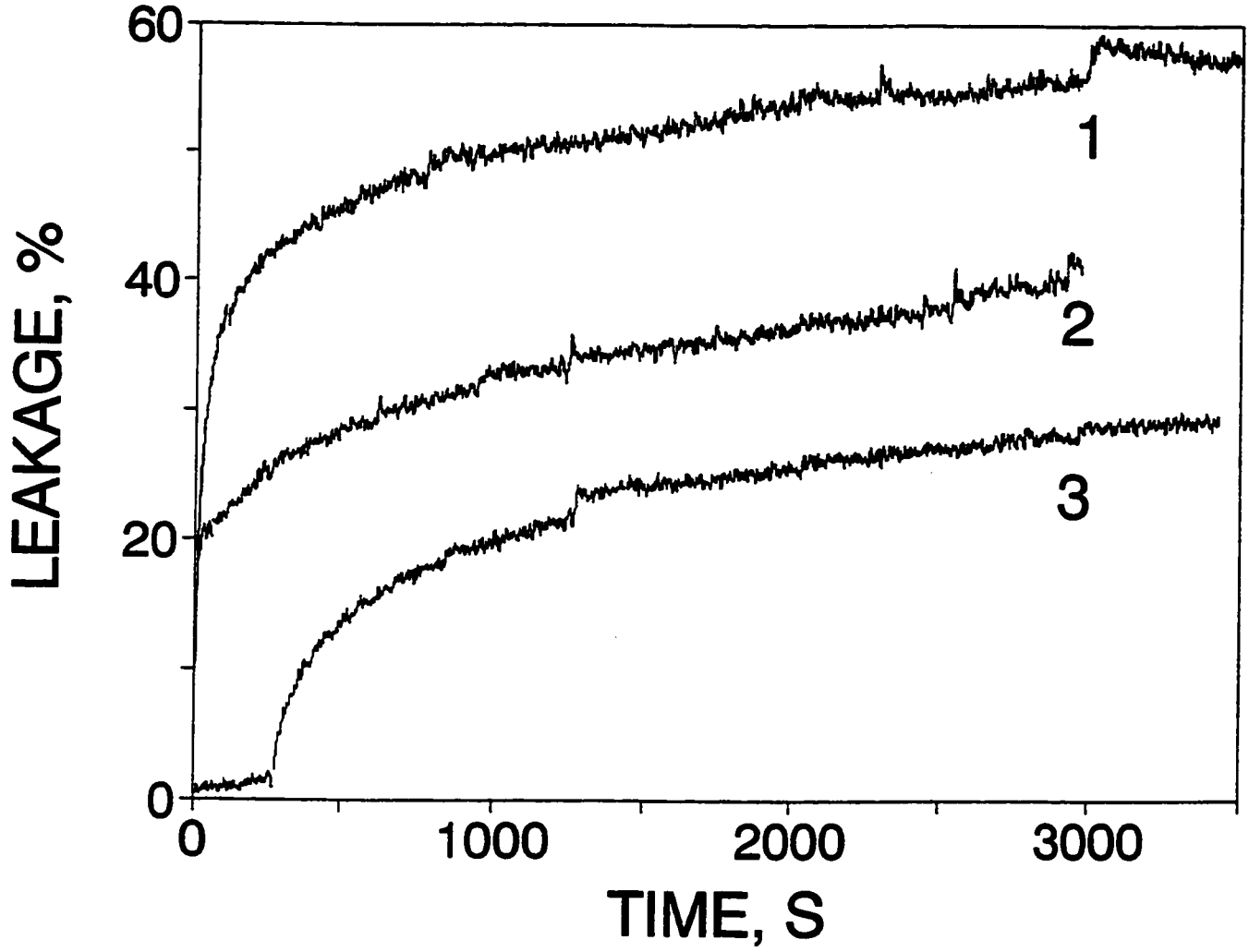

Figure 3.4.2. Effect of various order of peptide and vesicle addition. Curve 1 : Leakage induced by addition of 20 μM LUV (DOPC:DOPE (1:1)) into 1μM 18L solution . Curve 2: Leakage induced by addition of 20 μM LUV (DOPC:DOPE (1:1)) into 1μM 18L solution followed by addition of 1 μM Ac-18A-NH_2 after 20 seconds. Curve 3 : Leakage induced by addition of 20 μM LUV (DOPC:DOPE (1:1)) into 1μM Ac-18A-NH_2 solution followed by addition of 1 μM 18L after 300 seconds.

We studied how inhibition of 18L-induced leakage depended on Ac-18A-NH_2 concentration (Fig. 3.4.3A). For 20 μM DOPC:DOPE, 1:1, and 1 μM 18L, the maximum inhibition was observed at 4-8 μM of Ac-18A-NH_2. Further increase of Ac-18A-NH_2 concentration resulted in an increase of leakage.

The reciprocal effect on peptide-induced leakage also depended on the total lipid concentration. For example, for DOPC:DOPE, 1:1, the reciprocal effect on vesicle leakage was pronounced at low (20 μM) lipid concentrations, but was not observed at high (200 μM) concentrations. Indeed, at 200 μM lipid, the simultaneous addition of Ac-18A-NH_2 and 18L increased the extent of leakage above the sum of the independent additions of each peptide. This lipid concentration dependence is additional evidence of the complex interplay between leakage and fusion effects of 18L and Ac-18A-NH_2. We found that Ac-18A-NH_2 was able to inhibit 18L-induced fusion (Fig. 3.4.3B). Contrary to leakage activity, a sufficient amount of Ac-18A-NH_2 was able to inhibit fusion completely. It is possible that, at 200 μM, inhibition of 18L-induced fusion directed the peptide activity towards increased content leakage.

18L caused much faster (1-100 s) leakage from liposomes containing acidic lipids DOPG (Fig. 3.4.4) or DOPC:DOPG, 1:1 , although at peptide-lipid ratios comparable to that required for zwitterionic lipids. Resolution of initial leakage rates was possible only by stopped-flow. Leakage was not dependent on the total lipid concentration. 18L did not cause fusion of DOPG vesicles at the leakage-inducing concentrations. Ac-18A-NH_2 induced leakage of DOPG and DOPC:DOPG vesicles with

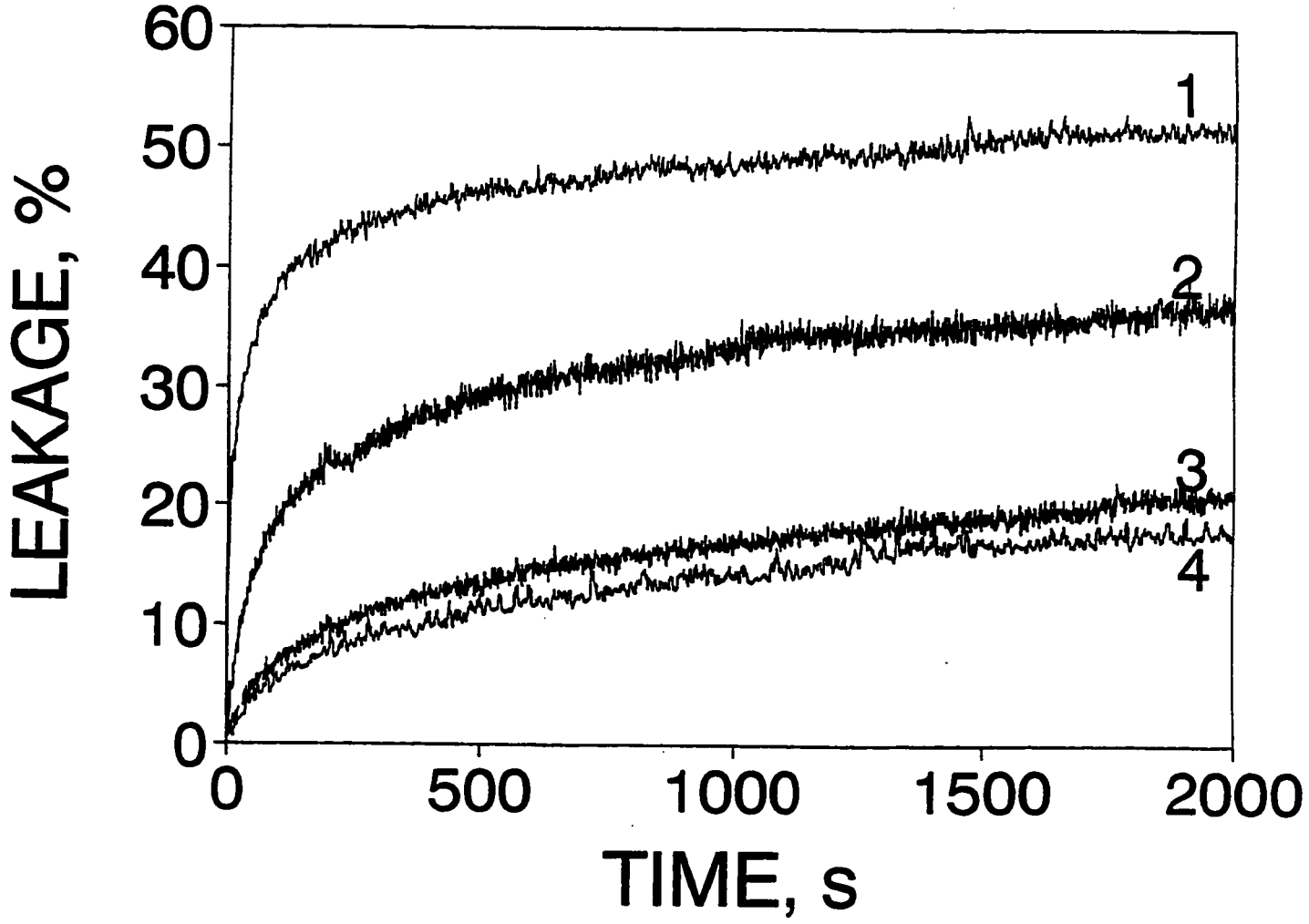

Figure 3.4.3. A. Inhibition by various amounts of Ac-18A-NH_2 of 18L-induced leakage of DOPC:DOPE (1:1) LUV. Lipid concentration 20 μM. 18L concentration 1 μM. Concentration of Ac-18A-NH_2: 1 - 0; 2 - 0,5 μM; 3 - 1 μM; 4 - 8 μM. Maximum inhibition was observed at 4-8 μM of Ac-18A-NH_2.

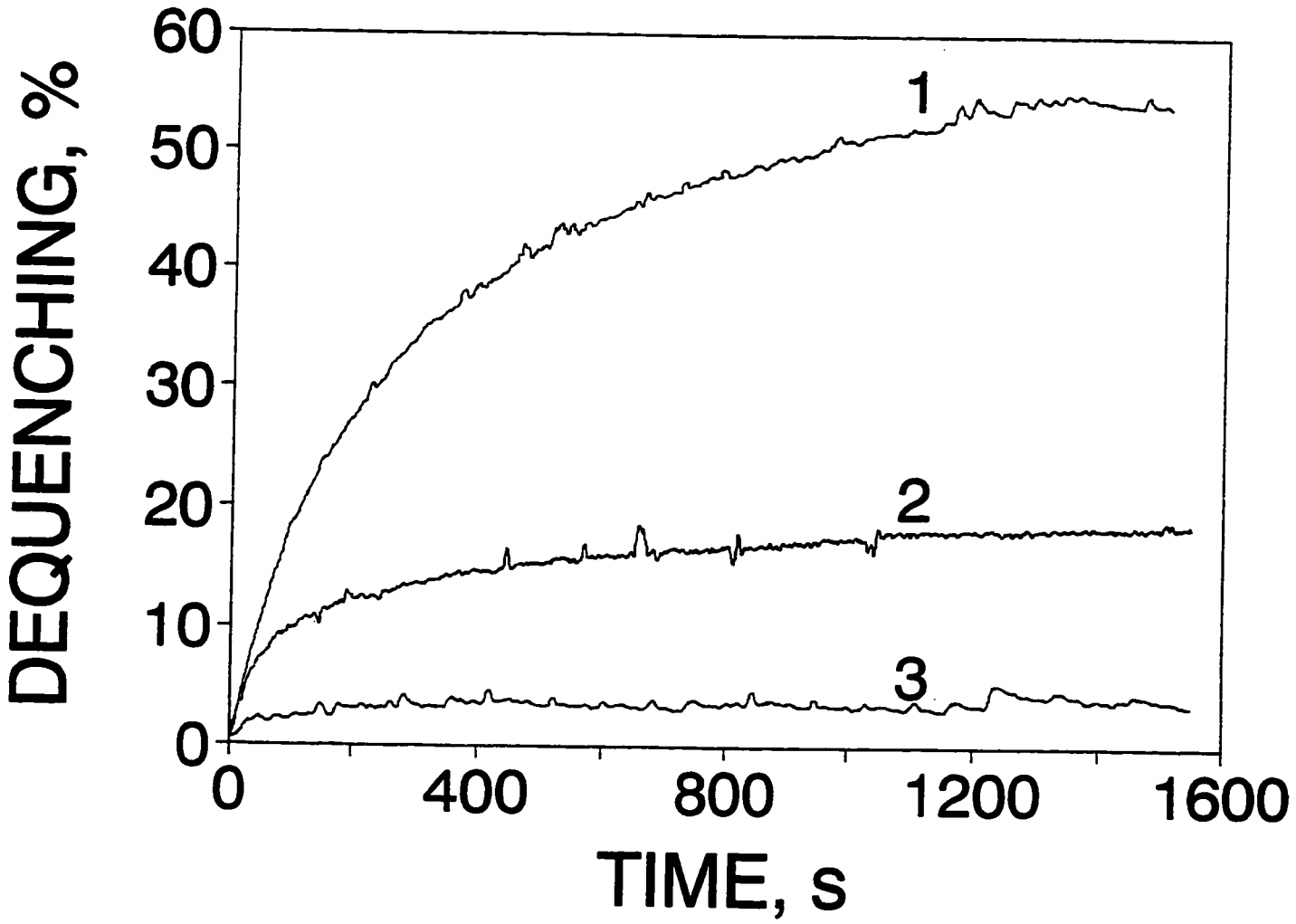

Figure 3.4.3. **B. DOPC:DOPE liposome fusion induced by 18L and its inhibition by Ac-18A-NH_2. Fusion monitored by a lipid-mixing assay, based on dequenching of anthrylvinyl fluorescence from anthrylvinylphosphatidylcholine (APC)-labelled liposomes upon fusion with unlabelled liposomes. Lipid concentration 200 μM. Curve 1- 18L - 20 μM. Curve 2- 18L - 20 μM, Ac-18A-NH_2 - 5 μM.Curve 3 - 18L - 20 μM, Ac-18A-NH_2 - 20 μM.**

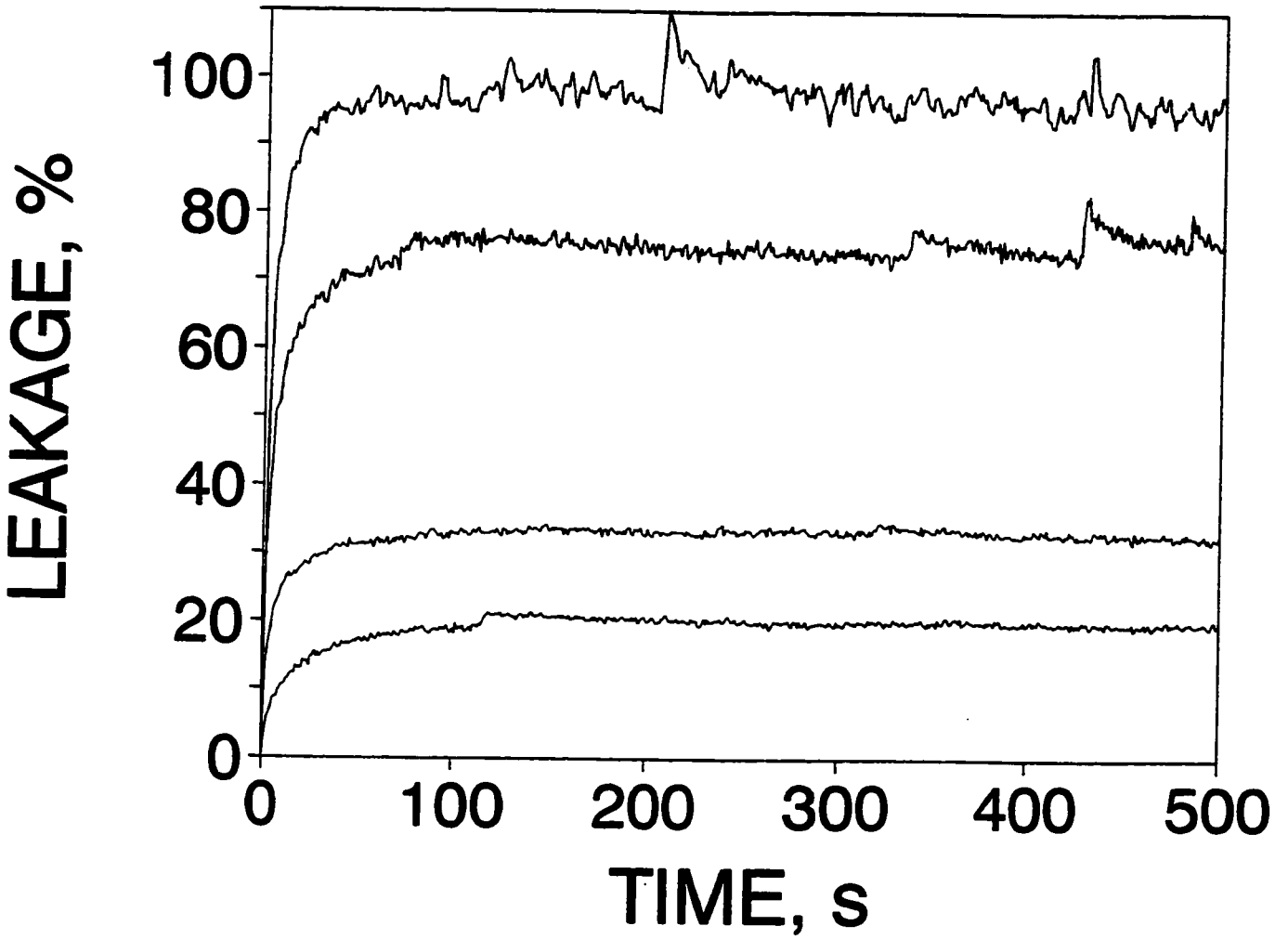

Figure 3.4.4. 18L -induced DOPG LUV aqueous contents leakage. Stopped-flow experiments. From top to the bottom, the peptide/lipid ratios were 0.2, 0.16, 0.08, 0.04, respectively. Lipid concentration was 130 μM.

kinetics very similar to that of 18L and also did not promote fusion. With acidic lipids, we did not observe a reciprocal effect between 18L and Ac-18A-NH_2. On the contrary, leakage was close to the sum of that contributed by each of the peptides individually, irrespective of lipid concentration or order of peptide addition.

3.5 Peptide Effect on Membrane Asymmetry and Lipid Flip-Flop

Difference in peptide effects in zwitterionic and anionic membranes brings up an interesting question about which of this is biologically relevant. The asymmetric composition of biomembranes suggest that a peptide first contacts with zwitterionic lipids. However, if a peptide is able to translocate to another bilayer leaflet and/or induce lipid flip-flop, then further stages of interaction will be dominated by peptide association with acidic lipids. As an approach to distinguish between these possibilities, we decided to study 18L peptide effects on lipid flip-flop. Thus this aspect of peptide-lipid interactions is directly connected with the mechanism of 18L-induced membrane permeabilization.

Elaboration of the assay was a prerequisite for these studies. As a starting point we used an assay for membrane asymmetry [McIntyre and Sleight, 1991] based on the incorporation of NBD-labelled phospholipids into the membrane and reduction of NBD by dithionite (DT), which results in formation of nonfluorescent ABD on the

surface accessible for dithionite. Vesicles labelled symmetrically, inside only or outside only were used in experiments.

Initially, we supposed that immediate surface accessibility (and fast decrease of NBD-fluorescence) can be distinguished from NBD-reduction due to membrane permeability to dithionite (slow NBD-reduction component), but we found that to be not unequivocal. The rate of quenching of NBD fluorescence on the accessible outer surface depended on DT concentration. At 10 mM DT, fluorescence quenching approached saturation within 2-3 minutes for NBD-PC in DOPC:DOPE, 1:1, vesicles. If within this timescale a significant concentration of DT can permeate into vesicles, then determination of outside only NBD-DT will be complicated. To adjust sodium dithionite solution to pH 7.4 approximately equimolar NaOH solution was used, as a result, the 10 mM DT solution had an osmotic strength of about 40 mOsm. As is discussed in Chapter 3.6, creation of such an osmotic gradient was sufficient to enhance significantly peptide induced membrane permeabilization.

In order to avoid interference from peptide-induced permeability vesicles were trypsin-treated after incubation with peptide and prior to DT addition. Trypsin treatment results in desorption of cut peptide fragments from the membrane and thus sealing of the membrane. Trypsin on its own was not causing any effect on probe distribution. Desorption of peptide from the membrane upon trypsin addition was observed by a decrease of fluorescence energy transfer from peptide to a membrane inserted probe, e.g. NBD or anthrylvinyl-labelled phospholipid. Concentrations of trypsin were adjusted depending on peptide concentration, approximately 50 μM of trypsin per 1 μm of peptide

was found sufficient for cutting all peptide within several minutes. Additions of varied amounts of trypsin and incubations at different times were used as a control.

Results from experiments with labelled inside-only vesicles are shown in Fig 3.5.1. Vesicles treated with trypsin after both two hours and two days of incubation with 18L peptide at peptide/lipid ratios up to 1:20-1:15 caused only relatively small probe redistribution. This redistribution was found to vary linearly with peptide/lipid ratio. Time dependence of peptide induced probe redistribution shows that probe redistribution occurs immediately after peptide addition and then proceeds relatively slowly, i.e. only 2-4 times faster than flip-flop in the absence of peptide (Fig. 3.5.2). We suppose that probe redistribution occurs immediately after peptide insertion in the membrane, although, due to the low time-resolution of the flip-flop assay we are unable to confirm this directly. Indirect support for this model goes from the peptide concentration dependence (Fig. 3.5.1). Values of the slope of the concentration dependence derived by linear regression are 2.6±0.3 moles lipid/mol peptide for 2 hours of incubation and 4.3±1.1 moles lipid/mol peptide for two days of incubation. That is insertion of 1 molecule of peptide in the bilayer results in fast redistribution to the outer leaflet of bilayer of 2-3 molecules of lipid and relatively slow redistribution of subsequent lipid molecules.

An interesting question is whether initial redistribution of lipids occurs concomitantly with the translocation of peptide to the inner leaflet of the bilayer. Matsuzaki et al. (1995) emphasized the view of the peptide-induced leakage as a relaxation process of peptide (magainin) translocation. With respect to 18L peptide, on the one hand, we have seen a decrease in membrane permeability after long times of peptide-lipid incubation

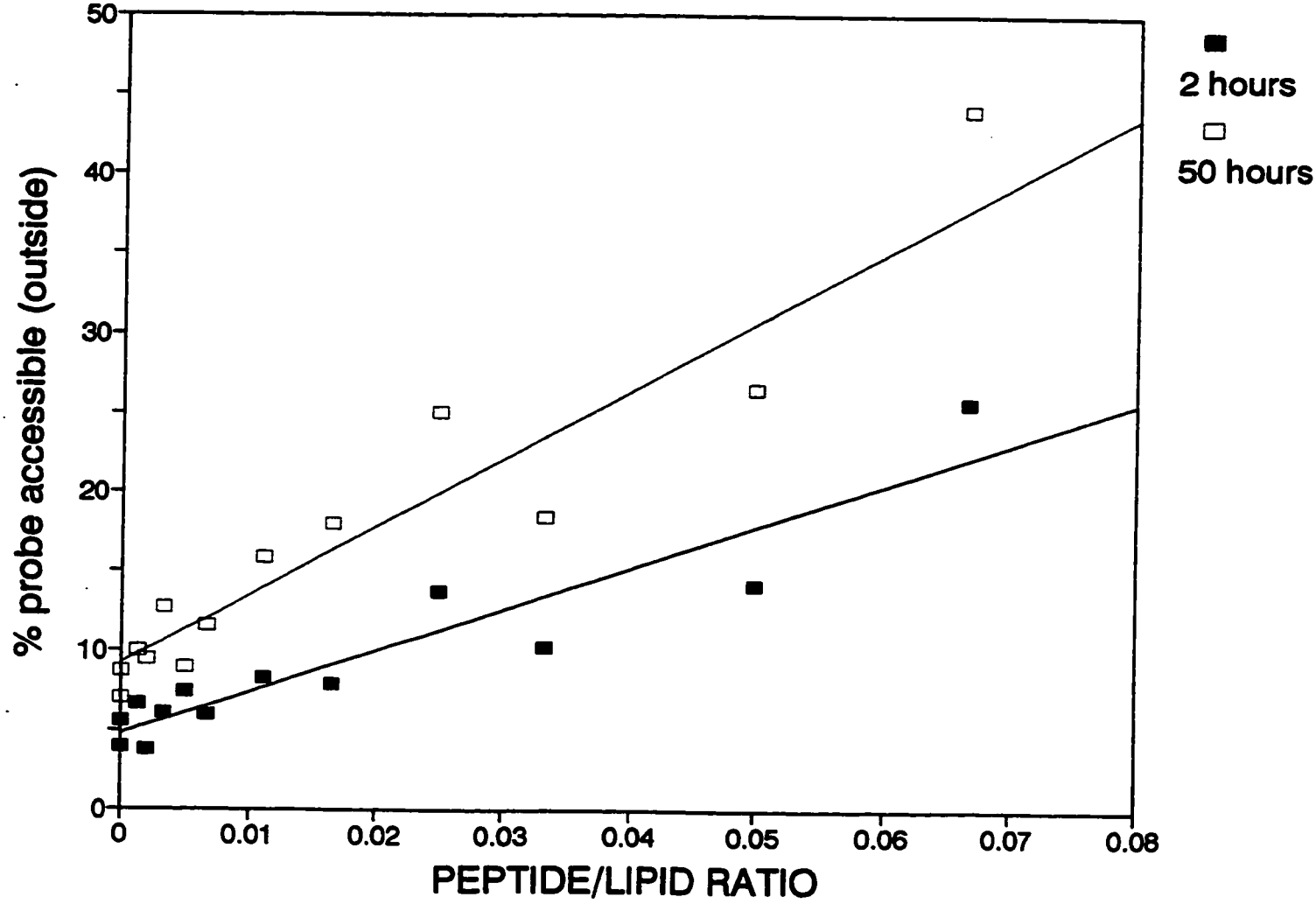

Figure 3.5.1. 18L peptide effects on phospholipid flip-flop, as revealed from the outward redistribution of NBD-PC in LUV (DOPC:DOPE, 1:1) initially labelled only inside with 1% NBD-PC. Vesicles were incubated at 25^0 C different time with the 18L peptide at different peptide lipid ratios and treated with trypsin before dithionite addition. ■ - 2 hours of incubation before trypsin treatment, dotted line obtained by linear regression. □ - 2 days (50 hours) incubation before trypsin addition, dashed line obtained by linear regression.

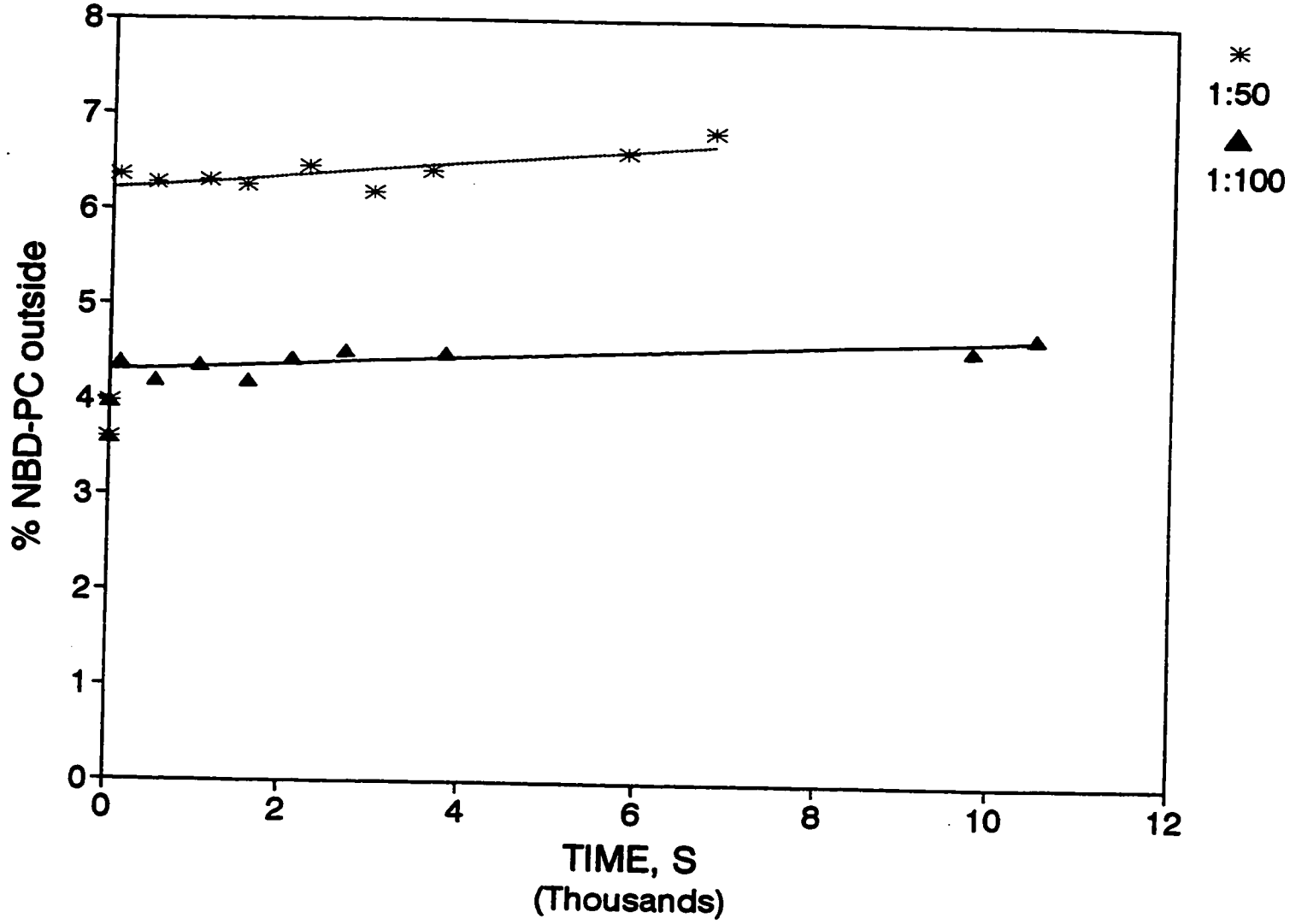

Figure 3.5.2. Time dependence of changes in distribution of NBD-PC in DOPC:DOPE (1:1) LUV labelled inside only after addition of 18L peptide. * - 18L/lipid ratio 1:50, Δ - 18L/lipid ratio 1:100. Trypsin was added before dithionite addition.

which can be due to slow peptide translocation. On the other hand, we observe fast lipid translocation (redistribution) to the outer leaflet of the bilayer, despite the fact that peptide insertion in the outer leaflet will create excess surface in the outer leaflet. This means that probably there is some fast peptide translocation inside the bilayer or that there is transient limited increase in the lipid random flip-flop rate.

As long as the original peptide insertion occurs in the outer leaflet we can expect redistribution of lipid to the inside, to compensate for the excess surface area. Vesicles labelled outside only were incubated with peptide in order to determine the inward movement of the probe. In this arrangement, increase with time of percentage of NBD-PC inaccessible to dithionite reduction is indicative of lipid flip-flop, despite interference with dithionite permeability (Fig. 3.5.3). Interference with dithionite permeability can be avoided by trypsin treatment. At the same peptide/lipid ratios, the percentage of lipid distributed from outside to inside (Fig. 3.5.3) is similar to lipid redistributed inside to outside (Fig. 3.5.1). Although all minor details are not clarified, we can conclude that in the PC:PE system, the 18L peptide at the leakage inducing peptide/lipid ratios, is causing only a relatively short time increase in lipid flip-flop rates which coincides with peptide insertion and/or translocation.

While it is interesting to see what the effects of the 18L peptide are on lipid flip-flop in acidic membranes, we found NBD/DT assay less helpful in this situation. Electrostatic repulsions between a DT anion and an anionic membrane surface, in accordance with Gouy-Chapman, theory results in several fold decrease of dithionite concentration in vicinity of bilayer [Kuchinka and Seelig, 1989; Beschiashchvili and Seelig, 1990; Mosior and McLaughlin, 1992]. As a consequence, DT quenching

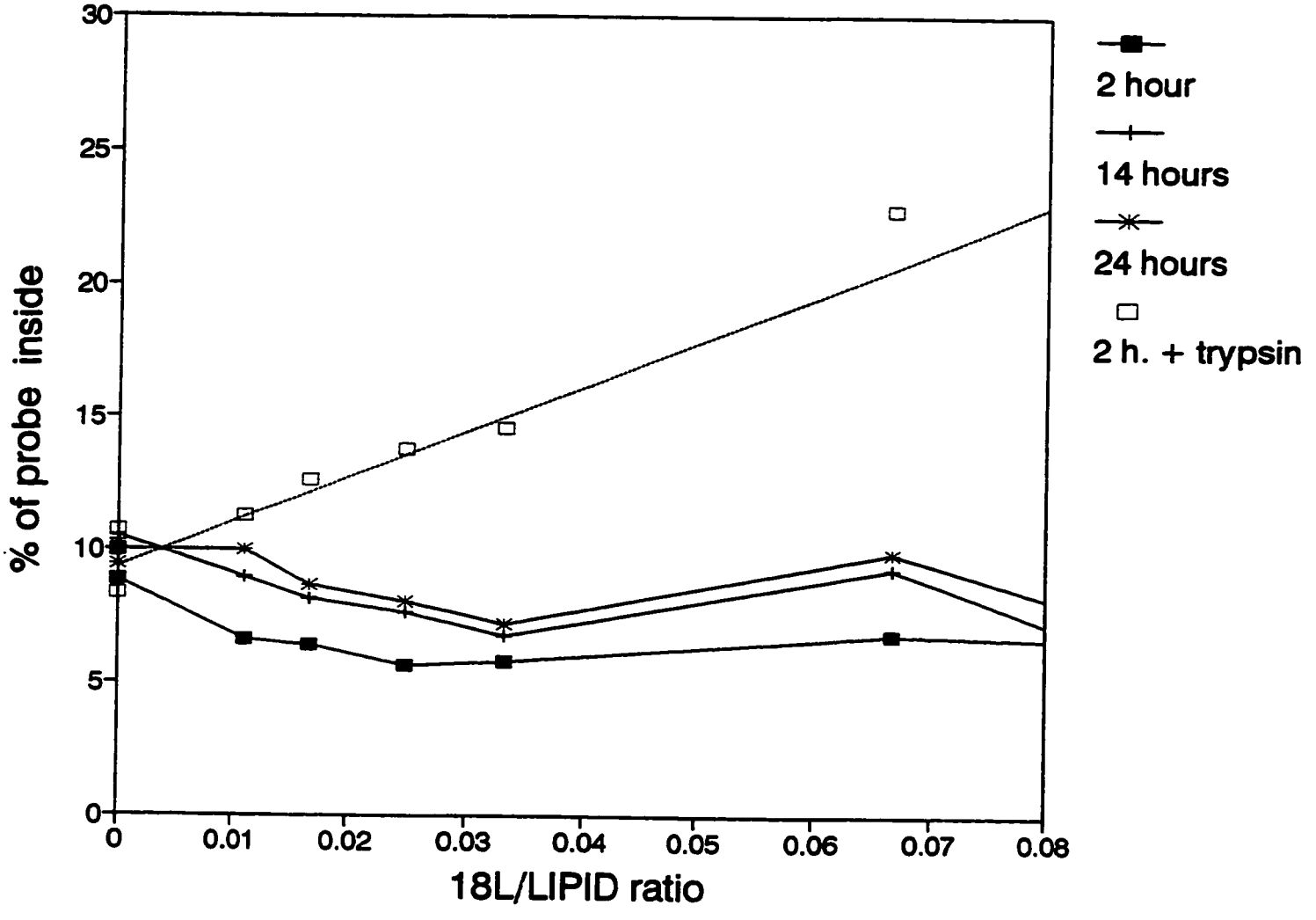

Figure 3.5.3. Dependence of the percentage of NBD-PC inaccessible for dithionite reduction after incubation of 18L with DOPC:DOPE (1:1) vesicles labelled with 1% NBD-PC in the outer leaflet. Incubation was conducted for 2 hours (■), 14 hours (+) or 24 hours (*). Vesicles were treated with trypsin before dithionite addition (□) after 2 hours of incubation.

proceeded significantly slower and the distinction between immediately accessible surface and that due to DT penetration through the bilayer was less certain. An increase in DT concentration had peculiar consequences. It looked like almost all membrane surfaces became accessible to DT quenching. An increase in DT concentration had a similar effect in the case of zwitterionic membranes. We conclude that this is a result of two contributing factors, first there is some residual membrane bound peptide after trypsin treatment, and second, high DT concentration creates an osmotic gradient across the membrane which attenuates peptide lytic activity, which is described in the next section [Chapter 3.6].

3.6 Membrane Tension and Peptide Effects

Problems with the dithionite assay on membrane asymmetry as well as previously observed effects of osmotic disbalance on 18L-induced vesicles contents leakage made us look more closely at this aspect of peptide-membrane interactions. The effect of osmotic modulation of peptide activities is related to the more general question of the modulation of membrane function by membrane tension. Both positive and negative tensions can be created by varying the direction of osmotic gradient. *In vivo* membrane tension can be of a variety of origins, including osmotic swelling and hydrodynamic shear stress. It is likely, that independent of the mechanism of membrane tension creation, there will be similar consequences for peptide-lipid interactions (and membrane protein functions). The effect of membrane tension on peptide-lipid interactions have not yet been studied in detail. Most of experiments on peptide-induced

leakage either specify that the vesicles studied have been osmotically compensated or recklessly does not pay attention to this aspect of the membrane state.

We found that an osmotic gradient as low as 5-10 mM NaCl affect peptide-membrane interactions. Fig. 3.6.1 shows leakage induced by the addition of 100 μM of DOPC:DOPE LUV to 3.3 μM 18L (peptide/lipid ratio 1:30). We found that the osmotic strength of the ANTS/DPX solutions entrapped in the vesicles is compensated best of all by 20 mM Tris-HCl buffer containing 25 mM NaCl. The osmotic strength of this buffer is about 95 mOsm. Addition of peptide to vesicles in this buffer, resulted in slow leakage of below 10% in 2 hours. Less concentrated buffer 80 mOsm (10 mM Tris-HCl, 25 mM NaCl), gives similar but faster leakage. Dilution of vesicles into 45 mOsm or 20 mOsm media changes the picture significantly. Essentially there appears a fast leakage component which results in a high percentage of leakage. It is interesting that osmotic stress applied in the other direction i.e. media more concentrated than the vesicles content also results in an increased leakage rate (case of 225 mOsm (10 mM Tris, 100 mM NaCl) shown on Fig. 3.6.1). We suppose that in the first approximation, at any particular peptide/lipid ratio vesicles can bear some critical membrane tension σ_c without additional fast leakage. However, if membrane tension exceeds this critical value then spontaneous pore formation occurs. Membrane tension (σ) depends on osmotic pressure **P** as

$$\sigma = P \cdot R/(2h) \qquad (3.6.1)$$

where **R** is the radius of vesicle and **h** - thickness of bilayer [Landau and Lifshits, 1986]. Thus σ_c corresponds to $P_c = \sigma_c \cdot 2h/R$ - osmotic pressure which vesicle can tolerate. Based

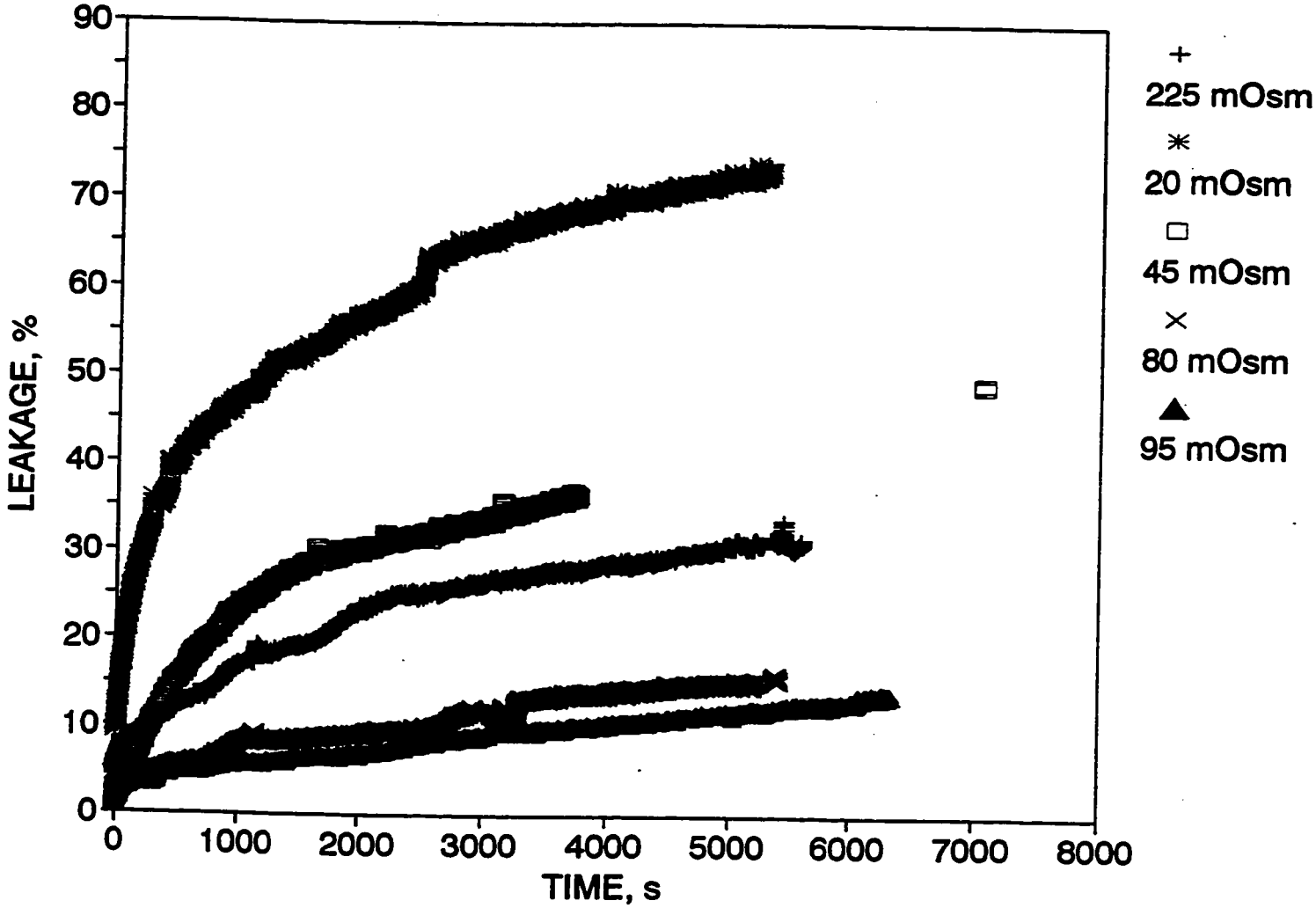

Figure 3.6.1. Time dependence of aqueous contents leakage of 100 μM DOPC:DOPE (1:1) LUV loaded with 12.5 μM ANTS and 45 μM DPX, pH 7.4 osmotic strength 95 mOsm/kg and diluted into media with different osmotic strength. Leakage was induced by addition of 3.3 μM 18L.

on this hypothesis the following equation can be proposed as an approximation of the expected leakage kinetics:

$$L(t) = 100\% \cdot \{ (P_o - P_m - P_c)/P_o \cdot (1 - e^{-k_1 t}) + (P_m + P_c)/P_o \cdot (1 - e^{-k_2 t}) \} \quad (3.6.2)$$

Where P_o - osmotic strength of vesicle content (95 mOsm in this case) and P_m - osmotic strength of media outside vesicles. The first term in the equation describes tension induced leakage. Generally, tension induced leakage rate (k_1) is a function of tension $k_1 = k_1(\sigma)$. But as a first approximation we can take k_1 as a constant. The second term is describing leakage from unstrained liposomes. Strictly speaking leakage from unstrained liposomes is not described by a simple exponential decay. But here we have the case of slow leakage with low leakage extent, which can be reasonably well approximated by exponent. As leakage from nontensed vesicles is much slower than from osmotically tensed, $k_2 << k_1$.

A fit of all of the time traces (Fig. 3.6.2) gives a value of $P_c = 11 \pm 1$ mOsm. It is interesting to discuss the origin of this P_c. The energy of pore formation in the tensed membrane can be presented as:

$$E = 2\pi\sigma_l \cdot r - \pi\sigma \cdot h \cdot r^2 \quad (3.6.3)$$

Where r - is the radius of the pore and σ_l is the line tension of the pore. Spontaneous pore formation is possible when $dE/dr < 0$, i.e. $\sigma_l - \sigma \cdot h \cdot r < 0$. Existence of the critical tension, σ_c, corresponds to existence of spontaneous fluctuations in the membrane of the size of $r_c = \sigma_l / (\sigma_c \cdot h)$. Experiments with stable pores made by electroporation in giant vesicles [Zhelev and Needham, 1993] give values of σ_l of $0.92 \cdot 10^{-6}$ dyn for SOPC and $3.05 \cdot 10^{-6}$ dyn for SOPC:Chol (1:1) bilayers. Mui et al. (1993) report that 100 nm LUV of EPC:Chol can tolerate osmotic gradients up to 400 mOsm which corresponds to $\sigma_c \cdot h = 40$ dyn·cm^{-1}. Thus

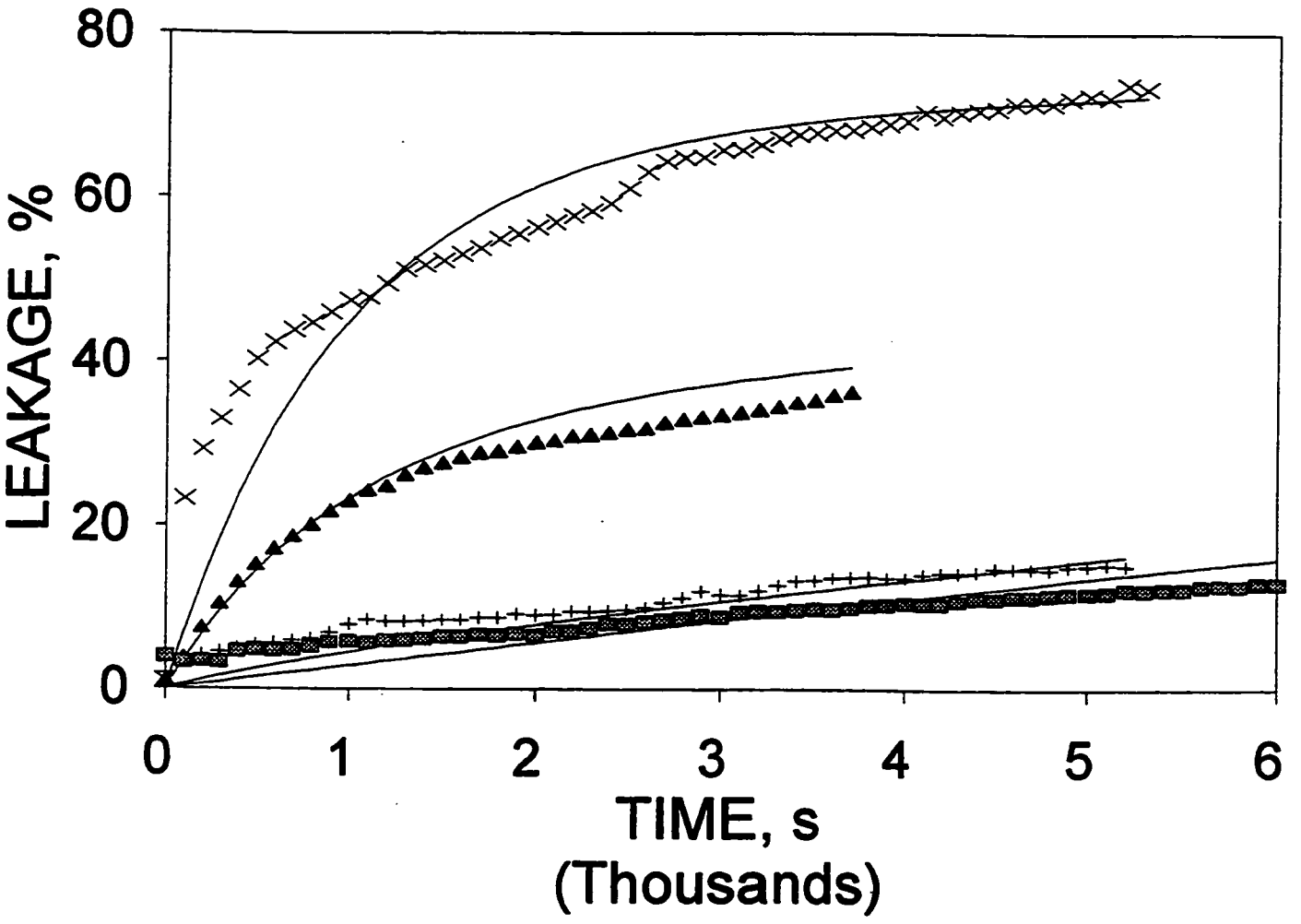

Figure 3.6.2. Fit of the leakage time traces from Figure 3.6.1 (shown by symbols) using equation (3.6.2). The best fit lines shown on the figure (as lines) were obtained using the following parameters: P_c=11 mOsm/kg, k_1= $1.04 \cdot 10^{-3}$ s^{-1}, k_2= $2.92 \cdot 10^{-5}$ s^{-1}.

we can estimate that for pure lipid systems vesicles don't leak until the size of fluctuation required for pore formation is on the subnanometer scale of $r_c \approx (1\text{-}3)\cdot 10^{-6}/40 = 0.25\text{-}0.75$ nm. Insertion of peptide into the tensed membrane creates sites for the formation of the pores and also potentially reduces linear tension of the pore (σ_l). Both of these factors favour the reduction in P_c, which in the case shown in Fig 3.6.1 is more than 10 times. Disregarding changes in σ_l this supposes the existence of defects on the scale of nanometres which essentially correlates with the size of the 18L peptide in the sided insertion model and suggest that monomeric peptide serves as a nucleation site for the pore formation.

Similar modulation of lytic activity was found for mastoparan, and K18L peptides. Since in the above description we never mentioned particular peptide sequence, this facilitation of vesicles osmotic lysis may apply not only to 18L lytic peptide, but may be one of general motif in peptide-lipid interactions.

4. Discussion

4.1 Mechanism of 18L-induced membrane permeabilization

Taken together, data on the mode of action of the lytic peptide 18L, suggest that lysis is mediated by a membrane destabilisation mechanism. We have seen no evidence of substantial peptide aggregation upon membrane binding. High peptide/lipid ratios were required for the lytic activity of 18L. The peptide caused leakage simultaneously with

fusion and at the same peptide/lipid ratios that it measurably affected lipid phase behavior. The size of the 18L-induced membrane defects is sufficient for the release of M.W. 20,000 fluorescent dextrans, which have average Stokes radii of 3.3 nm. Since 18L-induced membrane potential release is observed at the same peptide/lipid ratios and lipid concentrations at which dextran leakage occurs, we conclude that no small channels are formed. As the mode of ANTS/DPX leakage was found to be gradual rather than all-or-none release, we can conclude that the lifetime of the defect is very short. It is insufficient for the release of the entire vesicle contents, which in our case can be estimated as ~3 ms (pore area ~9 nm^2, vesicle radius ~50 nm) according to Schwarz and Robert (1990, 1992). Such a short lifetime of the leaky state further substantiates the idea that leakage is due to transient membrane defects. Theoretically it is possible that at the high peptide/lipid ratios, peptide membrane permeabilization activity is mediated by a small percent of helical bundles formed by associated peptides [Rapaport et al., 1996; Matsuzaki et al., 1995]. However this description seems unlikely for the formation of large, short-lived pores. The distinction between the helical bundle model and membrane destabilization concept is in the pore size, the lining of the pore, its life-time and also the forces or the mechanisms of the formation of the pores. Membrane destabilization suggests inclusion of lipid molecules in the pore lining. Peptide-induced increase in membrane permeability can be viewed as a result of a decreased activation energy for defect formation. This must be the result of peptide incorporation into the pore lining, reducing water exposure of the fatty acid chains. Leakage occurring through the flickering pore is likely to depend on the size of

the reporter. The absence of such a pronounced dependence suggests that the pore formation has a high activation energy, but once formed the pore rapidly grows in size and then collapses back. While there exist certain reservations about the relationship between conductance and leakage activity [Kerr et al., 1995], it is probable that these normally transient defects can be stabilized by an electric potential applied across the membrane (Fig. 3.3.5.1C). Conductance levels observed in the planar bilayer membrane experiments correspond to the surface of the aqueous pore in the range from 0.4 nm^2 (Fig. 3.3.5.1A) to ~100 nm^2 (Fig. 3.3.5.1C). Transient spikes in the conductance correspond to pore surfaces in the range of 1-10 nm^2 (Fig. 3.3.5.1B).

From geometric considerations and previous DSC studies [Tytler et al., 1993], Ac-18A-NH_2 and 18L affect the membrane intrinsic monolayer curvature (IMC) in opposite directions. Compensation of changes in intrinsic monolayer curvature leads to canceling of membrane effects when both peptides are added together, i.e. to the reciprocal effect of 18L and Ac-18A-NH_2. However, the present study shows that this reciprocal effect is pronounced only for systems with high nonbilayer phase propensity. The reason for this is that effects on IMC as the main mechanism responsible for leakage occur only when the membrane already has a negative IMC. Existence of negative IMC in bilayers had been shown to result in an instability [Epand and Epand, 1994]. For the unstrained bilayer, i.e. a bilayer with a very low IMC, addition of either peptide can not easily produce a state with high IMC strain and thus other mechanisms will be prevalent.

Induction of LUV fusion by 18L was pronounced in bilayers with a propensity for nonbilayer phase formation. This can be expected as structures with overall negative curvatures are thought to be structural intermediates in the process of fusion [Markin et al., 1984; Chernomordik et. al. 1985; Siegel, 1993]. Observation of 18L-induced fusion in parallel with leakage suggests that both processes are alternative ways of reducing strain created by peptide insertion. At high lipid concentration, when there are more frequent bilayer-bilayer contacts, membrane defects are more likely to result in fusion rather than leakage. Support for this explanation comes from the dependence of leakage on lipid concentration (Fig. 3.3.1.1C). At higher lipid concentrations (favorable for fusion) we saw less leakage at the same peptide to lipid ratios (in both cases the peptide was essentially totally bound).

Fusion and leakage caused by peptides is initiated by the incorporation of peptides into the outer bilayer leaflet. This insertion modulates the overall bilayer curvature stress (different from IMC) by creating excessive surface in the outer leaflet. This bilayer curvature stress has long been known to be responsible for changes in the shape of lipid vesicles or cells [Sheetz et al., 1976; Sackmann, 1994, 1995]. We think it is natural to apply this concept for the understanding of peptide-induced leakage and fusion. This mass imbalance concept is related to the view of Matsuzaki et al. (1995, 1996) of peptide-induced permeabilization as a relaxation process of peptide equilibration between two bilayer leaflets. Alternatively tension release can involve redistribution of both peptides and lipids between leaflets (flip-flop). Data in Fig. 3.5.2. suggest that transbilayer peptide and lipid redistribution occurs transiently after

peptide insertion as a relaxation process to reduce bilayer curvature strain. The initially high leakage rate in the system may be caused by such transient redistribution. Addition of Ac-18A-NH_2 may immediately release only the 18L-induced intrinsic monolayer curvature strain of the outer monolayer, but not the strain caused by the mass imbalance between monolayers. Only limited inhibition of 18L-induced leakage by Ac-18A-NH_2 (Fig. 3.4.3A) supports the importance of bilayer curvature stress for peptide-induced leakage. Contrary to that, complete inhibition of 18L-induced fusion by Ac-18A-NH_2 (Fig. 3.4.3B) suggests that bilayer curvature stress by itself is not sufficient to promote vesicle fusion.

4.2 Peptide effects on acidic membranes

For such lytic peptides as magainins, lytic activity towards acidic membranes is much higher than against zwitterionic ones [Matsuzaki, 1995]. Contrary to that, while melittin binds acidic membranes with higher affinity its lytic activity is reduced [Benachir and Lafleur, 1995]. 18L binding constants for acidic membranes are two-three orders of magnitude higher than for zwitterionic membranes, however, the 18L peptide is only two to three-fold more disruptive to vesicles of acidic lipids than to those with zwitterionic lipids (Fig. 3.3.1.1 and Fig. 3.4.4). However, the time course of leakage differed greatly. Leakage proceeded much faster for anionic compared with zwitterionic vesicles and could be resolved only by using a stopped flow apparatus. A reason for this altered behavior may be the inability to cause membrane fusion, due to electrostatic repulsion between charged vesicles. Also high peptide binding affinity for

acidic membranes correlated with longer times of peptide residence in the membrane (Table 3.1.2.1; Chapter 3.1.3) which might also correlate with the longer life-time of a permeable state of the membrane. It is interesting that the Ac-18A-NH_2 peptide was also considerably more lytic in the presence of acidic lipids and the simultaneous addition of Ac-18A-NH_2 and 18L results in an additive increase in leakage. The description in terms of curvature modulations proposed above for zwitterionic membranes neglects possible specific effects. For example, we have shown the preferential association of both 18L and Ac-18A-NH_2 peptides with PG in PC:PG membranes [Chapter 3.2.4; Polozov et al., 1995, 1997b]. In contrast, there was no preferential association of these peptides with either PC or PE in DOPC:DOPE mixtures. Thus a description of peptide effects in terms of curvature may be valid for the PC:PE system, but not for PC:PG.

4.3 Peptide effects in biological systems

The propensity for nonbilayer phase formation and the presence of anionic lipids were the characteristics of the lipid bilayer which modulated peptide-lipid interactions. These two aspects of membrane composition may play an important role in the regulation of lipid-protein interactions and membrane properties *in vivo*. Previously reciprocal effects of 18L and Ac-18A-NH_2 peptides in some biological activity assays have been reported [Chapter 1.2.3; Tytler et al., 1993]. In our studies of model membranes we found that this reciprocal effect of 18L and Ac-18A-NH_2 is pronounced only in lipid systems with a propensity for

nonbilayer phase formation. The extent of protection by Ac-18A-NH_2 against the effects of 18L correlated with an increase of intrinsic monolayer curvature. This finding suggests the importance of nonbilayer phase propensity for certain functions of biological membranes.

Certain L-type lytic peptides, originally extracted from amphibian skin [Zasloff, 1987; Zasloff et al., 1988], are suggested to protect the host from bacterial infection. From characterisation of the binding of 18L we can suggest that L-type peptides partition essentially completely into the membrane under physiological conditions. Peptides are nonlytic for the host cells *in vivo*, due to the low peptide to total lipid ratio. However, due to the dynamic character of binding and the high peptide affinity for acidic membranes, the redistribution and accumulation of peptide at a lytic concentration on the acidic membrane of bacteria may take place. We used 18L-induced vesicle contents leakage as a way to illustrate the dynamic character of peptide binding (Fig. 3.1.3.4). This data also show the possibility of selective induction of leakage from acidic liposomes without affecting zwitterionic ones. At the same bound peptide/lipid ratios 18L is similarly lytic to both zwitterionic and acidic vesicles (Fig. 3.3.1.1 and Fig. 3.4.4). Thus difference in membrane binding can explain why some L-type lytic peptides posses bactericidal activity at concentrations tolerant to the host cells. High peptide/lipid ratios, required for permeabilization of zwitterionic membranes, make possible the application of lytic peptides in host defense systems as natural antibiotics. Due to the background of non-specific peptide-membrane binding, peptide antibiotic activity is expected to be pronounced at relatively high peptide concentrations. Increased specificity for binding to acidic membranes can serve as a

guideline for the design of peptides for possible medical applications. Exposure of acidic lipids in malignant cells, can also serve as a method for targeting lytic peptides. This can explain the antitumor activity of magainins - L class peptide antibiotics [Cruciani et al., 1991]. Prebinding of peptides with liposomes can be used as a method for the reduction of acute toxicity upon peptide administration. The dynamic aspect binding of peptides is not the only stage of regulation of their membrane permeabilization properties [Matsuzaki et al., 1995; Tytler et al., 1995], but it is defenitely an important stage.

In the case of class L peptides that are lytic to mammalian cells, fast high affinity binding may be essential for their activity *in vivo*. For example, mastoparan, a L-class wasp venom peptide, is administered by local injection. In this case fast and tight binding (with slow exchange) of this peptide occurs, which results in a high local concentration of peptide causing cell lysis via the destabilisation of cell membranes around the site of peptide injection. The propensity of biological membranes for nonbilayer phase formation is exploited by lytic peptides for its disruption. These examples illustrate how physical properties of membranes and peptide structural motifs can modulate biological functions.

5. Summary and Perspectives

We have extensively characterised the mode of interaction of the amphipathic α-helical peptides, 18L and Ac-18A-NH_2, with membranes. We have shown a pronounced dependence of interactions on lipid type. Two characteristics of the lipid bilayer were found to be important with respect to peptide-lipid interactions, namely the presence of anionic

lipids and, in the case of zwitterionic membranes, nonbilayer phase formation propensity. There was also found metastability in peptide interactions with gel state lipids. Although Ac-18A-NH_2 is zwitterionic, and 18L cationic, both peptides were similarly affected by the presence of acidic lipids. Binding constants were increased by two-three orders of magnitude (that is above the Gouy-Chapman contribution). An increase in binding correlated with a longer time of membrane residence. Peptides were found to be in dynamic equilibrium with membranes, with an association rate close to the diffusion limit. Both peptides were able to induce lateral phase separation in membranes containing acidic lipids, and were able to cause fast vesicle content leakage. Overall charge-charge interactions is a very strong modulator of peptide membrane interaction.

While charge-charge interactions affected similarly both 18L and Ac-18A-NH_2 peptides, intrinsic monolayer curvature affected peptide activities in the opposing directions. And, ultimately, high negative intrinsic monolayer curvature was necessary for observation of the reciprocal effect of 18L and Ac-18A-NH_2. It can be formulated that lipid membrane nonbilayer phase propensity is necessary for membrane protection by class A peptides against the effects of class L lytic peptides.

Analysis of the mechanism of 18L induced permeabilization of zwitterionic membranes have shown that the 18L peptide destabilises membranes, leading to a transient formation of large defects (diameter > 3 nm) which generally results in contents leakage, but the presence of bilayer-bilayer contact can lead to vesicle fusion. Initial stages of peptide membrane permeabilization can also be viewed as a relaxation process, since it is initiated by peptide insertion only in the outer monolayer, and

followed with phospholipid flip-flop and/or peptide translocation. However, the liposome retains residual permeability on the scale of days, when initial translocation is essentially complete. Peptide insertion into the membrane also significantly reduces membrane stability to mechanical tension, making it susceptible to osmotic lysis. This mechanism may be general for the action of class L peptides.

Progress in membrane research is hampered by the lack of high precision quantitative methods available for solution chemistry. So one has to rely on a number of indirect assays of membrane activities. Several novel approaches were developed in this work, like a FITC-Dextrans leakage assay, NBD/DT assay of membrane permeabilization, APC/PPC lipid mixing fusion assay, FRET approaches in studies of lateral membrane organization. A modified quantitative approach was proposed for the use of tryptophan fluorescence in studies of the kinetics and equilibrium of peptide-membrane binding. These assays can be of general use for characterization of membrane active peptides.

6. References

Allan, D., and Kallen, K.-J. (1994) *Trends in Cell Biology, 4,* 350-353. Is plasma membrane lipid composition defined in the exocytic or the endocytic pathway?

Almeida, P.F.F, Vaz, W.L.C., and Thompson, T.E. (1993) *Biophys. J., 64,* 399-412. Percolation and diffusion in three component lipid bilayers: Effect of cholesterol on an equimolar mixture of two phosphatidylcholines.

Almeida, P.F.F., and Vaz, W.L.C. (1995) In "Structure and dynamics of membranes" , R. Lipowsky and E. Sackmann, eds., Elseveir, Amsterdam, 305-358. Lateral diffusion in membranes.

Ames, B. N. (1966) *Methods Enzymol.*, 8, 115-118. Assay of inorganic phosphate, total phosphate and phosphatases.

Anantharamaiah, G.M. (1986) *Methods Enzymol.*, 128, 627-647. Synthetic peptide analogs of apolipoproteins.

Anantharamaiah, G.M., Jones, M.K., Brouilette, C.G., Schmidt, C.F., Chung, B.H., Hughes, T.A., Bhown, A.S., and Segrest, J.P. (1985) *J. Biol. Chem., 260,* 10248-10255. Studies of synthetic peptide analogs of the amphipathic helix. Structure of complexes with dimyristoylphosphatidylcholine.

Anantharamaiah, G.M., Jones, M.K., and Segrest, J.P. (1993) in "The Amphipathic Helix", ed. Epand, R. M., CRC Press, Boca Raton, FL, 109-142. An atlas of the amphipathic helical domains of the human exchangeable plasma apolipoproteins.

Argiolas, A., and Pisano, J.J. (1985) *J. Biol. Chem., 260,* 1437-1441. Bombolitins, a new class of mast cell degranulating peptides from the venom of the bumblebee Megabombus pennsylvanicus.

Auland, M.E., Roufogalis, B.D., Devaux, P.F., and Zachowski, A.(1994) *Proc. Natl. Acad. Sci. U.S.A.*, 91, 10938-10942. Reconstitution of ATP-dependent aminophospholipid translocation in proteoliposomes.

Axelrod, D., Koppel, D.E., Schlessinger, J., Elson, E., and Webb, W.W. (1976) *Biophys. J., 16, 1055-1069.* Mobility measurements by analysis of fluorescence photobleaching recovery.

Batzri, S., and Korn, E.D. (1973) *Biochim. Biophys. Acta., 298,* 1015-1019. Single bilayer liposomes prepared without sonication.

Bear, R.S., Palmer, K.J., and Schmitt, F.O. (1941) *J. Cell. Comp. Physiol., 17,* 355-367. X-ray diffraction studies of nerve lipides.

Bechinger, B., Zasloff, M., and Opella, S.J. (1993) *Protein Sci., 2,* 2077-2084. Structure and orientation of the antibiotic peptide magainin in membranes by solid-state nuclear magnetic resonance spectroscopy.

Benachir, T., and Lafleur, M. (1995) *Biochim. Biophys. Acta, 1235,* 452-460. Study of vesicle leakage induced by melittin.

Benachir, T., and Lafleur, M. (1996) *Biophys J., 70,* 831-840. Osmotic and pH transmembrane gradients control the lytic power of melittin.

Bentz, J., Nir, S., and Covell, D. (1988) *Biophys. J., 54,* 449-462. Mass action kinetics of virus-cell aggregation and fusion.

Berclaz, T. and McConnell, H.M. (1981) *Biochemistry, 20,* 6635-6640. Phase equilibria in binary mixtures of dimyristoylphosphatidylcholine and cardiolipin.

Bergelson, L. D., Gawrisch, K., Ferretti, J. A., and Blumenthal, R., eds. (1995) Special Issue on Domain Organization in Biological Membranes. *Mol. Mem. Biol., 12,* 1-162.

Bergelson, L. D., Manevich, E. M., Molotkovsky, J. G., Muzya, G. I., and Martynova, M. A.(1987) *Biochim. Biophys. Acta, 921,* 182-190.The interaction of prostaglandins with high-density lipoproteins: a non-equilibrium model of ligand-receptor interaction.

Bergelson, L. D., Molotkovsky, J. G., and Manevich, Y. M. (1985) *Chem. Phys. Lipids, 37,* 165-193. Lipid-specific fluorescent probes in studies of biological membranes.

Bergelson, L.D. (1992) *FEBS Letters, 297,* 212-215. Lipid domain reorganization and receptor events. Results obtained with new fluorescent lipid probes.

Bergelson, L.D., and Barsukov, L.I. (1977) *Science, 197,* 224-230. Topological asymmetry of phospholipids in membranes.

Beschiaschvili, G., and Seelig, J. (1990) *Biochemistry, 29,* 52-58. Melittin binding to mixed phosphatidylglycerol/phosphatidylcholine membranes.

Bloom, M., Evans, E., and Mouritsen, O.G. (1991) *Q. Rev. Biophys., 24,* 293-397. Physical properties of the fluid lipid-bilayer component of cell membranes: a perspective.

Borovyagin, V.L., and Sabelnikov, A.G. (1989) *Electron. Microsc. Review, 2,* 75-115. Lipid polymorphism of model and cellular membranes as revealed by electron microscopy.

Chapman, C.J., Erdahl, W.E, Taylor, R.W., and Pfeiffer, D.R. (1991) *Chem. Phys. Lipids, 60,* 201-208. Effects of solute concentration on the entrapment of solutes in phospholipid vesicles prepared by freeze-thaw extrusion.

Cheetham, J.J. (1993) Ph.D. Thesis, McMaster University. The effects of bilayer stabilization on membrane fusion in model and biological systems.

Chen, C.-S., Martin, O.C., and Pagano, R.E. (1997) *Biophys. J., 72,* 37-50. Changes in the spectral properties of a plasma membrane lipid analog during the first seconds of endocytosis in living cells.

Chernomordik, L.V., Kozlov, M.M., Melikyan, G.B., Abidor, I.G., Markin, V.S., and Chizmadzhev, Yu. A. (1985) *Biochim. Biophys. Acta, 812,* 643-655. The shape of lipid molecules and monolayer membrane fusion.

Chung, B.H., Anantharamaiah, G.M., Brouillette, C.G., Nishida, T., and Segrest, J.P. (1985) *J. Biol. Chem., 260,* 10256-10262. Studies of synthetic peptide analogs of the amphipathic helix. Correlation of structure with function.

Clerc, S.G., and Thompson, T.E. (1994) *Biophys. J., 67,* 475-477. A possible mechanism for vesicle formation by extrusion.

Cornut, I., Desbat, B., Turlet, J.M., and Dufourcq, J. (1996) *Biophys. J., 70,* 305-312. In situ study by polarization modulated Fourier transform infrared spectroscopy of the structure and orientation of lipids and amphipathic peptides at the air-water interface.

Cornut, I., Buttner, K., Dasseux, J.L., and Dufourcq, J. (1994) *FEBS Letters, 349,* 29-33. The amphipathic alpha-helix concept. Application to the de novo design of ideally amphipathic Leu, Lys peptides with hemolytic activity higher than that of melittin.

Cruciani, R. A., Barker, J. L., Zasloff, M., Chen, H.-C., and Colamonici, O. (1991) *Proc. Natl. Acad. Sci. U.S.A., 88,* 3792-3796. Antibiotic magainins exert cytolytic activity against transformed cell lines through channel formation.

Cruciani, R.A., Barker, J.L., Durrel, S.R., Raghunathan, G., Guy, H.R., Zasloff, M., and Stanley, E.F. (1992) *Europ. J. Pharm., 226,* 287-296. Magainin 2, a natural antibiotic from frog skin, forms ion channels in lipid bilayer membranes.

Csonka, L.N., and Hanson, A.D. (1991) *Ann. Rev. Microbiol., 45,* 569-606, Prokaryotic Osmoregulation: Genetics and Physiology.

Cullis, P.R., de Kruijff, B. (1979) *Biochim. Biophys. Acta, 559,* 399-420. Lipid polymorphism and the functional roles of lipids in biological membranes.

Dathe, M., Schumann, M., Wieprecht, T., Winkler, A., Beyermann, M., Krause, E., Matsuzaki, K., Murase, O., and Bienert, M. (1996) *Biochemistry, 35,* 12612-12622. Peptide helicity and membrane surface charge modulate the balance of electrostatic and hydrophobic interactions with lipid bilayers and biological membranes.

Dathe, M., Wieprecht, T., Nikolenko, H., Handel, L., Maloy, W.L., Macdonald, D.L., Beyermann, M., and Bienert, M. (1997) *FEBS Letters, 403,* 208-212. Hydrophobicity, Hydrophobic Moment and Angle Subtended by Charged Residues Modulate Antibacterial and Hemolytic-Activity of Amphipathic Helical Peptides.

Davis, J. H., Bloom, M., Clare, D. M., and Hodges, R. S. (1983) *Biochemistry, 22,* 5298-5305. Interaction of a Synthetic Amphiphilic Polypeptide and Lipids in a Bilayer Structure.

De Bony, J. and J. F. Tocanne. (1984) *Eur. J. Biochem., 143*, 373-379. Photo-induced dimerization of anthracene phospholipids for the study of the lateral distribution of lipids in membranes.

de Kruijff B. (1997) *Nature, 386*, 129-130. Biomembranes. Lipids beyond the bilayer.

Deamer, D.W. (1996) *Biophys. J., 71*, 543-543.Water chains in lipid bilayers.

Devaux, P.F. (1992) *Annu. Rev. Bioph. Biomol. Struct., 21*, 417-439. Protein involvement in transmembrane lipid asymmetry.

Devaux, P.F. (1993) *Curr. Opin. Struct. Biol., 3*, 489-494. Lipid asymmetry and flip-flop in biological membranes and in lipid bilayers.

Disalvo, E.A., Campos, A.M., Abuin, E., and Lissi, E.A. (1996) *Chem. Phys. Lipids, 84*, 35-45. Surface changes induced by osmotic shrinkage on large unilamellar vesicles.

Dobereiner, H.G., Kas, J., Noppl, D., Sprenger, I., and Sackmann, E. (1994) *Biophys. J., 65*, 1396-1403. Budding and fission of vesicles.

Duclohier, H. (1994) *Toxicology, 87*, 175-188. Anion pores from magainins and related defensive peptides.

Edidin, M. (1993) *J. Cell Science, 17*, 165-169. Patches and fences: probing for plasma membrane domains.

Ellens, H., Bentz, J., and Szoka, F. C. (1984) *Biochemistry, 23*, 1532-1538. pH-induced destabilization of phosphatidylethanolamine-containing liposomes: role of bilayer contact.

Ellens, H., Bentz, J., and Szoka, F.C. (1985) *Biochemistry, 24*, 3099-3106. H+- and Ca2+-induced fusion and destabilization of liposomes.

Epand, R.M., Gawish, A., Iqbal, M., Gupta, K.B., Chen, C.H., Segrest, J.P., and Anantharamaiah, G.M. (1987) *J. Biol. Chem., 262*, 9389-9396. Studies of synthetic peptide analogs of the amphipathic helix. Effect of charge distribution, hydrophobicity, and secondary structure on lipid association and lecithin:cholesterol acyltransferase activation.

Epand, R.M., Surewicz, W.K., Hughes, D.W., Mantsch, H., Segrest, J.P., Allen, T.M., and Anantharamaiah, G.M. (1989) *J. Biol. Chem., 264*, 4628-4635. Properties of lipid complexes with amphipathic helix-forming peptides. Role of distribution of peptide charges.

Epand, R. M. (1978) *Biochim. Biophys. Acta, 514*, 185-197. Studies on the effect of the lipid phase transition on the interaction of glucagon with dimyristoyl-glycerophosphocholine.

Epand, R. M. (1982) *Biochim. Biophys. Acta, 712*, 146-151. The apparent preferential interaction of human plasma high density apolipoprotein A-I with gel-state phospholipids.

Epand, R. M., and Epand, R. F. (1980) *Biochim. Biophys. Acta, 602,* 600-609. The role of the phospholipid phase transition in the regulation of glucagon binding to lecithin.

Epand, R.M., ed. (1993) The Amphipathic Helix, CRC Press, Boca Raton, FL.

Epand, R.M., Shai, Y., Segrest, J.P., and Anantharamaiah, G.M. (1995) *Biopolymers (Peptide Science), 37,* 319-338. Mechanisms for the modulation of membrane bilayer properties by amphipathic helical peptides.

Epand, R.M., and Epand, R.F. (1994) *Biophys. J., 66,* 1450-1456. Calorimetric detection of curvature strain in phospholipid bilayers.

Epand, R.M., and Polozov, I.V. (1996) In "Nonmedical applications of liposomes", Y. Barenholz and D.D. Lasic, eds., CRC Press, Boca Raton, 105-111. Liposomes and Membrane Stability.

Epand, R.M., ed. (1996) *Chem. Phys Lipids, 81,* 101-264. Special Issue: The properties and Biological roles of Non-lamellar forming lipids.

Epand, R.M., ed. (1997) Lipid polymorphism and membrane properties. Academic Press, San Diego, in press. v.44 in the CURRENT TOPICS IN MEMBRANES Series.

Epand, R.M., Epand, R.F., Blackburn, W.D., Mishra, V.K., Tytler E.M., Segrest, J.P., and Anantharamaiah, G.M. (1993) Proceedings of the Thirteenth American Peptide Symposium, ESCOM, Leiden, 1041-1042. Properties of a potent cationic lytic amphipathic helical peptide.

Epand, R.M., Stafford, A., Leon, B., Lock, P.E., Tytler E.M., Segrest, J.P., and Anantharamaiah, G.M. (1994) *Arterioscler. Thromb., 14,* 1775-1783. HDL and apolipoprotein A-I protect erythrocytes against the generation of procoagulant activity.

Ertel, A., Marangoni, A.G., Marsh, J, Hallet, F.R., and Wood, J.M. (1993) *Biophys. J., 64,* 426-434. Mechanical properties of vesicles. I. Coordinated analyses of osmotic swelling and lysis.

Fattal, E., Nir, S., Parente, RA., and Szoka, F.C. Jr. (1994) *Biochemistry, 33,* 6721-6731. Pore-forming peptides induce rapid phospholipid flip-flop in membranes.

Findlay, E.J., and Barton, P.G. (1978) *Biochemistry, 17,* 2400-2405. Phase behavior of synthetic phosphatidylglycerols and binary mixtures with phosphatidylcholines in the presence and absence of calcium ions.

Fisher, P.J., Prendergast, F.G., Ehrhardt, M.R., Urbauer, J.L., Wand, A..J., Sedarous, S.S., McCormick, D.J., and Buckley, P.J. (1994) *Nature, 368,* 651-653. Calmodulin Interacts with Amphiphilic Peptides Composed of All D-Amino Acids.

Fung, B.K., and Stryer, L. (1978) *Biochemistry, 17,* 5241-5248. Surface density determination in membranes by fluorescence energy transfer.

Gawrisch, K., Han, K.-H., Yang, J.-S., Bergelson, L.D., and Ferretti, J.A. (1993) *Biochemistry, 32,* 3112-3118. Interaction of peptide fragment 828-848 of the envelope Glycoprotein of human immunodefficiency virus type I with lipid bilayers.

Gennis, R.B. (1989) Biomembranes. Springer, Berlin.

Gershfeld, N.L. (1989) *Biochim. Biophys. Acta, 988,* 335-350. The critical unilamellar state: a perspective for membrane bilayer assembly.

Gershfeld, N.L. and Murayama, M. (1988) *J. Membr. Biol., 101,* 67-72. Thermal instability of red cell membrane bilayers: temperature dependence of hemolysis.

Golding, C., Senior, S., Wilson, M. T., and O'Shea, P. (1996) *Biochemistry, 35,* 10931-10937. Time resolution of binding and membrane insertion of a mitochondrial signal peptide: correlation with structural changes and evidence for cooperativity.

Gorter, E. and Grendel, F. (1925) *J. Exp. Med., 41,* 439-443. On bimolecular layers of lipoids on the chromocytes in blood.

Gromova, I. A., Molotkovsky, J. G., and Bergelson, L. D. (1992) *Chem. Phys. Lipids, 60,* 235-246. Anthrylvinyl-labelled phospholipids as fluorescent membrane probes. The action of melittin on multilipid systems.

Grove, A., Tomich, J.M., Iwamoto, T., and Montal, M. (1993) *Protein Sci., 2,* 1918-1930. Design of a functional calcium channel protein: inferences about an ion channel-forming motif derived from the primary structure of voltage-gated calcium channels.

Gruner, S.M. (1985) *Proc. Natl. Acad. Sci. U.S.A., 82,* 3665-3669. Intrinsic curvature hypothesis for biomembrane lipid composition: A role for nonbilayer lipids.

Gruner, S.M. (1989) *J. Phys. Chem., 93,* 7562-7570. Stability of lyotropic phases with curved interfaces.

Gruner, S.M., Lenk, R.P., Janoff, A.S., and Ostro, M.J. (1985) *Biochemistry,* 24, 2833-2842. Novel multilayered lipid vesicles: comparison of physical characteristics of multilamellar liposomes and stable plurilamellar vesicles.

Gruner, S.M., Tate, M.W., Kirk, G.L., So, P.T.C., Turner, D.C., Keane, D.T., Tilcock, C.P.S., and Cullis, P.R. (1988) *Biochemistry, 27,* 2853-2866. X-ray diffraction studies of the polymorphic phase behavior of N-methylated dioleoyl phosphatidylethanolamine.

Hallet, F.R., Marsh, J., Nickel, B.G., and Wood, J.M. (1993) *Biophys. J., 64,* 435-442. Mechanical properties of vesicles. II. A model for osmotic swelling and lysis.

Haugland, R.P. (1996) Handbook of fluorescent probes and research chemicals. Molecular Probes, Eugene, OR.

Hirai, Y., Yasuhara, T., Yoshida, H., Nakjima, T., Fujino, M., and Kitada, C. (1979) *Chem. Pharm. Bull., 27,* 1942-1944. A new mast cell degranulating peptide "mastoparan" in the venom of Vespula lewisii.

Hong-wei, S. and McConnell, H.M. (1975) *Biochemistry, 14,* 847-854. Phase separations in phospholipid membranes.

Hwang, J., Tamm, L.K., Bohm, C., Ramalingam, T.S., Betzig, E., and Edidin, M. (1995) *Science, 270,* 610-614. Nanoscale complexity of phospholipid monolayers investigated by near-field scanning optical microscopy.

Israelachvilli, J.N., Marcelja, S., and Horn, R.G. (1980) *Q. Rev. Biophys., 13,* 121-200. Physical principles of membrane organization.

Israelachvilli, J.N., Mitchell, D.J., and Ninham, B.W. (1977) *Biochim. Biophys. Acta, 470,* 185-201. Theory of self assembly of lipid bilayers and vesicles.

Israelachvilli, J.N. (1991) "Intermolecular and Surface Forces". 2nd ed., Academic Press, London.

Jacobsen, K., and Vaz, W. L. C. eds. (1992) Topical Issue on Domains in Biological Membranes, *Commun. Mol. Cell. Biophys., 8,* 1-114.

Johansson, L. B. A., Molotkovsky, J.G., and Bergelson, L. D. (1990) *Chem. Phys. Lipids, 53,* 185-189. Fluorescence Properties of Anthrylvinyl Lipid Probes.

Jones, M.K., Anantharamaiah, G.M., and Segrest, J.P. (1992) *J. Lipid Res., 33,* 287-296. Computer programs to identify and classify amphipathic alpha helical domains.

Jovin, T.M., and Vaz, W.L.C. (1989) *Methods Enzymol., 172,* 471-513. Rotational and translational diffusion in membranes measured fluorescence and phosphorescence methods.

Kaplun, A.P., Basharuli, V.A., and Shvets, V.I. (1978) *Bioorgan. Khim. (in russian), 4,* 1567-1568. Synthesis of fluorescence labelled phosphatidylcholines with 11-(2-anthroyl)undecanoic acid residues.

Keller, S.L., Bezrukov, S.M., Gruner, S.M., Tate, M.W., Vodyanoy I., and Parsegian, V.A. (1993) *Biophys. J., 65,* 23-27. Probability of alamethicin conductance states varies with nonlamellar tendency of bilayer phospholipids.

Kerr, I.D., Dufourcq, J., Rice, J.A., Fredkin, D.R, and Sansom, M.S.P. (1995) *Biochim. Biophys. Acta, 1236,* 219-227. Ion channel formation by synthetic analogues of staphylococcal delta-toxin.

Kirk, G.L. and Gruner, S.M. (1985) *J. Phys. Paris, 46,* 761-769. Lyotropic effects of alkanes and headgroup composition on the L-H_{II} lipid liquid crystal phase transition: Hydrocarbon packing versus intrinsic curvature.

Kiyota,T., Lee, S., and Sugihara, G. (1996) *Biochemistry, 35,* 13196-13204. Design and synthesis of amphiphilic alpha-helical model peptides with systema-

tically varied hydrophobic-hydrophilic balance and their interaction with lipid membrane and biomembrane.

Knoll, W., Ibel, K., and Sackmann, E. (1981) *Biochemistry, 20,* 6379-6383. Small-angle neutron scattering study of lipid phase diagrams by the contrast variation method.

Knoll, W., Schmidt, G., and Sackmann, E. (1983) *J. Chem. Phys., 79,* 3439-3442. Critical demixing in fluid bilayers of phospholipid mixtures: A neutron diffraction study.

Kornberg, R.D., and McConnell, H.M. (1971) *Biochemistry, 10,* 1111-1120. Inside-outside transitions of phospholipids in vesicle membranes.

Kuchinka, E. and Seelig, J. (1989) *Biochemistry, 28,* 4216-4221. Interaction of melittin with phosphatidylcholine membranes. Binding isotherm and lipid head-group conformation.

Lakowicz, J. R. (1983) Principles of Fluorescence Spectroscopy, Plenum Press, New York, NY.

Landau, L.D. and Lifshitz, E.M. (1986) "Theory of Elasticity", 3 ed., Pergamon, Oxford.

Landh, T. (1995) *FEBS Letters, 369,* 13-17. From entangled membranes to eclectic morphologies: cubic membranes as subcellular space organizers.

Laneelle, G., and Tocanne, J.-F. (1982) *Eur. J. Biochem., 109,* 177-182. Evidence for penetration in liposomes and in mitochondrial membranes of a fluorescent analogue of cord factor.

Lee, A.G. (1975) *Biochim. Biophys. Acta, 413,* 11-23. Fluorescence studies of chlorophyll A incorporated into lipid mixtures, and the interpretation of "phase" diagrams.

Loew, L.M., Benson, L., Lazarovici, P., and Rosenberg, I. (1985) *Biochemistry, 24,* 2101-2104. Fluorometric analysis of transferable membrane pores.

Luan, P., Yang, L., and Glaser, M. (1995) *Biochemistry, 34,* 9874-9883. Formation of membrane domains created during the budding of vesicular stomatitis virus. A model for selective lipid and protein sorting in biological membranes.

Ludtke, S. J., He, K., Heller, W. T., Harroun, T. A., Yang, L., and Huang, H. W. (1996) *Biochemistry, 35,* 13723-13728. Membrane pores induced by magainin.

Ludtke, S., He, K., and Huang, H.W. (1995) *Biochemistry, 34,* 16764-16769. Membrane thinning caused by magainin 2.

Luna, E. J. and McConnell, H. M. (1978). *Biochim. Biophys. Acta, 509,* 462-473. Multiple phase equilibria in binary mixtures of phospholipids.

Luzzati, V.(1968) In " Biological Membranes: Physical Fact and Function" D. Chapman, ed., Academic Press, London, v. 1, 71-123. X-ray diffraction studies of lipid water systems.

Luzzati, V., and Husson, F. (1962) *J. Cell. Biol., 12*, 207-219, The structure of lipid crystalline phases of lipid-water systems.

Mantsch, H.H. and McElhaney, R.N. (1991) *Chem. Phys. Lipids, 57*, 213-226. Phospholipid phase transitions in model and biological membranes as studied by infrared spectroscopy.

Markin, V. S., Kozlov, M.M. and Borovjagin, V.L. (1984) *Gen. Physiol. Biophys. 3*, 361-377. On the theory of membrane fusion. The stalk mechanism.

Marrink, S.J., Jahnig, F., and Berendsen, H.J. (1996) *Biophys. J., 71*, 632-647. Proton transport across transient single-file water pores in a lipid membrane studied by molecular dynamics simulations.

Marsh, D. (1995) *Mol. Memb. Biol., 12*, 59-64. Lipid-protein interactions and heterogeneous lipid distribution in membranes.

Matsuzaki, K., Harada, M., Funakoshi, S., Fujii, N., and Miyajima, K. (1991) *Biochim. Biophys. Acta, 1063*, 162-170. Physicochemical determinants for the interactions of magainins 1 and 2 with acidic lipid bilayers.

Matsuzaki, K., Murase, O., Fujii, N., and Miyajima, K. (1995) *Biochemistry, 34*, 6521-6526. Translocation of a channel-forming antimicrobial peptide, magainin 2, across lipid bilayers by forming a pore.

Matsuzaki, K., Murase, O., Fujii, N., and Miyajima, K. (1996) *Biochemistry, 35*, 11361-11368. An antimicrobial peptide, magainin 2, induced rapid flip-flop of phospholipids coupled with pore formation and peptide translocation.

Matsuzaki, K., Murase, O., Tokuda, H., Funakoshi, S., Fujii, N., and Miyajima, K. (1994) *Biochemistry, 33*, 3342-3349. Orientational and aggregational states of magainin 2 in phospholipid bilayers.

Matsuzaki, K., Sugishita, K.-L., Fujii, N., and Miyajima, K. (1995) *Biochemistry, 34*, 3423-3429. Molecular basis for membrane selectivity of an antimicrobial peptide, magainin 2.

McIntyre, J.C., and Sleight, R.G. (1991) *Biochemistry, 30*, 11819-11827. Fluorescence assay for phospholipid membrane asymmetry.

McMullen, T.P. and McElhaney, R.N (1995) *Biochim Biophys. Acta, 1234*, 90-98. New aspects of interaction of cholesterol with dipalmitoylphosphatidylcholine bilayers as revealed by high sensitivity differential scanning calorimetry.

Mellor, I.R., and Sansom, M.S.P. (1990) *Proc. R. Soc. Lond. B, 239*, 383-400.

Mishra, V.K., Palgunachari, M.N., Lund-Katz, S., Phillips, M.C., Segrest, J.P., and Anantharamaiah, G.M. (1995) *J. Biol. Chem., 270*, 1602-1611. Effect of the arrangement of tandem repeating units of class A amphipathic alpha-helices on lipid interaction.

Mishra, V.K., Palgunachari, M.N., Segrest, J.P., and Anantharamaiah, G.M. (1994) *J. Biol. Chem., 269*, 7185-7191. Interactions of synthetic peptide

analogs of the class A amphipathic helix with lipids. Evidence for the snorkel hypothesis.

Molotkovsky, J. G, Dmitriev, P. I., Nikulina, L. F., and Bergelson, L. D. (1979) *Bioorgan. Khim.*, 5, 588-594. Synthesis of new fluorescence-labelled phosphatidylcholines.

Molotkovsky, J. G., and Bergelson, L. D. (1982) *Bioorgan. Khim.*, *8*, 1256-1262. Perylenoyl-labelled lipid specific fluorescent probes.

Molotkovsky, J. G., Bergelson, L. D. and Karyukhina, M. O. (1987) *Biol. Membrany*, *4*, 387-394. A fluorescence method for studying bilayer-membrane water permeability.

Molotkovsky, J.G., Bergelson, L. D., Karyukhina, M.O., and Smirnova, M.M. (1989) *Bioorgan. Khim.*, *15*, 686-689. Synthesis of Anthrylvinyl Phospholipid Probes.

Molotkovsky, J.G., Babak, V.I., Bergelson, L. D., and Manevich, Y. M. (1984) *Biochim. Biophys. Acta*, *778*, 281-288. Perylenoyl-Labelled and Anthrylvinyl-Labelled Lipids As Membrane Probes.

Molotkovsky, J. G., Unkovsky, V. I., and Bergelson, L. D. (1980) *Bioorgan. Khim.*, *6*, 144-145. Enzymatic synthesis of fluorescent phosphatidylethanolamine.

Molotkovsky, J.G., Manevich, Y.M., Gerasimova, E.N., Molotkovskaya, I.M., Polessky, V.A., and Bergelson, L.D. (1982) *Eur. J. Biochem.*, *122*, 573-579. Differential study of phosphatidylcholine and sphingomyelin in human high-density lipoproteins with lipid-specific fluorescent probes.

Molotkovsky, J.G., Mikhalyov, I.I., Imbs, A.B., and Bergelson, L.D. (1991) *Chem. Phys. Lipids*, *58*, 199-212. Synthesis and characterization of new fluorescent glycolipid probes. Molecular organization of glycosphingolipids in mixed composition lipid bilayers.

Morein S., Andersson A., Rilfors, L., and Lindblom, G. (1996) *J. Biol. Chem.*, *271*, 6801-6809. Wild-type Escherichia coli cells regulate the membrane lipid composition in a "window" between gel and non-lamellar structures.

Morris, C.E. (1990) *J. Membr. Biol.*, *113*, 93-107. Mechanosensitive Ion Channels.

Mosior, M., and McLaughlin, S. (1992) *Biochim. Biophys. Acta*, *1105*,185-7. Electrostatics and reduction of dimensionality produce apparent cooperativity when basic peptides bind to acidic lipids in membranes.

Mouritsen, O. G., and Jorgensen, K. (1994) *Chem. Phys. Lipids*, *73*, 3-25. Dynamical order and disorder in lipid bilayers.

Mouritsen, O. G., and Bloom, M.(1993) *Annu. Rev. Biophys. Biomol. Struct*, *22*, 145-171. Models of lipid-protein interactions in membranes.

Mueller, P., and Rudin, D.O. (1968) *Nature, 217,* 713-719. Action potentials induced in biomolecular lipid membranes.

Mui, B.L., Dobereiner, H.G., Madden, T.D., and Cullis, P.R. (1995) *Biophys. J., 69,* 930-941. Influence of transbilayer area asymmetry on the morphology of large unilamellar vesicles.

Mui, B.L.-S., Cullis, P.R., Evans, E.A., and Madden, T.D. (1993) *Biophys. J., 64,* 443-453. Osmotic properties of large unilamellar vesicles prepared by extrusion.

Mui, B.L.-S., Cullis, P.R., Pritchard, P.H., and Madden, T.D. (1994) *J. Biol. Chem., 269,* 7364-7370. Influence of plasma on the osmotic sensitivity of large unilamellar vesicles prepared by extrusion.

Nir, S., Peled, R., and Lee, K.-D.(1994) *Colloids and Surfaces A, 89,* 45-57.

Oblatt-Montal, M., Buhler, L.K., Iwamoto, T., Tomich, J.M., and Montal, M. (1993) *J. Biol. Chem.,* 268, 14601-14607. Synthetic peptides and four-helix bundle proteins as model systems for the pore-forming structure of channel proteins. I. Transmembrane segment M2 of the nicotinic cholinergic receptor channel is a key pore-lining structure.

Opsahl, L.R., and Webb, W.W. (1994) *Biophys. J., 66,* 71-74. Transduction of membrane tension by the ion channel alamethicin.

Oren, Z., Hong, Z., and Shai, Y. (1997) *J. Biol. Chem., 272,* 14643-14649. A repertoire of novel antibacterial diastereomeric peptides with selective cytolytic activity.

Österberg, F., Rilfors, L., Wieslander, A, Lindblom, G., and Grüner, S.M. (1995) *Biochim. Biophys. Acta, 1257,* 18-24. Lipid extracts from membranes of Acholeplasma laidlawii A grown with different fatty acids have a nearly constant spontaneous curvature.

Palmer, K.J., and Schmitt, F.O. (1941) *J. Cell. Comp. Physiol., 17,* 385-394. X-ray diffraction studies of lipid emulsions.

Paltauf, F. and Schmid H. H. O., eds. (1989) Special issue. Fluorescence in Membrane Biochemistry. *Chem. Phys. Lipids,* 50, 171-289.

Parente, R.A., Nir, S., and Szoka, F.C. (1990) *Biochemistry, 29,* 8720-8728. Mechanism of leakage of phospholipid vesicle contents induced by the peptide GALA.

Perutz, M.F., Kendrew, J.C., and Watson, H.C. (1965) *J. Mol. Biol., 13,* 669-678. Structure and function of haemoglobin II. Some relations between polypeptide chain configuration and aminoacid sequence.

Polozov, I. V., J. G. Molotkovsky, and L. D. Bergelson. (1994a) *Chem. Phys. Lipids,* 69, 209-218. Anthrylvinyl-labelled phospholipids as membrane probes: the phosphatidylcholine-phosphatidylethanolamine system..

Polozov, I.V., Polozova, A. I., Anantharamaiah, G. M., Segrest, J. P., and Epand,. R. M. (1994b) *Biochem. Mol. Biol. Intern., 33,* 1073-1079. Mixing rates can markedly affect the kinetics of peptide-induced leakage from liposomes.

Polozov, I. V., Polozova, A. I., Molotkovsky, J.G., Anantharamaiah, G. M., Segrest, J. P., and Epand, R. M. (1997b) *Biochim. Biophys. Acta,*(in press). Amphipathic Peptide Affects The Lateral Domain Organization Of Lipid Bilayers.

Polozov, I. V., Polozova, A. I., Tytler, E. M., Anantharamaiah, G. M., Segrest, J. P., Woolley, G.A. and Epand, R. M. (1997a) *Biochemistry (in press)* Role of lipids in the permeabilization of membranes by class L amphipathic helical peptides.

Polozov, I.V., Polozova, A.I., Molotkovsky, J.G., Anantharamaiah, G.M., Segrest, J.P., and Epand, R.M.. (1995) *Biophys. J., 68,* A433. Amphipathic peptides effects on the lateral domain organization of lipid bilayers.

Pomorski, T., Muller, P., Zimmermann, B., Burger, K., Devaux, P.F., and Herrmann, A. (1996) *J. Cell Science, 109,* 687-698. Transbilayer movement of fluorescent and spin-labelled phospholipids in the plasma membrane of human fibroblasts: a quantitative approach.

Pownall, H. J., Gotto, A.M. Jr., and Sparrow, J. (1984) *Biochim. Biophys. Acta, 793,* 149-156. Thermodynamics of lipid-protein associationand the activation of lecithin cholesterol acyltransferase by synthetic novel apolipopeptides.

Rapaport D., and Shai Y. (1994) *J. Biol. Chem., 269,* 15124-15131, Interaction of fluorescently labelled analogues of the amino-terminal fusion peptide of Sendai virus with phospholipid membranes.

Raudino, A. (1995) *Advances Coll. Inter. Sci.,* 57, 229-285. Lateral inhomogeneous lipid membranes: theoretical aspects.

Redwood, W.R., Pfeiffer, F.R., Weisbach, J.A., and Thompson, T.E. (1971) *Biochim. Biophys. Acta, 233,* 1-6. Physical properties of bilayer membranes formed from a synthetic saturated phospholipid in n-decane.

Reeves, J.P., and Dowben, R.M. (1970) *J. Membrane Biol., 3,* 123-123. Water permeability of phospholipid vesicles.

Rodgers, W., and Rose, J.K. (1996) *J. Cell Biology, 135,* 1515-23. Exclusion of CD45 inhibits activity of p56lck associated with glycolipid-enriched membrane domains.

Saberwal, G., and Nagaraj, N. (1994) *Biochim. Biophys. Acta, 1197,* 109-131. Cell-lytic and antibacterial peptides that act by perturbing the barrier function of membranes: facets of their conformational features, structure-function correlations and membrane-perturbing abilities.

Sackmann, E. (1994) *FEBS Letters, 346,* 3-16. The seventh Datta Lecture. Membrane bending energy concept of vesicle- and cell-shapes and shape-transitions.

Sackmann, E. (1995) In "Structure and dynamics of membranes" , R. Lipowsky and E. Sackmann, eds., Elseveir, Amsterdam, 1-65.

Sansom, M. S. P. (1991) *Prog. Biophys. Molec. Biol., 55,* 139-235. The biophysics of peptide models of ion channels.

Schroeder, R., London, E., and Brown, D. (1994) *Proc. Natl. Acad. Sci. U.S.A., 91,* 12130-12134. Interactions between saturated acyl chains confer detergent resistance on lipids and glycosylphosphatidylinositol (GPI)-anchored proteins: GPI-anchored proteins in liposomes and cells show similar behavior.

Schwarz, G., Gerke, H., Rizzo, V., and Stankowski, S. (1987) *Biophys. J., 52,* 685-92. Incorporation kinetics in a membrane, studied with the pore-forming peptide alamethicin.

Schwarz, G., and Beschiaschvili, G. (1989) *Biochim. Biophys. Acta, 979,* 82-90. Thermodynamic and kinetic studies on the association of melittin with a phospholipid bilayer.

Schwarz, G. (1987) *Biophys. Chemistry, 26* , 163-169. Basic kinetics of binding and incorporation with supramolecular aggregates.

Schwarz, G. (1989) *Biochimie, 71, 3-9.* Thermodynamics and kinetics of incorporation into a membrane

Schwarz, G. and Blochman, U. (1993) *FEBS Letters, 318, 172-176.* Association of the wasp venom peptide mastoparan with electrically neutral lipid vesicles. Salt effects on partitioning and conformational state.

Schwarz, G., and Robert, C. H. (1990) *Biophys. J., 58,* 577-583. Pore formation kinetics in membranes determined from the release of marker molecules out of molecules or cells.

Schwarz, G., and Robert, C.H. (1992) *Biophys. Chem., 42,* 291-296. Kinetics of pore-mediated release of marker molecules from liposomes or cells.

Seddon, J.M. (1990) *Biochim. Biophys. Acta, 1031,* 1-69. Structure of the inverted hexagonal (H_{II}) phase, and non-lamellar transitions of lipids.

Segrest, J.P., Garber, D.W., Brouillette, C.G., Harvey, S.C., and Anantharamaiah, G.M. (1994) *Advances in Protein Chemistry, 45,* 303-369. The amphipathic alpha helix: a multifunctional structural motif in plasma apolipoproteins.

Segrest, J. P., Chung, B. H., Brouillette, C. G., Kanellis, P., and McGan, R. (1983) *J. Biol. Chem., 258,* 2290-2295. Studies of synthetic peptide analogs of the amphipathic helix. Competitive displacement of exchangeable apolipoproteins from native lipoproteins.

Segrest, J. P., de Loof, H., Dohlman, J. G., Brouillette, C. G., and Anantharamaiah, G. M. (1990) *Proteins, 8,* 103-117. Amphipathic helix motif: classes and properties [published erratum appears in *Proteins* (1991) 9(1), 79].

Segrest, J. P., Jones, M.K., De Loof, H., Brouillette, C. G., Venkatachalapathi, Y.V., and Anantharamaiah, G. M. (1992). *J. Lipid Res., 33,* 141-166. Amphipathic helix in exchangeable apolipoproteins, a review of secondary structure and function.

Segrest, J.P., Jackson, R.L., Morrisett, J.D., and Gotto, A.M., Jr. (1974) *FEBS Letters, 38,* 247-253. A molecular theory for protein-lipid interactions in plasma lipoproteins.

Sekharam, K. M., Bradrick, T. D., and Georghiou, S. (1991) *Biochim. Biophys. Acta, 1063,* 171-174. Kinetics of melittin binding to phospholipid small unilamellar vesicles.

Shai, Y., and Oren, Z. (1996) *J. Biol. Chem., 271,* 7305-7308. Diastereoisomers of cytolysins, a novel class of potent antibacterial peptides

Sheets, E.D., Simson, R., and Jacobson, K.(1995) *Curr. Opin. Cell Biol., 7,* 707-14. New insights into membrane dynamics from the analysis of cell surface interactions by physical methods.

Sheetz, M.P., Painter, R.G., and Singer, S.J. (1976) *J. Cell Biol. 70,* 193-203. Biological membranes as bilayer couples. III. Compensatory shape changes induced in membranes.

Sheetz, M.P., Turney, H., Quian, H., and Elson, E.L. (1989) *Nature, 340,* 284-288. Nanometer-level analysis demonstrates that lipid flow does not drive membrane glycoprotein movements.

Shinitzky, M. (1984) In "Physiology of Membrane Fluidity", Shinitzky, M., ed., CRC Press, Boca Raton, v.1, 1-53.

Siegel, D.P. (1993) *Biophys. J., 65,* 2124-2140. Energetics of intermediates in membrane fusion: Comparison of stalk and inverted micellar intermediate mechanisms.

Siegel, D.P., Banschbach, J.L., and Yeagle, P.L. (1989) *Biochemistry, 24,* 5010-5019. Stabilization of H_{II} phases by low levels of diglyceride and alkanes: An NMR, calorimetric and X-ray diffraction study.

Singer, S.J. (1992) *J. Membrane Biol.*, 129, 3-12. The structure and function of membranes - a personal memoir.

Singer, S.J., and Nicolson, G.L. (1972) *Science, 175,* 720-731. The fluid mosaic model of the structure of cell membranes.

Sjolund, M., Lindblom, G., Rilfors, L., and Arvidson, G. (1987) *Biophys. J., 52,* 145-153. Hydrophobic molecules in lecithin water systems. I. Formation of reversed hexagonal phases at high an low water contents.

Smirnov, O. N., Surin, A. M., Astashkin, E. I., Mikhalyov, I. L., and Molotkovsky, J. G. (1995) *Biol. Membrany*, 12, 174-184. Study on the Interaction of Cholera-Toxin and Its B-Subunit with Liposomes Containing Ganglioside GM1 and Fluorescent-Labelled Gangliosides.

Smit, J.J., Schinkel, A.H., Oude Elferink, R.P., Groen, A.K., Wagenaar, E., van Deemter, L., Mol, C.A.., Ottenhoff, R., van der Lugt, N.M., and van Roon, M.A. (1993) *Cell, 75*, 451-462, Homozygous disruption of the murine mdr2 P-glycoprotein gene leads to a complete absence of phospholipid from bile and to liver disease.

Smith, A.J., Timmermans-Hereijgers, J.L., Roelofsen, B., Wirtz, K.W., van Blitterswijk, W.J., Smit, J.J., Schinkel, A.H., and Borst, P. (1994) *FEBS Letters, 354*, 263-266. The human MDR3 P-glycoprotein promotes translocation of phosphatidylcholine through the plasma membrane of fibroblasts from transgenic mice.

Smolarsky, M., Teitelbaum, D., Sela, M., and Gitler, C. (1977) *J. Immunol. Meth., 15*, 255-265. A simple fluorescent method to determine complement-mediated liposome immune lysis.

Spuhler, P., Anantharamaiah, G. M., Segrest, J. P., and Seelig, J. (1994) *J. Biol. Chem., 269*, 23904-23910. Binding of apolipoprotein A-I model peptides to lipid bilayers. Measurement of binding isotherms and peptide-lipid headgroup interactions.

Srinivas, R.V., Bridal, B., Owens, R.J., Anantharamaiah, G.M., Segrest, J.P., and Compans, R.W. (1990) *Virology, 176*, 48-57. Antiviral effects of apolipoprotein A-I and its synthetic amphipathic peptide analogs.

Stoffel, W., and Michaelis,G. (1976) *Hoppe-Seylers's Z. Physiol. Chem., 357*, 7-19. Chemical syntheses of novel fluorescent-labelled fatty acids, phosphatidyl-cholines and cholesterol esters.

Sulpice, J.C., Moreau, C., Devaux, P.F., Zachowski, A., and Giraud, F. (1996) *Biochemistry, 35*, 13345-13352. Antagonist effects of Ca2+ and spermine on phosphatidylinositol 4,5-bisphosphate-mediated transmembrane redistribution of phospholipids in large unilamellar vesicles and in erythrocytes.

Tytler, E. M., Anantharamaiah, G. M., Walker, D. E., Mishra, V. K., Palgunachari, M. N., and Segrest, J. P. (1995) *Biochemistry, 34*, 4393-4401. Molecular basis for prokaryotic specificity of magainin-induced lysis.

Tytler, E. M., J. P. Segrest, R. M. Epand, S. Q. Nie, R. F. Epand, V. K. Mishra, Y. V. Venkatachalapathi, and G. M. Anantharamaiah. (1993) *J. Biol. Chem.*, 268, 22112-22118. Reciprocal effects of apolipoprotein and lytic peptide analogs on membranes. Cross-sectional molecular shapes of amphipathic alpha helices control membrane stability.

Van Dijck, P. W., de Kruijff, B., Verkleij, A. J., van Deenen, L. L., and de Gier, J. (1978) *Biochim. Biophys. Acta, 512*, 84-96. Comparative studies on the effects

of pH and Ca^{2+} on bilayers of various negatively charged phospholipids and their mixtures with phosphatidylcholine.

Venkatachalapathi, Y. V., Phillips, M. C., Epand, R. M., Epand, R. F., Tytler, E. M., Segrest, J. P., and Anantharamaiah, G. M. (1993) *Proteins, 15*, 349-359. Effect of end group blockage on the properties of a class A amphipathic helical peptide.

Vist, M.R. and Davis, J.H. (1990) *Biochemistry, 29*, 451-464. Phase equilibria of cholesterol/dipalmitoylphosphatidylcholine mixtures: 2H nuclear magnetic resonance and differential scanning calorimetry.

Waggoner, A.S., and Stryer, L. (1970) *Proc. Natl. Acad. Sci. U.S.A., 67*, 579-589. Fluorescent probes of biological membranes.

Watts, A., Harlos, K., and Marsh, D. (1981) *Biochim. Biophys. Acta, 641*, 91-95. Charge-induced tilt in ordered-phase phosphatidylglycerol bilayers evidence from X-ray diffraction.

Wegener, J., and Galla, H.-J. (1996) *Chem. Phys. Lipids, 81*, 229-256. The role of non-lamellar lipid structures in he formation of tight junctions.

Welti, R., and Glaser, M. (1994) *Chem. Phys. Lipids, 73*, 121-137. Lipid domains in model and biological membranes.

Welti, R., and Silbert, D. (1982) *Biochemistry, 21*, 5685-5689. Partition of parinaroyl phospholipid probes between solid and fluid phosphatidylcholine phases.

White, G., Pencer, J., Nickel, B.G., Wood, J.M., and Hallett, F.R.(1996) *Biophys. J., 71*, 2701-2715.Optical changes in unilamellar vesicles experiencing osmotic stress.

Wieprecht, T., Dathe, M., Schumann, M., Krause, E., Beyermann, M., and Bienert, M. (1996) *Biochemistry, 35*, 10844-10853. Conformational and functional study of magainin 2 in model membrane environments using the new approach of systematic double-D-amino acid replacement.

Wilschut, J., Duzgunes, N., Fraley, R., and Papahadjopoulos, D. (1980) *Biochemistry, 19*, 6011-6021. Studies on the mechanism of membrane fusion, kinetics of calcium ion induced fusion of phosphatidylserine vesicles followed by a new assay for mixing of aqueous vesicle contents.

Wiseman, T., Williston, S., Brandts, J. F., and Lung-Nau, L. (1989) *Anal. Biochemistry, 179*, 131-137. Rapid measurement of binding constants and heats of binding using a new titration calorimeter.

Wu, Y., He, K., Ludtke, S. J., and Huang, H. W. (1995) *Biophys. J., 68*, 2361-2369. X-ray diffraction study of lipid bilayer membranes interacting with amphiphilic helical peptides: diphytanoyl phosphatidylcholine with alamethicin at low concentrations.

Yaroslavov, A.A., Kul'kov, V.E., Polinsky, A.S., Baibakov, B.A., and Kabanov, V.A.. (1994) *FEBS Letters, 340,* 121-123. A polycation causes migration of negatively charged phospholipids from the inner to outer leaflet of the liposomal membrane.

Zasloff, M. (1987) *Proc. Natl. Acad. Sci. U.S.A., 84,* 5449-5453. Magainins, a class of antimicrobial peptides from Xenopus skin: isolation, characterization of two active forms, and partial cDNA sequence of a precursor.

Zasloff, M., Martin, B., and Chen, H.-C. (1988) *Proc. Natl. Acad. Sci. U.S.A., 85,* 910-913. Antimicrobial activity of synthetic magainin peptides and several analogues.

Zhelev, D.V., and Needham, D. (1993) *Biochim. Biophys. Acta, 1147,* 89-104. Tension-stabilized pores in giant vesicles: determination of pore size and pore line tension.

Appendix 1. Note on calculations

Software packages used in this work

There exist some mathematical functions in the software used for running AB-2 fluorescence spectrophotometer. However, generally they are of limited usability. For calculations, data from fluorescence measurements were converted into the ASCII format and imported into the spreadsheets. Initially, I used for calculations and presentations the spreadsheet Quattro Pro 4.0 for DOS. In my experience, the main disadvantage of this spreadsheet was the limit of six lines per graph as well as general orientation on the business rather than scientific graphic, e.g. no error bars. The first drawback was overcome with introduction of a Windows version (the latest version I tried was Quattro Pro 6.0 for Windows) the second is intrinsic and will not go away anytime soon. On the positive side of this package was the high computational speed, ease of use, thought out and convenient set of functions and features. I used scientific graphic packages Sigma Plot (2.2 for Windows) and MicroCal Origin (4.0 for Windows) to overcome presentation limitations inherent to Quattro Pro. This use of software was a history dependent personal choice. The same calculations obviously can be reproduced with other computer packages.

Determination of binding

Deconvolution of fluorescence spectra was performed using Optimizer block in Quattro Pro (tools section in DOS version, tools/numerical methods in Windows version) according to equation (3.1.2.1) and with constraint (3.1.2.2). Essentially the concentration of peptide in membrane (P_b) was determined as a value of P ($0<P<P_o$) at

which the error of the fit of experimental curve with two components reached the minimum:

$$\min_{P=0..P0} \{ \sum_{\lambda=300..480} (I_\lambda - [(P_o - P)\cdot I_{\lambda 0} + P \cdot I_{\lambda \infty}])^2 \}$$

Concentration of peptide in solution (P_f) was then determined by subtraction of the bound peptide concentration (P_b) from the total peptide concentration (P_o): $P_f = P_o - P_b$

Kinetics of binding

Monoexponential fit of the kinetic curves was also performed in Quattro Pro, using Optimizer block. Three parameters were determined by simultaneous minimisation of the sum of the squares of the error. The range of rate constant (error bars on the Fig. 3.1.3.2) was estimated manually by calculating and plotting the error of the fit the around the optimal value of the rate constant.

Leakage time traces

Time traces of aqueous contents leakage of osmotically stressed vesicles were fitted according to equation (3.6.2), also using Optimizer block in Quattro Pro. All the time traces were fitted simultaneously. To reduce the number of calculations only each one hundredth experimental data point was used for the fitting (Fig. 3.6.2) after preliminary smoothing of the data.

IMAGE EVALUATION TEST TARGET (QA-3)

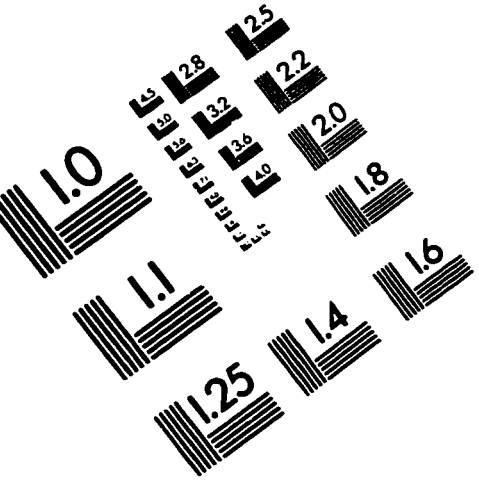

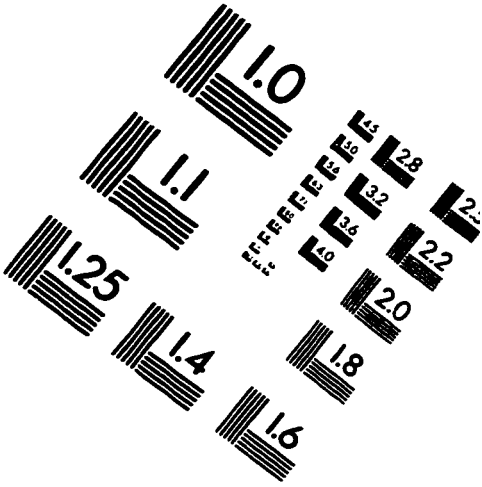

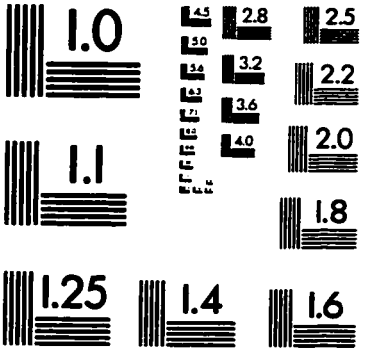

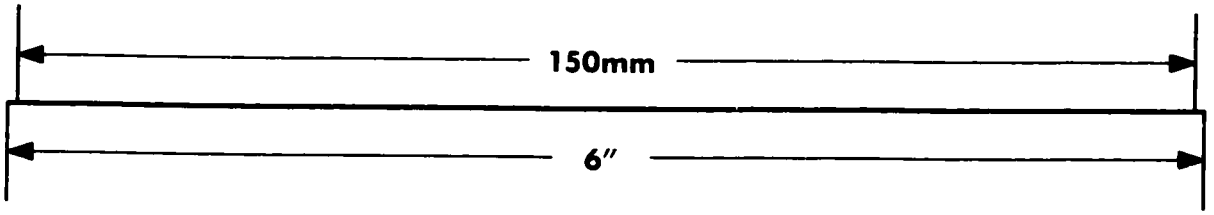

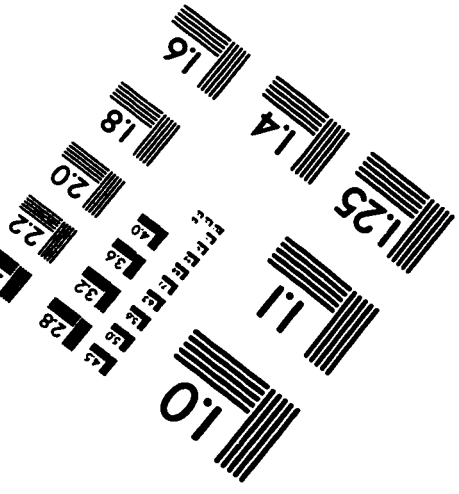

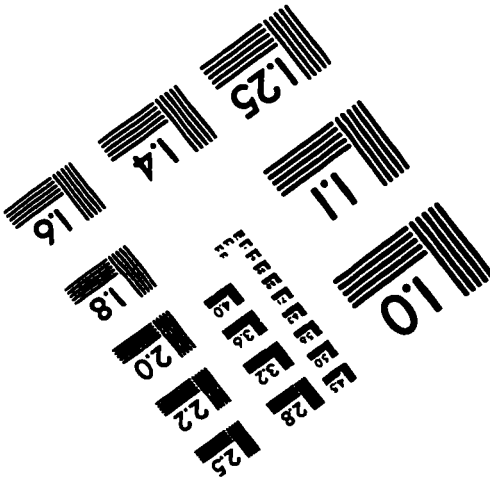

APPLIED IMAGE, Inc
1653 East Main Street
Rochester, NY 14609 USA
Phone: 716/482-0300
Fax: 716/288-5989